00591

UNIVERSIDAD NACIONAL AUTONOMA DE MEXICO

FACULTAD DE QUIMICA

PROGRAMA DE MAESTRIA Y DOCTORADO EN CIENCIAS BIOQUIMICAS

PARTICIPACION DE LAS DESHIDROGENASAS LACTICAS MITOCONDRIALES DE *Euglena gracilis* EN EL METABOLISMO ENERGETICO

T E S I S

QUE PARA OBTENER EL GRADO DE:

DOCTOR EN CIENCIAS BIOQUIMICAS

P R E S E N T A :

M. EN C. RICARDO JASSO CHAVEZ

ASESOR: DR. RAFAEL MORENO SANCHEZ

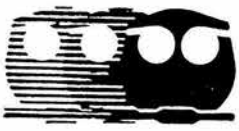

CIUDAD UNIVERSITARIA. 2004

La presente tesis se realizó en el Departamento de Bioquímica del Instituto Nacional de Cardiología Ignacio Chávez, bajo la tutoría del Dr. Rafael Moreno Sánchez.

Este proyecto fue apoyado parcialmente por el donativo 203313 del PAEP, Facultad de Química, UNAM.

Jurado Asignado:

Dra. Victoria Chagoya de Sánchez	Presidente
Dra. Irma Bernal Lugo	Vocal
Dr. Georges Dreyfus	Vocal
Dr. Juan Pablo Pardo Vázquez	Vocal
Dr. José de Jesús García Valdés	Secretario
Dr. Juan Luis Rendón Gómez	Suplente
Dr. Edgardo Escamilla Marván	Suplente

Asesor: Rafael Moreno Sánchez.

Sustentante: Ricardo Jasso Chávez.

Agradecimientos

- A mis papás, por inculcarme el AMOR, el trabajo Y la honestidad….

- A mis hermanos otra vez, ¿cómo agradecer tanto cariño, apoyo y confianza? Mil gracias los quiero mucho…

- A toda mi familia, sobrinos, cuñadas, tíos, primos, etc., principalmente a mi tías Esther y chole y a mis tíos toño y chayo. Gracias por su confianza…

- A los que ya no están en cuerpo, a mis abuelos toño y aurelia, A mis tios maro y guille, a mi primo arturo. Y Especialmente a mi amigo y hermano césar avilés: manito, va por ti, espero que estés en mi examen….

- A todas las personas que amo y quiero, a los amigos y compañeros. Gracias por su confianza, amor, amistad y por su tiempo. Gracias por estar ahí en los buenos y tristes momentos. Ustedes saben quienes son. Perdón por ser tan escueto pero son demasiados sentimientos para tan poco espacio…

- Al Dr. Rafael moreno Sánchez, gracias por permitirme ser parte de su grupo y por inculcarme el trabajo y la crítica….

- A mi dios que está conmigo siempre, principalmente cuando siento que ya no hay más…. Por darme consuelo.

"La ciencia avanza de puntillas, no a pasos,
éstos hacen demasiado ruido." (Anónimo)

"Todos somos científicos cuando somos niños,
pero al crecer, solo algunos conservan
un poco de esa curiosidad
que es la madre de la ciencia."

"El hombre encuentra a Dios
detrás de cada puerta
que la ciencia logra abrir."
— Albert Einstein

"PARTICIPACIÓN DE LAS DESHIDROGENASAS LÁCTICAS MITOCONDRIALES DE *Euglena gracilis* EN EL METABOLISMO ENERGÉTICO"

RESUMEN

El protista *Euglena gracilis* no tiene la capacidad de oxidar piruvato para la síntesis de acetil-CoA cuando se le cultiva en condiciones aeróbicas. En cambio, tiene la habilidad de acoplar la oxidación de D- y L-lactato a la fosforilación oxidativa por medio de enzimas isómero específicas. Estas lactato deshidrogenasas reducen directamente a la poza de quinonas, están unidas a la membrana interna mitocondrial y son independientes de NAD^+, por lo que se les conoce como lactato deshidrogenasas independientes de piridín nucleótidos (D-iLDH y L-iLDH). Estas enzimas presentaron valores de *Km* de 2.7 y 2.5 mM por D- y L-lactato respectivamente. Fueron inhibidas de forma competitiva por oxamato y de forma mixta por oxalato, aunque la D-iLDH fue más sensible a ambos inhibidores. La D-iLDH fue termorresistente hasta los 70°C mientras que la L-iLDH lo fue hasta los 50°C.

En un intento por dilucidar la participación de la D- y L-iLDH en el metabolismo energético de la célula, y determinar si el metabolismo del lactato aportaba los equivalentes reductores necesarios para soportar la síntesis de ATP, *Euglena* se cultivó en diferentes fuentes de carbono (glutamato/malato, lactato y glucosa) y se determinaron las actividades de D- y L-iLDH durante el crecimiento. Se analizaron también los niveles de D- y L-lactato, ATP, piruvato y paramilo (cadena lineal de glucosa con enlaces β-1,3). Los resultados mostraron que ambas actividades de iLDH se encontraron en las células cultivadas en todas las fuentes de carbono y en todas las fases de crecimiento. Las concentraciones de D- y L-lactato fueron lo suficientemente altas para mantener cerca de su velocidad máxima a ambas iLDH. El incremento en la actividad de ambas iLDH correlacionó con el abatimiento de la fuente de carbono externa y el inicio de la degradación de la fuente de carbono interna, el paramilo. El efecto del oxalato sobre el crecimiento celular, la respiración asociada a la fosforilación oxidativa y el contenido de ATP, fue mayor en las células cultivadas en lactato con respecto a las cultivadas en glutamato/malato. La adición de citosol (cuya actividad de lactato deshidrogenasa

dependiente de NAD^+ fue 40-80 veces mayor hacia la producción de lactato), NADH y piruvato a mitocondrias incubadas con rotenona y flavona; promovieron el consumo de oxígeno el cual fue bloqueado por oxalato. Los resultados obtenidos sugieren que en *E. gracilis* la expresión de ambas iLDH es independiente de la disponibilidad de substrato y que tienen un papel clave en la transferencia de electrones del citosol a la cadena respiratoria. Así, las iLDH oxidan al lactato producido por la NAD^+-LDH citosólica a partir de piruvato y NADH para la síntesis de ATP. Este conjunto de enzimas conforman una lanzadera de lactato.

Finalmente, el análisis estructural de los componentes de la lanzadera de lactato reveló que, similar a las D-iLDH de bacterias, la de *E. gracilis* fue una enzima de aprox. 62 kDa con una molécula de FAD como cofactor y capaz de reducir quinonas de alto y bajo potencial redox. Fue específica para D-lactato. El L-lactato fue capaz de inhibirla con un valor de *Ki* de 10 mM. En el caso de la L-iLDH, los esfuerzos por purificar a la enzima no fueron exitosos, sin embargo, se logró extraer de la membrana con actividad suficiente para poder determinar algunos de sus parámetros cinéticos, entre otros la capacidad de reducir directamente a la ubiquinona-1. La NAD^+-LDH citosólica presentó una activación alostérica por fructosa-1,6-bisfosfato, lo que produjo una mayor afinidad por piruvato y NADH. Los esfuerzos por purificarla mostraron el enriquecimiento de un monómero de 40 kDa de masa molecular. El perfil de elusión de la NAD^+-LDH obtenido cuando se pasó un extracto citosólico por una resina de afinidad acoplada a una molécula de oxamato, mostró dos picos de actividad; en el primero la NAD^+-LDH no se unió a la resina y produjo D-lactato, mientras que el segundo pico la NAD^+-LDH se eluyó cuando se eliminó el NADH del buffer de lavado y produjo L-lactato. Estas características cinéticas de la NAD^+-LDH de *E. gracilis* sólo se han reportado para proteínas presentes en algunas bacterias homofermentativas, lo que sugiere un origen común entre las enzimas de bacterias y *Euglena*.

SUMMARY

The protist *Euglena gracilis* is unable to oxidize pyruvate for acetyl-coA synthesis when is cultured under aerobic conditions. Instead, it couples D- and L-lactate oxidation to oxidative phosphorylation by means of isomer-specific lactate dehydrogenases. These enzymes directly reduce the quinone pool, are membrane-bound enzymes and NAD^+-independent (D-iLDH and L-iLDH). The *Km* values were 2.7 and 2.5 mM for D- and L-lactate respectively. Both enzymes were inhibited competitively by oxamate and in mixed fashion by oxalate, although D-iLDH was more sensitive to these inhibitors. D-iLDH was thermo-resistant up to 70°C, while the L-iLDH was up to 50°C.

In an attempt to elucidate the role of iLDH in cellular energy metabolism, and assess whether lactate metabolism of lactate supplies the reducing equivalents to support ATP synthesis; cells were grown in different carbon sources (glutamate/malate, lactate and glucose) and D- and L-iLDH activities were determined throughout the growth curve. We also analyzed the level of D- and L-lactate, ATP, pyruvate and paramylon (lineal chain of glucose with β-1, 3 bonds). Results showed that both iLDH activities were present in all carbon sources in each growth phase. Intracellular concentrations of D- and L-lactate were high enough to get near *Vmax* rates of iLDH. Moreover, the intracellular concentrations of lactate increased at the end of the growth curve. An increase in the activity of both enzymes in the log phase, correlated with the exhaustion of the external carbon source and the start of paramylon degradation. The oxalate effect on cell growth, respiration linked to oxidative phosphorylation, and ATP levels, was higher when cells were cultured in lactate than in cells cultured in glutamate/malate. Addition of cytosolic extract, (which activity of NAD^+-dependent lactate dehydrogenase was 40-80 fold high toward lactate production), NADH and pyruvate to isolated mitochondria previously incubated with rotenone and flavone, prompted an oxalate-sensitive O_2-uptake. These data suggest that in *Euglena*, the expression of both iLDH is substrate-independent and that they play a key role in

transferring the reducing equivalents from cytosol to respiratory chain. Then, the mitochondrial D- and L-iLDH oxidize the lactate produced by mean of cytosolic NAD^+-LDH from pyruvate and NADH for the ATP synthesis. All these enzymes are the components of the lactate shuttle.

Finally, the structural analysis of the lactate shuttle components showed that D-iLDH was a 60 kDa protein containing FAD as cofactor. This enzyme was able to reduce high and low redox potential quinones as electron acceptors. D-iLDH was specific to the D-isomer. L-lactate was able to inhibit this activity with a *Ki* value of 10 mM. L-iLDH was inactivated when the enzyme was extracted from the membrane by detergents and it purification was unsuccessful. Despite this, we solubilized it with enough activity to determine some kinetic parameters, among others, its ability to reduce ubiquinone-1. The cytosolic NAD^+-LDH showed allosteric activation by fructose-1, 6-biphosphate, inducing an increased affinity for pyruvate and NADH. The efforts to purify the enzyme have shown the enrichment of a 40kDa of molecular mass monomer. The elution of NAD^+-LDH after passing the cytosolic extract through affinity resin coupled to insoluble oxamate, showed two peaks of NAD^+-LDH activity: The first one did not bind to the resin and the activity produced D-lactate. The second peak was eluted when NADH was absent in the washing-buffer and the enzyme produced L-lactate. These kinetic characteristics of the NAD^+-LDH from *E. gracilis*, have been reported in some homo-fermentative bacteria only, which suggests a common origin between bacteria and *E. gracilis* enzymes.

Nota: Esta tesis está dividida en 5 capítulos y un anexo. En el capítulo I se describen las generalidades del metabolismo energético de *Euglena*. El capítulo II comprende los antecedentes que se dividen a su vez en tres partes: la primera de ellas analiza las características generales de las deshidrogenasas lácticas independientes de NAD^+ (iLDH) en diversos microorganismos. Aquí se incluye una revisión en español en donde se hace un estudio más profundo de este tema (Boletín de Educación Bioquímica, 2001). La segunda parte del capítulo II es sobre la iLDH en *Euglena gracilis*. Se incluye un artículo publicado en los *Archives of Biochemistry and Biohysics* (2001) en donde se estableció la existencia de enzimas específicas para la oxidación de D- y L-lactato (D-iLDH y L-iLDH) y dos problemas bioquímicos publicados en el *Boletín de Educación Bioquímica*. La tercera parte de los antecedentes trata de la capacidad de ambas iLDH para reducir distintos tipos de quinonas. Estas publicaciones se encuentran en su forma completa en el anexo. El capítulo IV incluye una sección de métodos y otra de resultados. En esta sección se analiza la participación de la D- y L-iLDH en la fisiología del microorganismo y se describe por primera vez la existencia de una lanzadera de lactato en las mitocondrias de *Euglena* (de este trabajo se publicó un artículo en el *European Journal of Biocemistry*, 2003). Además se describe la purificación y caracterización de los componentes de la lanzadera de lactato; este trabajo se encuentra en preparación y se muestra la primera versión del artículo. Finalmente, el capítulo V incluye la discusión general, conclusiones, perspectivas y la bibliografía.

INDICE

I
INTRODUCCIÓN

1. *Euglena gracilis* y su metabolismo energético

Desde hace muchos años, el metabolismo de *Euglena gracilis* ha sido muy estudiado debido a la gran capacidad que posee este protista de vida libre para crecer en muy variadas condiciones nutrimentales. Esta capacidad esta dada probablemente por las características metabólicas que comparte con animales y plantas superiores, además de las que son exclusivas de su grupo, como la de obtener energía por medio de la fermentación de ésteres de cera o por la oxidación de acetato, succinato, succinato-semialdehído, glutamato/malato, glucosa, lactato o etanol. Incluso, las diferentes cepas de *Euglena gracilis* se diferencian entre sí, ya que algunas de ellas tienen la capacidad de crecer en galactosa y otras no. Tienen necesidades orgánicas diferenciales respecto de aminoácidos, purinas, pirimidinas y factores de crecimiento, según si se desarrollan heterotróficamente o fototróficamente, y presentan una amplia capacidad biosintética, por lo cual necesitan incorporar además nutrientes inorgánicos (Buetow, 1989).

La relación evolutiva que se ha establecido entre Euglénidos y Tripanosomátidos, ha mostrado que son los protozoarios mitocondriados más primitivos que existen (Nordnes y col., 1994; Linton y col., 1999). A pesar de que se ha establecido claramente la teoría endosimbiótica para el origen de la mitocondria y de que en general, la maquinaria necesaria para obtener ATP se ha conservado entre las mitocondrias y las bacterias que les dieron su origen (Müller y col., 1999), es relevante que las mitocondrias de *E. gracilis* tengan aspectos metabólicos únicos con respecto a las mitocondrias de otros organismos. De particular importancia son las enzimas $NADP^+$-piruvato-oxidorreductasa y las deshidrogenasas lácticas independientes de NAD^+ (iLDH). La primera se encuentra solamente en las mitocondrias de *Euglena* y en los hidrogenosomas de algunos parásitos, organelos que al igual que las mitocondrias, provienen al parecer, de un mismo ancestro (α-proteobacterias) (Philip, J. 1987;

Muller, M. y Martin, W. 1999). De manera semejante, las iLDH son enzimas que sólo se han encontrado en las mitocondrias de *Euglena,* de tripanosomátidos (Jasso-Chávez y cols. 2001) y en bacterias tan lejanas evolutivamente como *Paracoccus denitrificans* e incluso en archeabacterias como *Archaeglobus fulgidus* (Zboril y Wernerová, 1996; Reed y Hartzell, 1999). Estos datos sugieren que metabolicamente, las mitocondrias de *Euglena* tienen mayores semejanzas con los organismos que les dieron origen que con las mitocondrias de organismos actuales.

2. La cadena respiratoria de *Euglena*

La organización de la cadena respiratoria de las mitocondrias de *Euglena* es compleja. Aunque existen los cuatro componentes respiratorios clásicos, estas mitocondrias pueden oxidar también NADH externo por una enzima que es insensible a rotenona. Por el efecto de inhibidores como la antimicina y el mixotiazol sobre la reducción del citocromo *c* y el consumo de oxígeno, se ha propuesto que las mitocondrias de *Euglena* poseen al igual que *Leishmania*, una quinol: citocromo *c* oxidorreductasa distinta al complejo bc_1. Además, las mitocondrias de *Euglena* poseen también una oxidasa alterna resistente a cianuro, la cual parece ser diferente a la de plantas y bacterias, asemejándose más a la encontrada en *Trypanosoma* (Castro-Guerrero y cols., 2004).

Como ya se ha mencionado, la oxidación de D- y L-lactato acoplada al bombeo de protones para la producción de ATP, es otra de las particularidades que tiene la cadena respiratoria de *Euglena* (Uribe y Moreno-Sánchez, 1992). Moreno-Sánchez y cols. (2000), propusieron un modelo de la cadena respiratoria donde la oxidación del L-lactato por la iLDH es el principal sustrato oxidable en las mitocondrias aisladas de *Euglena* (esquema I). En el siguiente capítulo se explican las características enzimáticas y funcionales de las iLDH, además de su distribución en algunos microorganismos.

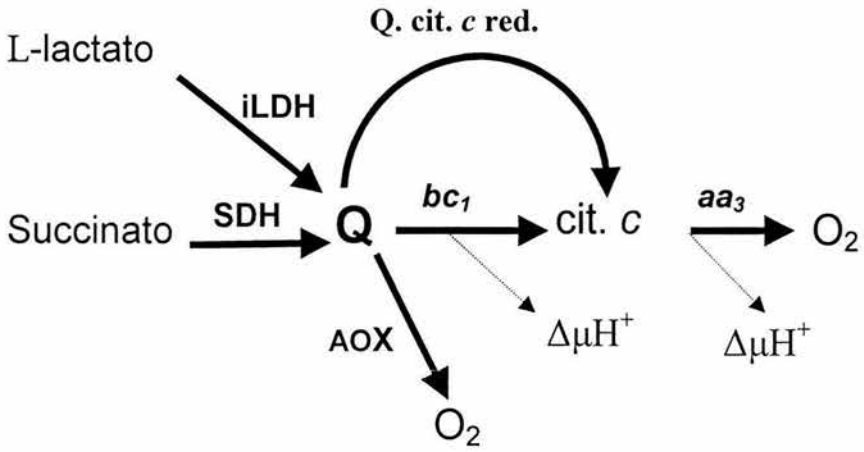

Esquema 1. **Cadena respiratoria de *Euglena gracilis*. SDH**, succinato deshidrogenasa; **iLDH**, lactato deshidrogenasa independiente de NAD^+; ***bc*$_1$**, quinol citocromo c oxidorreductasa (sensible a antimicina); **Q. cit. *c* red.**, quinol citocromo c oxidorreductasa (insensible a antimicina y sensible a mixotiazol); ***aa*$_3$**, citocromo *c* oxidasa; **AOX**, oxidasa alterna insensible a cianuro. Modificado de Moreno-Sánchez y cols. 2000.

II

ANTECEDENTES

Las deshidrogenasas lácticas independientes de NAD^+

1. Deshidrogenasas lácticas en microorganismos

Las enzimas más conocidas que oxidan lactato son las deshidrogenasas lácticas citosólicas dependientes de NAD^+. Sin embargo, en algunos organismos unicelulares se han detectado iso-enzimas que son independientes de NAD^+. Estas enzimas están ampliamente distribuidas en las bacterias, tanto en las empleadas en la industria de alimentos (*Lactobacillus casei*, *Leuconostoc mesenteroides*, *Acinetobacter calcoaceticus*, etc), como en las patógenas (*Neisseria sp, Salmonella sp, Haemophilus influenza*, etc.) y hasta en las inocuas utilizadas ampliamente en la investigación bioquímica (*Escherichia coli*, *Rhodobacter sphaeroides*, *Paracoccus denitrificans*, etc.) (Garvie, 1980; Allison y cols, 1985; Erwin y Gotchlich, 1993; Zboril y Wernerová, 1996). Aunque las iLDH se pueden encontrar en forma soluble (Díez-Gonzalez y cols, 1997), son las unidas a membranas las que se han estudiado ampliamente. Se encuentran localizadas en la membrana interna y tienen orientado su sitio activo hacia el citosol, la oxidación de D- o L-lactato está acoplada a la cadena respiratoria a través de la poza de quinonas (Garvie, 1980) y el gradiente de protones generado por la oxidación de lactato se utiliza para el transporte de aminoácidos y carbohidratos (Kaback, and Millner, 1970). La purificación y caracterización cinética de las iLDH bacterianas ha revelado que son flavoproteínas monoméricas y en general, específicas por su sustrato (Futai, 1970; Fewson, y cols. 1993). En bacterias, sólo una enzima (D- o L-iLDH) se expresa constitutivamente, mientras que la otra puede ser inducida en presencia de glucosa o de su sustrato, pero siempre en condiciones de aerobiosis.

Las levaduras como *Saccharomyces cerevisiae* y *Hansenula anomala*, son los otros organismos que presentan actividad de iLDH y, aunque llevan a cabo la misma

reacción que las enzimas bacterianas, éstas son flavocitocromos constituidos por una flavina y un citocromo tipo *b* (Gondry and Lederer, 1996) que se localizan en el espacio intermembranal de la mitocondria y su sitio activo se encuentra localizado hacia el citosol. El mecanismo molecular de la transferencia de los electrones también es diferente, ya que las enzimas de levadura tienen al citocromo *c* de la cadena respiratoria como su aceptor de electrones (Somlo, 1965). La L-iLDH de las levaduras es un homotetrámero y la D-iLDH un monómero (Lodi y Ferrero, 1996). En las levaduras, estas enzimas se expresan sólo en presencia de lactato en el medio y en aerobiosis; se ha propuesto que la función de la D-iLDH está relacionada con la destoxificación del metilglioxal (Lodi y Ferrero, 1996) (Esquema II). En el trabajo de revisión del *Boletín de Educación Bioquímica* de 2001, se hace un análisis más detallado acerca de éste tema (ver anexo).

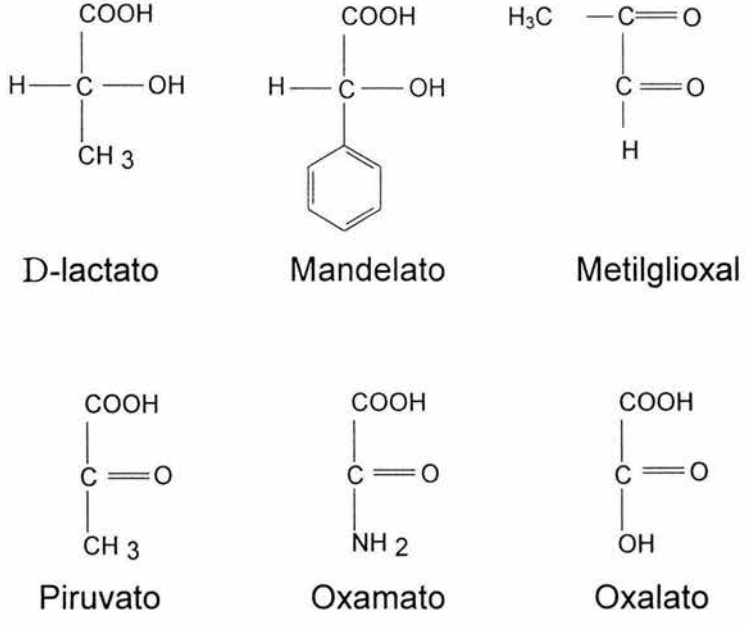

Esquema 2. **Estructura del D-lactato y otras estructuras similares mencionadas en este trabajo.**

2. Las deshidrogenasas lácticas isómero-específicas mitocondriales de *Euglena*

En 1961, Price reportó que la fracción no soluble (particulada) de un homogenado de *E. gracilis*, era capaz de oxidar D-lactato de una forma dependiente de zinc e independiente de piridín nucleótidos. El L-lactato también se oxidaba pero a velocidades más lentas (Price, 1961). Yokota y Kitaoka también reportaron actividades de iLDH con D- y con L-lactato en las mitocondrias y en la fracción microsomal, y ambas actividades fueron resistentes a 1 mM de cianuro (Yokota y Kitaoka, 1979). Años después Uribe y Moreno-Sánchez reportaron que las mitocondrias aisladas de *Euglena* oxidaban preferentemente L-lactato y que generaban un potencial de membrana sensible a desacoplante (Uribe y Moreno-Sánchez, 1992). En el volumen IV de su libro "The Biology of *Euglena*", Buetow propuso un esquema de la cadena respiratoria mitocondrial, donde la oxidación del L-lactato podía ceder sus electrones a la poza de quinonas o directamente al citocromo *c*; la última propuesta se fundamentó en el hecho de que la oxidación del D- y L-lactato presentó 50% de resistencia a antimicina (Buetow, 1989). Sin embargo, Moreno-Sánchez y cols., determinaron que la respiración y síntesis de ATP impulsadas por la oxidación de lactato resistentes a la antimicina, eran debidas a un componente alterno con actividad de citocromo *c* oxidorreductasa (resistente a la antimicina pero sensible a mixotiazol), el cual reduce al citocromo *c* y oxida al quinol (ver esquema I). Todos estos datos sugirieron que la iLDH de *Euglena* se encontraba en las mitocondrias, que podía oxidar D- y L-lactato y que estaba conectada a la cadena respiratoria directamente con la poza de quinonas (Moreno-Sánchez y cols., 2000).

Aunque el modelo de la cadena respiratoria de *Euglena* propuesto en nuestro laboratorio contesta muchas interrogantes acerca de su composición y secuencia (Esquema I), no establece si la oxidación del lactato se lleva a cabo por una enzima capaz de oxidar a los dos isómeros ó si son oxidados por enzimas isómero-específicas, como sucede en bacterias. En un primer trabajo, caracterizamos cinéticamente a la iLDH en mitocondrias aisladas con la finalidad de determinar si en *E. gracilis* al igual

que en las bacterias, existían enzimas isómero-específicas para la oxidación del lactato. Estudiamos la cinética de oxidación de D- y L-lactato midiendo directamente la reducción de DCPIP (un aceptor artificial de electrones) o de la ubiquinona-1 (análogo de la ubiquinona-9, presente en la poza de quinonas en *Euglena*). Se determinó que la oxidación de L-lactato era menos afín por la ubiquinona-1 que la de D-lactato. La velocidad máxima y la eficiencia catalítica fueron mayores para la oxidación de D-lactato. El efecto del oxamato y del oxalato, inhibidores clásicos de las iLDH, fue mayor cuando se utilizó D-lactato como substrato. La oxidación de D-lactato resultó ser estable hasta los 70°C mientras que la L-iLDH se inactivó a partir de los 50°C. Demostramos también que parámetros termodinámicos como el cambio de entropía ($\Delta S°$) y el cambio en la entalpía ($\Delta H°$) de la disociación del complejo enzima-sustrato fue de diferente signo cuando se usó D- o L-lactato como substrato. Sin embargo, el cambio en la energía libre de la reacción fue el mismo ($\Delta G°$). Estos datos indicaron que, igual que en las bacterias, las mitocondrias de *Euglena* tienen dos enzimas iLDH isómero-específicas (D-iLDH y L-iLDH). En el anexo que se encuentra al final de la tesis, se incluye el artículo que se publicó en los *Archives of Biochemistry and Biophysics* en 2001, como resultado de este trabajo. Además, se anexan dos problemas bioquímicos publicados en el *Boletín de Educación Bioquímica* en donde se explica a detalle los experimentos del efecto de la temperatura y de los inhibidores sobre la oxidación del D- y L-lactato, los cuales fueron importantes para determinar la existencia de las dos especies enzimáticas.

Los experimentos del efecto de la temperatura sobre la oxidación del D- y L-lactato en las mitocondrias aisladas de *Euglena*, mostraron que la desnaturalización de la D-iLDH involucró dos procesos:

$$E \leftrightarrow I \rightarrow D,$$

donde E es la enzima nativa, I es la enzima inactiva que puede revertir a E, y D es la enzima desnaturalizada irreversiblemente. Como se muestra en la figura 2 del artículo de los *Archives of Biochemistry and Biophysics* (2001), la exposición de las mitocondrias a temperaturas crecientes por arriba de 60°C, indujo una concomitante disminución en la actividad de la D-iLDH, lo que sugiere la inactivación de la enzima

(Fig. 1A). Sin embargo, si graficábamos las k_{inac} contra el inverso de la temperatura (gráfico de Arrhenius), se observaron dos pendientes que muestran dos eventos en la disminución de la actividad de la enzima (Fig. 1B). Estos datos sugirieron que para la D-iLDH, entre 45 y 75°C hay un paso de inactivación el cual es reversible (E ←→ I), esto se apoyó por el hecho de que cuando se calentaron las mitocondrias a 70°C y se midió la actividad de la D-iLDH los parámetros cinéticos no cambiaron (Fig. 4A del artículo de los *Archives of Biochemistry and Biophysics*, 2001). En la figura 1B se observa que, entre 80-90°C ocurre un cambio en la pendiente, lo que sugiere que a esta temperatura se lleva a cabo el paso de desnaturalización, el cual es irreversible (I → D). En cambio, cuando se incubaron a las mitocondrias a 70°C y se midió la actividad de L-iLDH 30°C, no hubo actividad, lo que sugiere que la desnaturalización de la L-iLDH involucra un solo proceso (Fig. 4A del artículo).

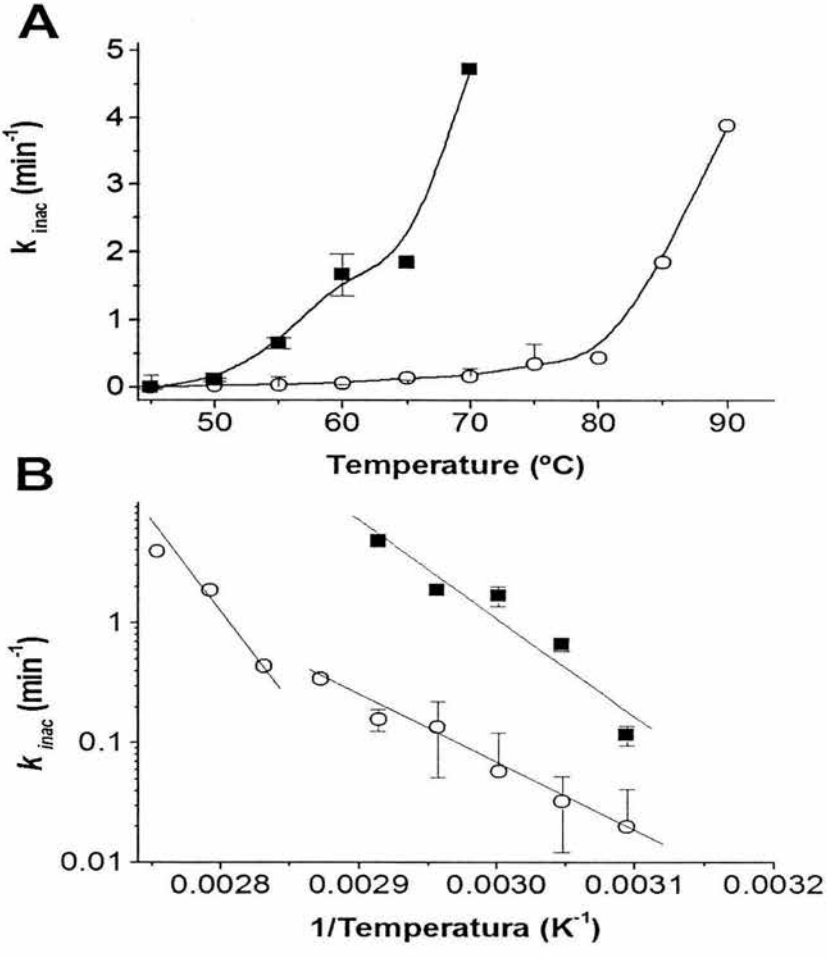

Figura 1. **Energía de desnaturalización de la iLDH mitocondrial de *Euglena*.** (A), las constantes de inactivación (k_{inac}) obtenidas para L-lactato (■) y para D-lactato (○) se graficaron contra la temperatura o (B), contra el inverso de la temperatura absoluta. Los datos muestran el promedio ± E. S. de 4 preparaciones distintas de mitocondrias.

3. Las deshidrogenas lácticas mitocondriales de *Euglena* reducen a quinonas de diferente potencial redox

Como se mencionó anteriormente, las iLDH de bacterias transfieren los electrones del lactato a la poza de quinonas, a diferencia de las levaduras que lo hacen directamente al citocromo *c*. En *Euglena* reportamos previamente que el consumo de oxígeno con D-lactato es mayor que con L-lactato pero la síntesis de ATP es igual (Moreno-Sánchez y cols., 2000). Este dato sugiere que los electrones provenientes del D-lactato siguen un camino alterno que no bombea protones (por ejemplo, la oxidasa alterna o el componente resistente a antimicina), aunque esto sólo puede explicarse si la D-iLDH y los componentes alternos de la cadena respiratoria tuvieran preferencia por uno de los dos tipos de quinonas presentes en las mitocondrias de *Euglena*: la ubiquinona-9 (Q9) y la rodoquinona-9 (RQ9). La RQ9 es una quinona con un grupo amino en vez del grupo metoxilo en la posición 2 del anillo, esta sustitución le confiere un potencial redox bajo (-65 mV). La rodoquinona es sustrato para la fumarato reductasa, una enzima muy importante para la obtención de energía en los organismos que viven en condiciones de baja tensión de oxígeno (Tielens y Van Hellemond, 1998). Aunque se ha reportado la actividad de esta enzima en *Euglena*, no se sabe si se expresa sólo en condiciones de anoxia. Sin embargo, la RQ9 se sintetiza en cantidades similares a la Q9 aún en condiciones aerobias (Castro-Guerrero y cols., 2004), por lo que probablemente, la RQ9 al formar parte de la poza de quinonas, podría también ser un sustrato para las iLDH. Así, se trató de establecer si había diferencias en las constantes cinéticas de la D- y la L-iLDH en la reducción de quinonas de alto potencial redox como la Q1, Q2 y DBQ (+100 mV) o de bajo potencial redox como la tetraclorohidroquinona (TCHQ, -8 mV) (Kim y cols., 2001). En estos experimentos no fue posible utilizar rodoquinona debido a que no está disponible comercialmente y su extracción y purificación de las membranas es complicado. En la tabla 1 se muestran los valores de los parámetros cinéticos de la reducción, de las ubiquinonas y de la TCHQ.

Tabla 1. **Parámetros cinéticos de la reducción de quinonas con diferente número de cadenas isoprenoides y distinto potencial redox por la D- y L-iLDH en mitocondrias de *Euglena***

		L-iLDH			D-iLDH *		
aceptor de ē	Potencial redox (mV)	K_m (μM)	V_m ^	V_m / K_m ^^	K_m (μM)	V_m	V_m / K_m
Q1	+ 100	41 ± 7	427 ± 35	10	19 ± 5	618 ± 71	33
Q2	+100	15 ± 2	184 ± 34	13	11 ± 2	304 ± 47	28
DBQ	+100	3.4 (2)	75	22	12 ± 2	232 ± 67	19
TCHQ	- 8	40 (2)	300	7.5	30 (2)	310	10.3
DCPIP	+ 117	35 ± 10	268 ± 31	8	35 ± 5	477 ± 44	14

Las cinéticas se realizaron a 30°C a pH de 7.6 y concentraciones saturantes de L-lactato y de D-lactato. La reducción de la Q1, Q2 y DBQ se midió por la disminución de la absorbancia a 273 nm y un coeficiente de extinción molar de 18 mM^{-1} cm^{-1}. La velocidad de reducción de la TCHQ se determinó polarográficamente midiendo el consumo de oxígeno (concentración inicial 200 μM de O_2). En este caso, las mitocondrias se incubaron a 25°C por 30 minutos con 0.5 mM ADP y 0.2% (p/v) BSA deslipidada para eliminar los sustratos endógenos. ^ para Q1, Q2 y DBQ, la V_m está en nmol de quinona reducida (min * mg prot)$^{-1}$, para TCHQ en nano átomos de oxígeno (min * mg prot)$^{-1}$. ^^ Para Q1, Q2, DBQ y DCPIP, la relación V_m / K_m está en min^{-1} * mg^{-1} * mL; y para TCHQ en nano átomos de oxígeno * min^{-1} * mL* $nmol^{-1}$. Los valores son el promedio ± ES de al menos 3 experimentos independientes, (n) es el número de experimentos. * Valores tomados de (Jasso-Chávez y cols, 2001) excepto para la TCHQ.

Las cinéticas de reducción de los diferentes aceptores de electrones mostraron que las eficiencias catalíticas (V_m / K_m) son mayores con la D-iLDH con respecto a la L-iLDH para las quinonas Q1 y Q2 (de potenciales redox similares al de la Q9). Conforme la hidrofobicidad de la quinona aumentó (DBQ>Q2>Q1), la actividad específica disminuyó en ambas enzimas, pero la K_m disminuyó para la L-iLDH, lo que

sugiere que el sitio catalítico de esta enzima se encuentra en un ambiente más hidrofóbico. Para la D-iLDH, la K_m por las diferentes quinonas se mantuvo en general, sin cambios (Tabla I). Sorprendente fue el hecho de que las iLDH pudieran reducir a la TCHQ (de un potencial redox similar al de la RQ9), ya que las únicas enzimas que se han reportado que tienen la capacidad de reducir quinonas de bajo potencial son las fumarato reductasa y en mucho menor grado, la succinato deshidrogenasa. Estos datos sugieren que en las mitocondrias de *Euglena* la D- y la L–iLDH podrían reducir a ambos tipos de quinonas (Q9 y RQ9) presentes en la cadena respiratoria; aunque tal vez con diferente afinidad y capacidad catalítica.

III

JUSTIFICACIÓN DEL PROYECTO

Uno de los puntos de más interés que surgió de los trabajos anteriores fue que en bacterias sólo una de las iLDH es constitutiva, mientras que la otra se induce sólo en presencia de su sustrato o de glucosa y en aerobiosis, mientras que en las levaduras la expresión de las dos iLDH está sujeta a la presencia de lactato y a la disponibilidad de oxígeno. Incluso, en bacterias, la síntesis de la iLDH es reprimida por metabolitos respiratorios como glutamato y succinato. Así, es sorprendente que las mitocondrias de *Euglena gracilis* hayan presentado las dos actividades de iLDH, aun cuando las células fueron cultivadas en fuentes de carbono como glutamato/malato. Una posible explicación a este comportamiento es que cuando la fuente de carbono externa en el que se cultiva a *Euglena* se ha terminado, las células degradan grandes cantidades de paramilo, el polisacárido de reserva constituido por unidades de glucosa que, a través de la glucólisis, produce el lactato necesario para estimular la síntesis de la D- y L-iLDH.

HIPÓTESIS

Como lactato es el mejor substrato oxidable para la síntesis de ATP en las mitocondrias aisladas de *E. gracilis*, cabe esperar que la D-iLDH y L-iLDH tengan una contribución esencial en proporcionar la energía necesaria para la duplicación celular y su expresión estará regulada por la disponibilidad del lactato externo o intracelular.

OBJETIVO GENERAL

Determinar la participación de la D-iLDH y L-iLDH mitocondriales de *Euglena* en el metabolismo energético.

Objetivos particulares:

1) Determinar la cinética de crecimiento de las células con diferentes fuentes de carbono.

2) Determinar la actividad de ambas iLDH en todas las condiciones de crecimiento.

3) Determinar las concentraciones intracelulares de D-lactato, L-lactato, ATP y piruvato; así como la desaparición de la fuente externa de carbono y la cantidad de paramilo a lo largo de la curva de crecimiento.

4) Determinar el efecto del oxalato (un inhibidor de ambas iLDH) sobre el crecimiento celular, la respiración basal y el contenido de ATP.

IV

MÉTODOS Y RESULTADOS

1. Métodos

La parte correspondiente a materiales y métodos se encuentra en el artículo de investigación, en la sección de los resultados.

1.1 Metodología complementaria. Determinación de metabolitos

Para la determinación de los metabolitos energéticamente importantes como ATP, piruvato, D-lactato y L-lactato, así como los de la fuente de carbono externa, se realizaron extractos ácidos de células cosechadas en las diferentes fases de crecimiento y se neutralizaron inmediatamente a un pH aproximado entre 7-8. La cuantificación de todos ellos se realizó espectrofluorométricamente, detectando la aparición (ATP, D-lactato, L-lactato, malato, glutamato y glucosa) o la desaparición (piruvato) de NADH o NADPH, los cuales fluorescen a una λ de excitación y emisión de 340 nm y 460 nm, respectivamente.

La determinación de ATP se llevó a cabo en 2 mL de una solución que contenía HEPES 100 mM, EGTA 1mM y Mg^{2+} 2mM a pH 7.4 (buffer HEM), acoplando la fosforilación de la glucosa (5mM) por la hexocinasa (1 UI), con el ATP presente en el extracto, con la oxidación de la glucosa-6-fosfato (G6P) por la G6P deshidrogenasa (1 UI) y la producción de NADPH:

Glucosa + ATP → ADP + G6P + NADP → gluconolactona + **NADPH**

En esta determinación se adicionó primero la G6P deshidrogenasa para oxidar a la G6P endógena y no se sobreestimara la cantidad de ATP presente (Figura 2).

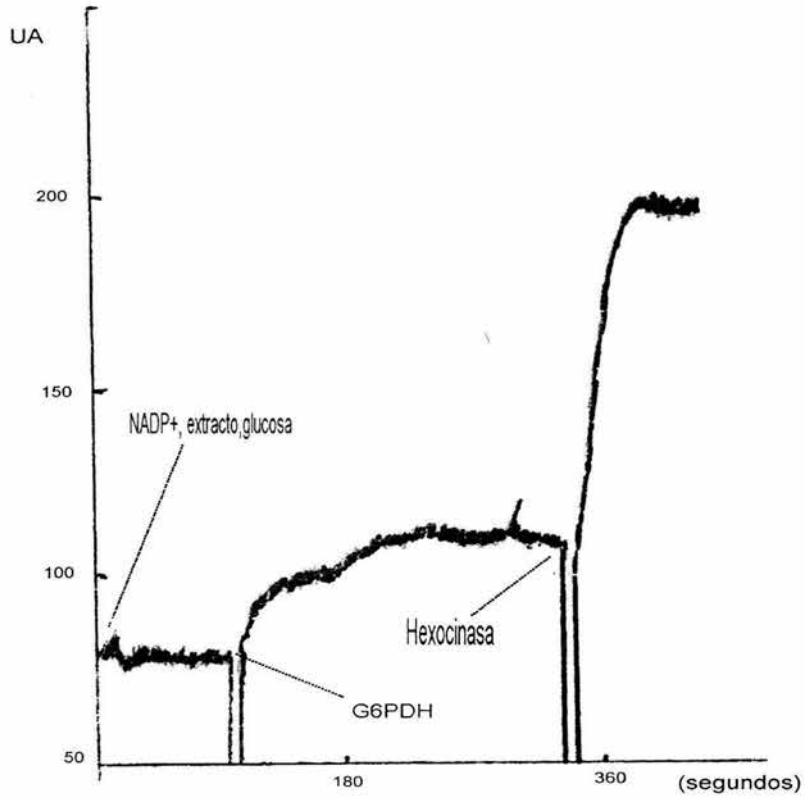

Figura 2. **Determinación espectrofluorométrica de ATP en extractos de *Euglena*.** En este caso, los extractos son de células cultivadas 72 horas en glu/mal. Este trazo corresponde a 7.5 nmol de ATP / 10^7 células. La adición de G6PDH (glucosa-6-fosfato deshidrogenasa) cuantifica la glucosa-6-fosfato del extracto. Así, la adición posterior de la hexocinasa determina la cantidad de ATP presente en el extracto. La caída en la señal de la fluorescencia se debe a la apertura de la puerta para cada nueva adición. UA, unidades arbitrarias de fluorescencia.

La cuantificación de piruvato se realizó en buffer HEM midiendo directamente la desaparición de NADH (0.6 mM) en presencia de los extractos celulares y de la

deshidrogenasa láctica de músculo de conejo comercial (0.5 UI) (Figura 3), de acuerdo con la reacción:

Piruvato + **NADH** → L-lactato + NAD^+

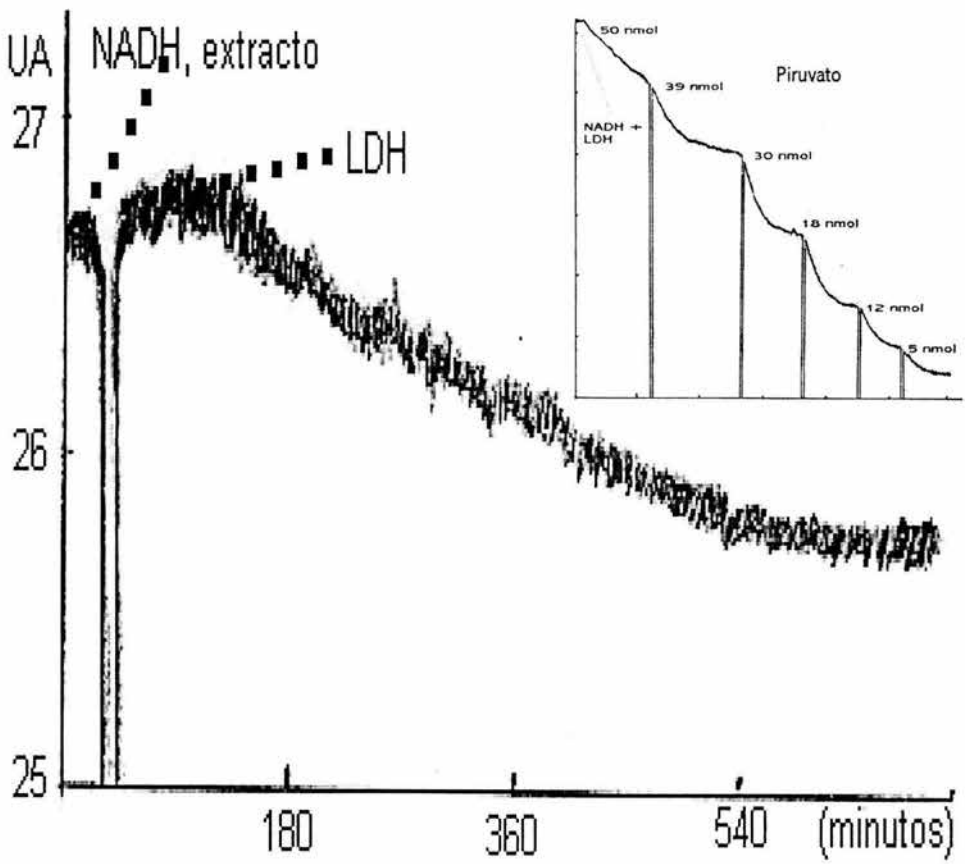

Figura 3. **Determinación espectrofluorométrica de piruvato en extractos de *Euglena*.** Extractos de células de 20 horas en un cultivo con glu/mal. Este trazo corresponde a 2.1 nmol de piruvato / 10^7 células. El recuadro muestra una curva de oxidación de NADH a diferentes adiciones de piruvato. Nótese que la disminución en la señal es efecto único de la presencia de piruvato. Ver pie de figura 2 para más detalles.

Para la cuantificación de lactato se utilizaron 2 mL de una solución que contenía NAD^+ (0.6 mM), glicina 400 mM e hidracina 500mM a pH 9 (Buffer HG) para asegurar que la reacción fuera unidireccional hacia la oxidación de lactato, ya que la hidracina forma un complejo con el piruvato (figura 4):

L-lactato + NAD^+ → Piruvato + **NADH** + H^+, (5 UI de L-lactato deshidrogenasa de músculo de conejo comercial) y

D-lactato + NAD^+ → Piruvato + **NADH** + H^+ (11 UI de D-lactato deshidrogenasa de *Lactobacillus leichmannii*)

La cuantificación de la glucosa se realizó con la misma reacción acoplada usada para cuantificar ATP, solo que en este caso se adicionó 2 mM ATP y se determinó la variación de la glucosa del medio durante el tiempo del cultivo. La cuantificación del malato se determinó en el mismo buffer usado para cuantificar lactato con malato deshidrogenasa comercial (10 UI) y NAD^+ (0.6 mM), midiendo la aparición de NADH:

Malato + NAD^+ → oxaloacetato + **NADH** + H^+

El glutamato se determinó en buffer HG pero la glicina se suplantó por Tris (ya que la glicina puede inhibir a la glutamato deshidrogenasa) y con la glutamato deshidrogenasa comercial (40 UI) y $NADP^+$ (0.6 mM) midiendo la aparición de NADPH. Para esta reacción fue necesaria la adición de ADP 5 mM, ya que es un activador de la enzima:

Glutamato + $NADP^+$ → 2-oxoglutarato + NH_4^+ + **NADPH** + H^+

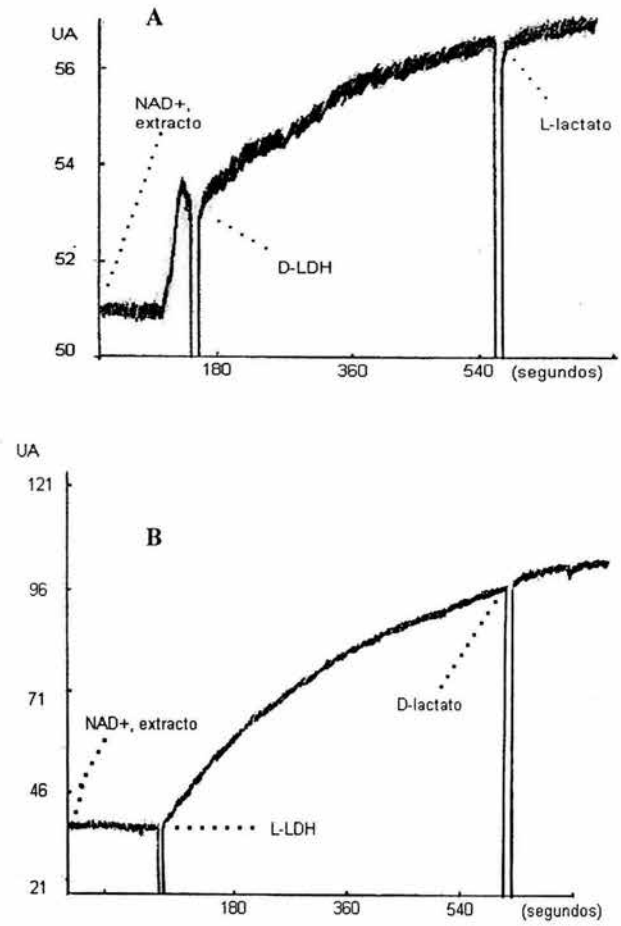

Figura 4. **Determinación espectrofluorométrica de D-lactato (A) y L-lactato (B) en extractos de *Euglena***. Extractos de células cultivadas durante 90 horas en glu/mal. A) el trazo corresponde a 21.3 nmol de D-lactato/ 10^7 células y el trazo B a 61 nmol de L-lactato / 10^7 células. Nótese que la adición de L-lactato en **A** y de D-lactato en **B**, no promueve un aumento en la fluorescencia (síntesis de NADH), lo que indica que cada LDH es específica para su propio sustrato. Ver pie de figura 2 para más detalles.

2. Resultados

2.1. La lanzadera de lactato de *Euglena*

La oxidación de lactato por las iLDH en las bacterias es muy importante ya que forma un gradiente de protones (Matsushita y Kaback, 1986) necesario para el transporte de carbohidratos y aminoácidos a través de la membrana citoplasmática (Kaback y Millner, 1970). En el caso de las levaduras, las iLDH se expresan sólo en aerobiosis y cuando la fuente de carbono externa es lactato. En este caso, debido a que las levaduras no expresan a la deshidrogenasa láctica dependiente de NAD^+, las iLDH son el único camino con el que cuenta la levadura para obtener energía (Somlo, 1965).

En el caso de *Euglena gracilis*, la oxidación del lactato no pareciera ser esencial para la obtención de energía, debido a la capacidad que tienen sus mitocondrias para oxidar una gran variedad de metabolitos, como glutamato/malato, NADH, succinato, succinato semialdehído, glicolato, glioxilato, etc. (Buetow, 1989; Uribe y Moreno-Sánchez, 1992). Sin embargo, el mayor consumo de oxígeno y la mayor velocidad de síntesis de ATP en mitocondrias aisladas, se logran utilizando al lactato como sustrato oxidable (Uribe y Moreno-Sánchez, 1992; Moreno-Sánchez y cols. 2000), probablemente por su incapacidad para oxidar al piruvato. Esta incapacidad se da por el hecho de que la enzima atípica que se encarga de oxidar al piruvato, la $NADP^+$-piruvato oxidorreductasa, se encuentra inactiva en nuestras condiciones de cultivo, ya que se inhibe fuertemente por oxígeno (Inui, y cols. 1985). Por esta razón, probablemente la célula reduce al piruvato para regenerar el NAD^+ utilizado en la glucólisis y produce lactato, que es oxidado por las iLDH, para así obtener un máximo provecho de los equivalentes reductores producidos en el citosol.

En el siguiente trabajo, publicado en el *European Journal of Biochemistry*, reportamos la importancia en *Euglena* de la D-iLDH y L-iLDH en el metabolismo energético y la existencia de un nuevo tipo de lanzadera de poder reductor (de lactato), la cual transfiere equivalentes reductores desde el citosol con la reducción del piruvato

por la lactato deshidrogenasa citosólica dependiente de NAD^+ (NAD^+-LDH) y la oxidación del lactato por ambas iLDH mitocondriales.

Eur. J. Biochem. **270**, 4942–4951 (2003) © FEBS 2003 doi:10.1046/j.1432-1033.2003.03896.x

Cytosol–mitochondria transfer of reducing equivalents by a lactate shuttle in heterotrophic *Euglena*

Ricardo Jasso-Chávez and Rafael Moreno-Sánchez

Departamento de Bioquímica, Instituto Nacional de Cardiología, Tlalpan, México D. F., México

To assess the expression and physiological role of the mitochondrial NAD^+-independent lactate dehydrogenase (iLDH) in *Euglena gracilis*, cells were grown with different carbon sources, and the D- and L-iLDH activities and several key metabolic intermediates were examined. iLDH activity was significant throughout the growth period, increasing by three- to fourfold from latency to the stationary phase. Intracellular levels of D- and L-lactate were high (5–40 mM) from the start of the culture and increased (20–80 mM) when the stationary phase was entered. All external carbon sources were actively consumed, reaching a minimum upon entering the stationary phase, when degradation of paramylon started. The level of ATP was essentially unchanged under all experimental conditions. Oxalate, an inhibitor of iLDH, strongly inhibited oligomycin-sensitive respiration and growth, whereas rotenone, an inhibitor of respiratory complex I, only slightly affected these parameters in lactate-grown cells. Isolated mitochondria exhibited external NADH-supported respiration, which was sensitive to rotenone and flavone, and an inability to oxidize pyruvate. Addition of cytosol, NADH and pyruvate to mitochondria incubated with rotenone and flavone prompted significant O_2 uptake, which was blocked by oxalate. The data suggested that iLDH expression in *Euglena* is independent of substrate availability and that iLDHs play a key role in the transfer of reducing equivalents from the cytosol to the respiratory chain (lactate shuttle).

Keywords: energy metabolism; lactate metabolism; NAD^+-lactate dehydrogenase; NAD^+-independent lactate dehydrogenase.

The respiratory chain of mitochondria isolated from heterotrophic *Euglena* exhibits several unusual characteristics. It has a cyanide-insensitive alternative oxidase and an antimycin-insensitive, myxothiazol-sensitive, quinol-cytochrome *c* oxidoreductase [1]. It also contains active membrane-bound NAD^+-independent D- and L-lactate dehydrogenases (D- and L-iLDH) that directly transfer electrons to the quinone pool [2]. Similar enzymes that contain FAD or FMN as prosthetic groups have also been described in bacterial respiratory chains [3]. In addition, the quinone pool in *Euglena* mitochondria has equal concentrations of ubiquinone-9 and rhodoquinone-9 [4], which is a low redox-potential quinone also found in purple bacteria [5].

We described recently that mitochondria, isolated from *Euglena* cultured with glutamate/malate (glu/mal) as the carbon source and harvested in the early stationary growth phase, exhibited stereospecific D- and L-iLDH activities [2]. Both enzymes were able to reduce the artificial high redox-potential ubiquinones-1 and -2; D-iLDH showed a higher catalytic efficiency than L-iLDH, a pattern also observed in bacterial systems [6]. It was remarkable that *Euglena* mitochondria showed both enzyme activities because cells were grown with a carbon source different from DL-lactate or glucose. In other systems, only one of these enzymes is constitutive. In bacteria, the inducible enzyme is expressed in the presence of glucose or D- or L-lactate [7,8], and repressed in the presence of the respiratory metabolites succinate or glutamate [8–10]. In yeast, iLDH is expressed in aerobiosis and repressed by anaerobiosis [11]. Exceptions to this general behavior in bacterial systems are *Neisseria meningitidis* and *N. gonorrhoeae*, which constitutively express both enzymes [6,12].

The highest rates of electron transport and ATP synthesis in *Euglena* mitochondria are achieved with D- and L-lactate as oxidizable substrates [1,13]. Pyruvate cannot be oxidized under aerobiosis, as these mitochondria lack the pyruvate dehydrogenase complex [4] and the pyruvate/$NADP^+$ oxidoreductase is inactivated by O_2 [14]. In consequence, to obtain a maximal benefit from glycolytic intermediates, cytosolic lactate oxidation could proceed through the mitochondrial iLDH. Therefore, to elucidate the participation of iLDH in the energy metabolism of heterotrophic *Euglena*, cells were grown with different carbon sources, such as glu/mal, DL-lactate, or D-glucose. The variation in concentrations of several relevant metabolites (D-lactate, L-lactate, pyruvate, paramylon, ATP) and carbon sources was determined. The respiratory rates and the activities of the iLDHs were also measured at all the different growth stages in an attempt to establish whether the oxidation of lactate supports the cellular supply of ATP.

Correspondence to R. Jasso Chávez, Departamento de Bioquímica, Instituto Nacional de Cardiología, Juan Badiano No. 1, Col. Sección XVI, Tlalpan, México D. F. 14080, México.
Fax: + 52 555 573 0926, Tel.: + 52 555 573 2911,
E-mail: rjassoch@aol.com

Abbreviations: COX, cytochrome *c* oxidase; glu/mal, glutamate/malate; iLDH, independent lactate dehydrogenase; LDH, lactate dehydrogenase.

(Received 15 September 2003, revised 15 October 2003, accepted 23 October 2003)

Materials and methods

Materials

D-glucose, 2,6-dichloroindophenol, L-lactate, D-lactate, pyruvate, *N,N,N′,N′*-tetramethylphenylenediamine, stigmatellin, SDS, phenylmethanesulfonyl fluoride, carbonyl cyanide *m*-chlorophenylhydrazone, safranine O, 1-bromododecane, rotenone, flavone, and BSA were from Sigma. $[^3H]H_2O$ and ^3H-labeled inulin were from New England Nuclear. NAD^+, NADH, hexokinase, NAD^+-malate dehydrogenase, NAD^+-glutamate dehydrogenase, $NADP^+$-glucose-6-phosphate dehydrogenase, and NAD^+-L-LDH were from Boheringer. NAD^+-D-LDH was from Roche.

Cell culture and isolation of cellular fractions

Culture of *E. gracilis* strain Z with 33 mM glutamate + 17 mM malate (glu/mal), 33 mM DL-lactate [15] or 75 mM glucose as the carbon source, and preparation of mitochondria, were carried out as described previously [2]. The cell number was determined by counting in a hemocytometer. Mitochondrial yields from 1 L cultures with glu/mal or lactate media were 50–70 or 30–40 mg of protein, respectively.

Isolation of the cytosolic fraction was carried out using the postmitochondrial supernatant (usually 70 mL), which was centrifuged for 45 min at 225 000 *g*. The resulting supernatant was concentrated in an Amicon ultrafiltration cell, using a YM30 ultrafiltration membrane from Millipore. The concentrated fraction, containing ≈ 250 mg of protein in 15–18 mL of 120 mM sucrose, 10 mM Hepes and 1 mM EGTA, pH 7.4 (SHE buffer), plus 10% (v/v) glycerol, was stored at −72 °C until use. All steps were performed at 4 °C and in the presence of 1 mM phenylmethanesulfonyl fluoride, a serine-threonine protease inhibitor.

Enzyme assays

The cytochrome *c* oxidase and the L- and D-iLDH activities were measured at 30 °C, as reported previously [2]. When cytochrome *c* oxidase activity was determined *in vivo*, the cells were incubated in 120 mM KCl, 20 mM Mops, 1 mM EGTA, pH 7.2 (KME buffer), with 10 μM stigmatellin, for 10 min. Then, the reaction was started with 2 mM *N,N,N′,N′*-tetramethylphenylenediamine and stopped, 1–3 min later, by the addition of 20 mM azide. NAD^+-LDH activity was measured at room temperature using a standard assay [16].

Intracellular volume determinations

The distribution of $[^3H]$-H_2O and ^3H-labeled inulin across the plasma membrane was used to determine the intracellular water volume [17]. Cells (1×10^7), cultured with different carbon sources and harvested at different times of culture, were washed once in SHE buffer. Cells were then incubated at 25 °C in SHE buffer with either 15 μL of $[^3H]H_2O$ (specific activity 13 300 c.p.m.·mL^{-1}) or 0.3 mg of ^3H-labeled inulin (specific activity 660–700 c.p.m.·μg^{-1}). After 30 s, the incubation mixture was poured into a 1.5 mL microfuge tube that contained, from the bottom, 0.3 mL of 30% (v/v) perchloric acid, 0.3 mL of 1-bromododecane ($\delta = 1.04$ g·mL^{-1}) and 0.3 mL of SHE buffer. The reaction was stopped by centrifugation at 14 000 *g* for 2 min at 4 °C. The radioactivity of both top and bottom layers was determined in a liquid scintillation counter. The internal water volume was calculated according to the formulations proposed by Rottenberg [18].

Mitochondrial respiration and membrane potential

Oxygen uptake was measured using a Clark-type O_2 electrode in mitochondria (1 mg of protein) incubated in air-saturated KME buffer. Rate values were determined using an oxygen solubility of 420 ng of atoms per mL (210 μM O_2) at 2240 m altitude and 25 °C. The membrane potential was determined in mitochondrial suspensions (0.5–1 mg of protein) incubated at 25 °C in 2 mL of KME buffer plus 5 μM safranine O and 5 mM potassium phosphate. The fluorescent signal of the dye was measured at 586 nm, with the excitation wavelength set at 495 nm [19].

Cellular break and metabolite extraction

A 0.9 mL suspension containing ≈ 1×10^8 washed cells, which were harvested by centrifugation at different culture time-points, was mixed with 0.1 mL of ice-cold 30% (v/v) perchloric acid containing 20 mM EGTA, and stirred vigorously for 1 min. Samples were centrifuged at 1250 *g* for 2 min. The supernatant was neutralized with 3 M KOH/0.05 M Tris, centrifuged again at 1250 *g* for 2 min, and the new supernatant was frozen immediately at −72 °C until use.

Metabolite determination

L-lactate, pyruvate, ATP, L-malate, glutamate, and D-glucose were determined fluorometrically at 30 °C according to standard methods [16]. For D-lactate determination, a large amount of NAD^+-dependent D-LDH (11 units) and a relatively long time of reaction (30 min) were used in the assay, to ensure complete transformation of D-lactate. In a previous report [1], 1 U of NAD^+-dependent D-LDH and a short incubation (< 10 min) were used, which led to an underestimation of cellular D-lactate. For glutamate, 70 U of glutamate dehydrogenase was used. The content of cytochromes $a+a_3$, b, and $c+c_1$ was determined as described previously [20].

Paramylon was determined spectrophotometrically as described by Ono *et al.* [21], with some modifications. Cells were mixed with perchloric acid, as described above; after centrifugation, the pellet was mixed with 1 mL of 1% SDS and stirred until homogenization. The mixture was incubated in a boiling waterbath for 15 min and samples were centrifuged at 1800 *g* for 15 min. The pellet was resuspended with 1 mL of 0.1% SDS and centrifuged again. The washed pellet was resuspended and hydrolyzed in 1 mL of 1 M NaOH and frozen immediately at −72 °C. Because hydrolysis of paramylon produces high quantities of D-glucose, the sensitive enzymatic method was replaced with a colorimetric assay, which yielded reliable results under these conditions [21].

Effect of respiratory inhibitors on O_2 uptake in whole cells

The rate of oxygen consumption in whole cells, harvested at different phases of growth, was measured polarographically by using a Clark-type O_2 electrode under the same culture conditions (25 °C and air-saturated cell-free culture medium obtained from each phase of growth). As pH values and other unknown factors in the culture medium changed throughout the growth period, we decided to use the same culture medium for respiratory rate measurements at each phase of culture, to maintain a more strict correlation with the growth rate, cell density and viability. In the glu/mal medium, pH values were 3.5 ± 0.1, 3.5 ± 0.09 and 6.1 ± 0.1 for 20, 44, and 93 h of culture, respectively. In the lactate medium, pH values were 3.9 ± 0.1, 3.5 ± 0.1, and 7.1 ± 0.3 for the same culture time-points (mean ± SE, $n = 4$).

The protein content in mitochondria was determined using the Biuret method with BSA as standard, as previously described [1,2].

Results

Growth

Euglena cells cultured in the dark showed a faster rate of duplication and reached a higher density in the stationary phase (phase III) when cultured with glu/mal than with lactate [22] or glucose [23] (Fig. 1). The cell density attained with lactate or glucose was similar, although with glucose, the latency period (phase I) lasted longer. Cell viability was always > 95% under all culture conditions.

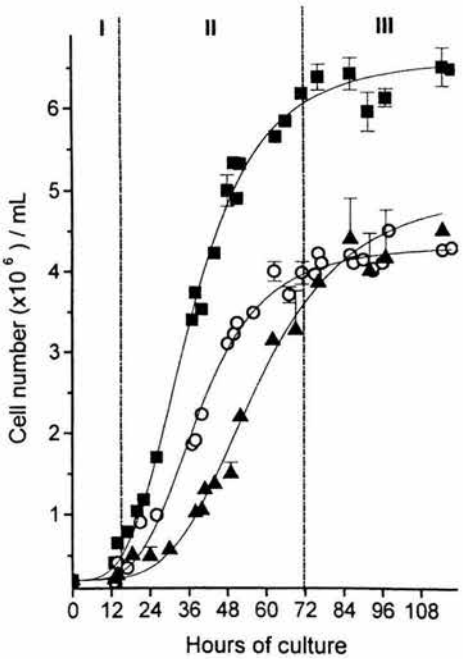

Fig. 1. Growth of *Euglena gracilis*. The initial inoculum was 0.2×10^6 cells·mL^{-1} for all culture conditions. Carbon sources were glutamate/malate (glu/mal) (■), DL-lactate (○), or glucose (▲). Roman numerals represent the different phases of growth: I, latency (0–15 h); II, exponential (15–72 h); and III, stationary (72–114 h). Values represent the mean ± SEM of at least five different cultures.

iLDH and cytochrome *c* oxidase (COX)

Mitochondria isolated from cells harvested at different culture time-points showed significant L- and D-iLDH activities throughout the growth period, even during phase I (Fig. 2). D-iLDH activity was higher than L-iLDH at all phases of growth. Surprisingly, the higher activities were attained in the glu/mal medium, whereas the lowest rates were observed with glucose. Oxidation of glucose for ATP generation may form lactate, but oxidation of glutamate and malate does not directly lead to formation of the iLDH substrates. All mitochondrial preparations were able to generate a significant uncoupler-sensitive membrane potential, as judged by the change in the safranine fluorescent signal (data not shown). They exhibited respiratory control values (rate of respiration with ADP/rate of respiration without ADP) of 1.4–1.9, with L-lactate as an oxidizable substrate, and a respiratory stimulation by the uncoupler carbonyl cyanide *m*-chlorophenylhydrazone of 35–95%. These observations indicated preservation of the membrane intactness in at least a fraction of organelles.

The increase in iLDH activity observed with progression of cell growth (Fig. 2) might be related to an increase in the cellular content of mitochondria or to a specific enhancement of iLDH. To distinguish between these two possibilities, the level of COX, a mitochondrial inner membrane enzyme, was determined in intact cells throughout the growth period (Table 1). Determination of the COX activity in isolated mitochondria yielded less reliable results, probably owing to a loss of cytochrome *c* during the sonication step in the isolation procedure. After an initial burst in COX activity when cells initiated phase II of growth, this mitochondrial activity (the concentration of COX) remained constant in lactate and glucose media; in glu/mal medium, COX activity stabilized after reaching phase III. In consequence, the iLDH/COX ratio increased in the three culture media, from 0.4 to 0.5 in phase I, to 0.8–2.0 in phase III. Determination of the cytochrome $a + a_3$ content in isolated mitochondria from cells grown in lactate medium also showed a significant increase ($P < 0.025$) from phase I (47 ± 13 pmol·mg^{-1} of protein; $n = 3$) to phase II (70 ± 10 pmol·mg^{-1} of protein; $n = 10$) and III (89 ± 18 pmol·mg^{-1} of protein; $n = 4$). Therefore, these data may be interpreted in terms of an enhancement in both iLDH activities with the progression of growth in the three culture media (Table 1).

L- and D-lactate

The presence of very active iLDH suggested that the intracellular concentration of D- and L-lactate might be

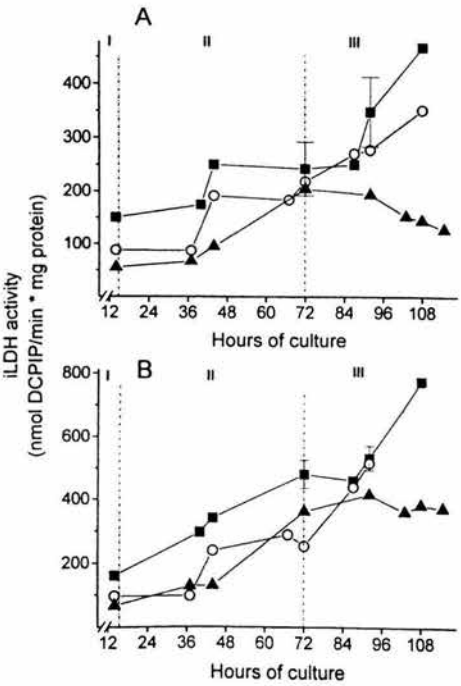

Fig. 2. L- and D-NAD$^+$ independent lactate dehydrogenase (iLDH) activities. (A) L-iLDH. (B) D-iLDH. Freshly prepared mitochondria (0.05 mg of protein·mL^{-1}), isolated from cells cultured with glutamate/malate (glu/mal) (■), DL-lactate (○), or glucose (▲), were incubated as described in the Materials and methods. The reaction was started by addition of 30 mM L- or D-lactate. Values represent the mean ± SEM of at least three different preparations. See the legend to Fig. 1 for other experimental details.

maintained at a low level throughout the growth curve as a consequence of the high enzyme content. To estimate the concentration of these and other metabolites, the intracellular water volume was determined at different time-points of culture. There was a significant decrease ($P < 0.005$) in the cell volume (given as μL per 10^7 cells) from phase II (1.4 ± 0.2; $n = 9$) to phase III (0.7 ± 0.1; $n = 4$) with glucose; in contrast, with glu/mal (2 ± 0.2; $n = 13$) and lactate (1.86 ± 0.16; $n = 8$), it remained constant.

Unexpectedly, the concentrations of D- and L-lactate were high and sufficient to maintain high rates of iLDH (Fig. 3). A minimal concentration was reached by the time of transition between phase II and III; the initiation of the stationary phase induced a significant elevation in the concentration of L-lactate with the three carbon sources, and of D-lactate with glucose. Under all culture conditions and culture time-points, the intracellular concentration of L-lactate was always higher than that of D-lactate, except for the initial 15 h of culture with DL-lactate (Fig. 3).

Table 1. *N,N,N′,N′*-tetramethylphenylenediamine oxidase activities in whole *Euglena* cells. Cells (0.2–0.5 × 10^6) were incubated in SHE buffer (120 mM sucrose, 10 mM Hepes, 1 mM EGTA, pH 7.4) with 10 μM stigmatellin for 10 min, and the reaction was started by the addition of 2 mM *N,N,N′,N′*-tetramethylphenylenediamine, as described in the Materials and methods. Addition of ascorbate did not increase the *N,N,N′,N′*-tetramethylphenylenediamine oxidase activity, probably owing to a low cellular permeability. The data shown represent the mean ± SEM, with the number of preparations assayed shown in parenthesis.

Hours in culture	Nanogram atoms of oxygen per min per 10^7 cells		
	Glu/mal medium	Lactate medium	Glucose medium
20 ± 2	263 ± 53 (5)[a,b]	223 ± 24 (7)	115 ± 21 (4)[a]
43 ± 3	282 ± 58 (4)	200 ± 26 (6)	168 ± 25 (5)
72 ± 2	532 ± 48 (3)[b,c]	296 ± 61 (4)[c]	216 (2)
92 ± 3	546 ± 38 (5)[d,e]	205 ± 41 (6)[d]	130 ± 24 (4)[e]
115	568 (2)	290 (2)	190 (2)

Significant differences were found for values with the same superscript letter. [a,c] $P = 0.05$; [b] $P = 0.025$; [d,e] $P < 0.005$.

Paramylon, carbon sources and ATP

The content in cells of paramylon, a linear polymer of glucose with β1–3 glycosidic bonds and the *Euglena* main fuel storage [24], varied with the progression of growth, reaching a maximum around the time of transition from phase II to phase III (Fig. 4A). The paramylon content was two to three times lower in cells cultured with glu/mal than with lactate or glucose, as expected from the respective metabolic routes of transformation. A net degradation of paramylon commenced with the start of the stationary phase in the three culture media.

Exhaustion of both external D- and L-lactate correlated with the start of the stationary phase (Fig. 4B). Arrival at the stationary phase in the glu/mal medium also coincided with limitation of L-malate (< 2 mM). With glucose, net cell growth stopped when the concentration fell to < 30 mM; culture media with initial glucose concentrations of ≤ 25 mM were also unable to support growth (data not shown).

The intracellular ATP concentrations were maintained at an approximately constant level throughout the growth period in the three culture media. In glu/mal and lactate media, the ATP concentrations were 1.0, 1.4–1.7 and 0.6 mM in phases I, II and III, respectively. In glucose medium, the ATP level varied between 1.5 and 1.9 mM during the growth period.

Effect of oxalate on growth and respiration

To assess whether iLDH activities were essential for supplying reducing equivalents to the respiratory chain for ATP synthesis, cells were cultured in the presence of 20 mM oxalate, which is a potent inhibitor of D- and L-iLDH [2]. In the glu/mal medium, oxalate added at the beginning of the culture did not alter the growth rate; when added after 50 h of culture, oxalate exerted a small, but significant, inhibition of the cell growth (Fig. 5A). In contrast, in the lactate medium, oxalate markedly affected cell growth (Fig. 5B).

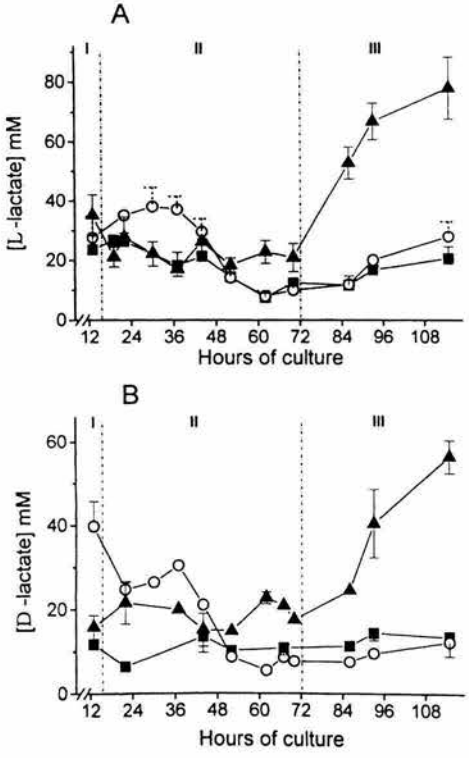

Fig. 3. Intracellular concentrations of L-lactate and D-lactate in *Euglena*. (A) [L-lactate]. (B) [D-lactate]. Cultures with glutamate/malate (glu/mal) (■), DL-lactate (○), or glucose (▲). See the text for values of intracellular water volumes. See the legend to Fig. 1 for other experimental details. Values represent the mean ± SEM of at least three different preparations.

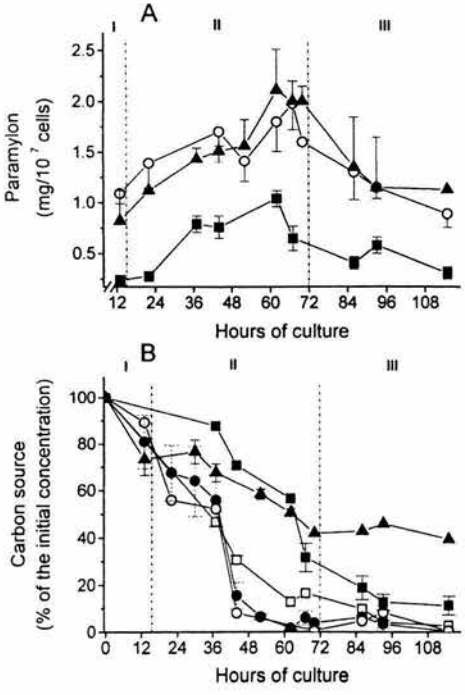

Fig. 4. Changes in paramylon and carbon sources in *Euglena*. (A) Paramylon from cells cultured with glutamate/malate (glu/mal) (■), DL-lactate (○), or glucose (▲). (B) Carbon source. Initial concentrations of carbon source were 35 mM glutamate (■), 17 mM malate (□), 23 mM L-lactate (●), 11 mM D-lactate (○), and 75 mM glucose (▲). The rate of disappearance of the external carbon sources at the start of culture was faster for glucose (15 mM·day^{-1}) and slower for L-malate (6.6 mM·day^{-1}), L-lactate (4.9 mM·day^{-1}), D-lactate (3.1 mM·day^{-1}), and glutamate (2.3 mM·day^{-1}). Values represent the mean ± SEM of three different preparations.

The rate of endogenous respiration of glu/mal-grown cells was higher than that of lactate-grown cells throughout the growth period (Fig. 6, insets). Azide-sensitive O_2 uptake accounted for 90–100% of total respiration in both culture conditions, whereas oligomycin, an inhibitor of the ATP synthase, induced 70–80% inhibition of total respiration (Fig. 6). Thus, cellular respiration in heterotrophic *Euglena* was almost exclusively of mitochondrial origin and associated with oxidative phosphorylation.

In turn, rotenone, an inhibitor of respiratory complex I, blocked respiration as effectively as oligomycin in glu/mal-grown cells (Fig. 6A), except for a significantly lower potency in the stationary phase. Oxalate exerted a small effect on respiration in the two initial growth phases, but showed a high inhibitory effect, similar to that of oligomycin, in the stationary phase. In contrast, in lactate-grown cells, rotenone exhibited a diminished inhibition on respiration, whereas oxalate exerted a stronger inhibition in the latency and logarithmic phases (Fig. 6B). These data suggested a lower contribution of complex I to electron flux, which was compensated for by an increased contribution of iLDHs.

In agreement with the cellular respiration data, oxalate produced a marked reduction in the ATP levels in the three growth phases of the lactate-grown cells as well as in the logarithmic and stationary phases of glu/mal-grown cells (Table 2).

Cytosol-dependent pyruvate oxidation in *Euglena* mitochondria

The high rate of oxidative phosphorylation attained with lactate in mitochondria isolated from *Euglena* [1,13] suggested that this substrate might provide a direct link between glycolysis and the respiratory chain, for an efficient energy supply. The metabolic link might be mediated by the cytosolic NAD^+-LDH (by reducing pyruvate to generate

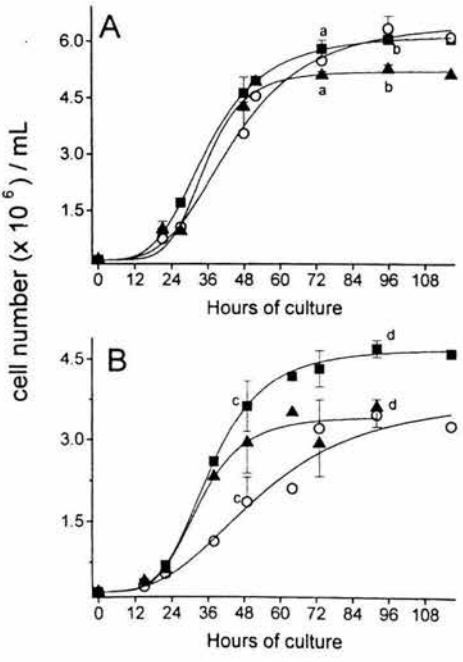

Fig. 5. Effect of oxalate on *Euglena* growth. Cells were cultured in glutamate/malate (glu/mal) (A) or lactate medium (B), with no further additions (■), or with 20 mM oxalate added at the start of culture (○) or after 52 h in glu/mal grown cells (A, ▲) or 38 h in lactate grown cells (B, ▲). Data represent the mean ± SEM of three different cultures. $^{a,b}P < 0.05$, Student's *t*-test for nonpaired samples; $^{c}P < 0.025$; $^{d}P < 0.01$.

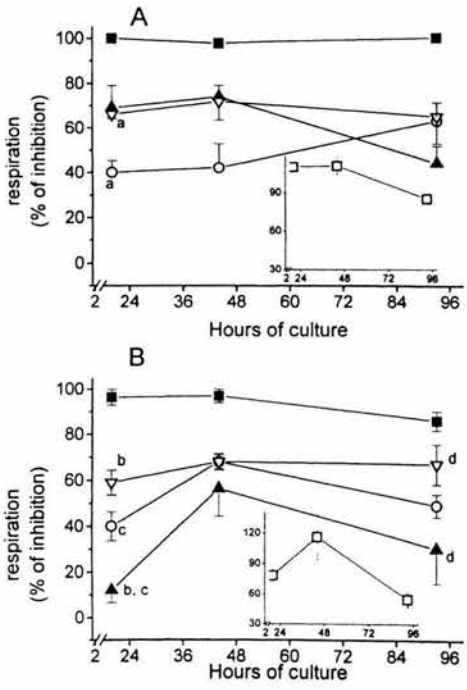

Fig. 6. Cellular respiration of *Euglena*. Cells (3–6 × 10^6), harvested from glutamate/malate (glu/mal) (A) or lactate media (B) by centrifugation and resuspended without washing, were incubated in the same air-saturated, cell-free culture medium at 25 °C for 15–20 min in the presence of 20 mM azide (■), 20 mM oxalate (○), 10 μM rotenone (△) or 30 μM oligomycin (▲). The rate of respiration was measured as indicated in the Materials and methods. Inset *y*-axis: basal respiration, without inhibitors, in nanogram atoms of oxygen per min per 10^7 cells. Values represent the mean ± SEM of three different cultures. $^{a,c,d}P < 0.025$; $^{b}P < 0.005$.

lactate) and the mitochondrial iLDH. To test this hypothesis, the oxidation of pyruvate by mitochondria in a cytosol-dependent reaction was assayed (Table 3).

Oxidation of D- and L-lactate was completely blocked by oxalate, whereas oxidation of external NADH [13] was fully inhibited by rotenone plus flavone (an inhibitor of external, rotenone-insensitive NADH dehydrogenases [25]). *Euglena* mitochondria were unable to oxidize added pyruvate (Table 3), in agreement with previous reports [4,14,26]. However, in the presence of a concentrated cytosolic fraction, mitochondria isolated from cells grown in glu/mal medium exhibited an active oxidation of pyruvate. This pyruvate oxidation was insensitive to rotenone and flavone, but was NADH dependent and sensitive to oxalate (Table 3); an identical result was attained when NADH and the cytosolic fraction were added to mitochondria previously inhibited by rotenone and flavone, and pyruvate was added last (data not shown). Substitution of the *Euglena* cytosolic fraction with commercial NAD^+-LDH from rabbit skeletal muscle also resulted in the activation of pyruvate oxidation. Addition of oxalate prior to NADH or pyruvate abolished the cytosol-dependent oxidation of pyruvate (not shown). These observations suggested that NAD^+-LDH was the specific protein component from the cytosol required to reconstitute pyruvate oxidation by *Euglena* mitochondria.

Discussion

Control of growth by the carbon source

The faster rate of cell duplication and higher cell density reached in the stationary phase with glu/mal suggested a more efficient oxidation of these two mitochondrial substrates and a comparable, lower, rate of oxidation of glycolytic substrates (Fig. 1), i.e. glycolysis limits growth in heterotrophic *Euglena*. With DL-lactate as the carbon source, glycolysis was bypassed and the growth rate was accelerated, but it was still slower than with glu/mal. These observations may also derive from (a) a faster delivery of reducing equivalents to the respiratory chain by the Krebs cycle enzymes than by iLDH, (b) a low availability of

Table 2. ATP and lactate levels in *Euglena*. Values represent nmol of ATP or L-lactate per 10^7 cells. Cells, harvested at the indicated time-points of culture and from the media shown, were incubated with no inhibitors, or with 20 mM oxalate or 30 μM oligomycin, for 15–20 min at 25 °C with orbital shaking. Then, the cell suspension was mixed with 3% perchloric acid. The metabolites were determined as described in the Materials and methods. The data shown represent the mean ± SEM, with the number of preparations indicated in parenthesis.

	Glu/mal medium		Lactate medium	
	ATP	L-lactate	ATP	L-lactate
18 h of culture				
Control	0.74 ± 0.10 (3)[a]	23.3 (2)	1.68 ± 0.30 (3)[a,b]	160 (2)
+ oxalate	1.01 ± 0.15 (3)	32 (2)	0.70 ± 0.08 (3)[b]	156 (2)
+ oligomycin	0.42 (2)	21 (2)	0.91 (2)	164
43 h of culture				
Control	0.54 ± 0.20 (3)	16 (2)	0.44 ± 0.03 (3)[c,d]	106 (2)
+ oxalate	0.22 ± 0.13 (3)	17 (2)	0.18 ± 0.09 (3)[c]	131 (2)
+ oligomycin	0.30 ± 0.16 (3)	14 (2)	0.11 ± 0.06 (3)[d]	102 (2)
92 h of culture				
Control	0.46 ± 0.14 (3)	7.9 (2)	0.70 ± 0.10 (3)	82 (2)
+ oxalate	0.33 (2)	10 (2)	0.46 ± 0.12 (3)	92 (2)
+ oligomycin	0.13 ± 0.07 (3)	8.6 (2)	0.26 ± 0.14 (3)	83

[a,b,c] $P < 0.05$; [d] $P < 0.01$.

Table 3. Cytosol-dependent pyruvate oxidation in *Euglena* mitochondria. Mitochondria (1 mg of protein), isolated from cells grown for 96 h in glutamate/malate (glu/mal) medium, were added to 1.5 mL of KME buffer (120 mM KCl, 20 mM Mops, 1 mM EGTA, pH 7.2) at 25 °C. The rate of respiration was determined in the presence of the indicated additions, as described in the Materials and methods. Oxalate was added after the oxidizable substrate. Additions: 4 mM L-lactate or D-lactate, 1 mM NADH, 4 mM pyruvate (Pyr), cytosolic fraction [170 mU NAD^+-lactate dehydrogenase (LDH)], commercial NAD^+-LDH (≈170 mU), rotenone (Rot), flavone (Flav). Data shown represent the mean ± SEM, with the number of experiments indicated in parenthesis.

	O_2 uptake rate (nanogram atoms of oxygen $min \cdot mg^{-1}$ of protein)
L-lactate	68.5 ± 13 (4)
+ 3 mM oxalate	10 ± 7
D-lactate	259 ± 31 (4)
+ 3 mM oxalate	5 ± 4
NADH	180 (2)
+ 3 mM oxalate	170
NADH	171 ± 26 (4)
+ 7 μM rotenone	6 ± 5
NADH	230 (2)
+ 50 μM flavone	16
Pyruvate	3.7 ± 2.7 (4)
No substrate added	11 ± 4 (3)
Rot + Flav + NADH + cytosolic fraction + Pyr	90 ± 9 (4)
+ 3 mM oxalate	5 ± 3
Rot + Flav + NADH + (commercial NAD ± LDH) + Pyr	123 (1)
+ 3 mM oxalate	2

organic nitrogen (and carbon) or (c) a diminution of the anaplerotic reactions of the Krebs cycle with lactate as the carbon source.

The lower capacity of *Euglena* to grow with carbohydrates as the carbon source has been previously described [24]. The slower growth in the glucose medium might involve a glucose transporter with a low affinity for glucose and probably with a strong product inhibition, together with a small transporter content, as glucose concentrations lower than 30 mM were unable to support cell growth. Other groups have also reported a similar growth requirement for high concentrations of glucose in *Euglena* [27–29].

In agreement with previous reports [21,23,30], it was observed that the degradation of paramylon in *Euglena* started upon arrival at the stationary growth phase, when the external carbon source was exhausted. The concomitant elevation in the concentration of both lactate isomers could probably proceed from paramylon, through the glycolytic pathway, which is functional in *Euglena* extracts [31] (also see below). The content of paramylon was lower in cells with a higher rate of growth (glu/mal-grown cells), and three- to fourfold higher in cells with lower growth rates (lactate- and glucose-grown cells). Thus, the carbohydrate storage in heterotrophic *Euglena* seemed to depend inversely on the ability of cells to duplicate. Recycling of stored carbohydrates is also apparently essential for growth in *Mycobacterium smegmatis* [32].

Expression of iLDH

In contrast to bacteria and yeast, significant activities of both D- and L-iLDH were detected in *Euglena* grown in the absence of lactate or glucose as an external carbon source [7,8,11]. In *Escherichia coli*, the induction of L-iLDH is highly sensitive to modulation by the carbon source in the culture medium [33]. In this work, it was found that *Euglena* mitochondria showed an increase in D- and L-iLDH activities throughout the growth period, and under all experimental conditions, despite the presence of saturating intracellular concentrations of D- and L-lactate. These data indicated that, in contrast to bacteria, the expression of iLDH in *Euglena* is not dependent on substrate availability.

Aerobiosis might be the condition that regulates mitocondrial iLDH expression, as observed in yeast [11]. Indeed, isolated mitochondria from *Euglena*, cultured with glu/mal under partially anoxic conditions, showed a six- to ninefold reduction in D- and L-iLDH activities (data not shown). Furthermore, other metabolic changes in *Euglena*, such as paramylon degradation, might also induce iLDH expression. In this regard, incubation of *Euglena* cells in 0.2 M NaCl for 2 h showed 35% reduction in paramylon, which was probably used to synthesize trehalose [34]. Interestingly, an enhancement of three- or fourfold in D- and L-iLDH activities accompanied increased utilization of paramylon under saline (0.2 M NaCl) stress, suggesting that iLDH expression in *Euglena* was associated with aerobic paramylon degradation (data not shown).

The observation that the intracellular steady-state concentration of L-lactate was higher than that of D-lactate suggested that the cytosolic synthesis of the former metabolite was faster, i.e. the NAD^+-dependent (glycolytic) L-LDH was more efficient than the NAD^+-dependent (glycolytic) D-LDH. Indeed, the NAD^+-LDH activity contained in the cytosolic fraction produced 74 ± 25 and 24 ± 7 nmol of L- and D-lactate/(min × mg protein), respectively (mean ± SE, $n = 3$). These data correlated with the catalytic efficiency of the mitochondrial L-iLDH and D-iLDH, which was higher with the latter enzyme [2], resulting in a lower intracellular level of D-lactate than of L-lactate.

Most of the lactate formed remained trapped intracellularly, resulting in a massive accumulation of this metabolite (Fig. 4). This observation suggested that the reverse reaction of the plasma membrane lactate transporter was negligible. In this regard, the accumulation of intracellular proline and the growth rate of *Saccharomyces cerevisiae* inversely correlate, when cells are grown under normal osmotic conditions [35]. By comparison, *Euglena* accumulated high levels of D- and L-lactate (up to 80 mM in glucose-grown cells), but growth was similar to that achieved by lactate-grown cells, which accumulated a much lower level of lactate (Figs 1 and 3). Thus, an inverse correlation was rather found between lactate accumulation and internal water volume, in which the synthesis and discharge of metabolites such as trehalose [34], or balancing the Na^+ and K^+ concentrations [17], probably attenuated osmotic stress.

Lactate shuttle

The effect of oxalate on growth, O_2 consumption, and ATP levels in *Euglena* cells was determined in an attempt to establish the role of iLDH in the energy metabolism. However, oxalate may also affect several other different enzymes, not only the mitochondrial iLDH, in addition to altering Mg^{2+} and Ca^{2+} homeostasis by forming insoluble complexes. For instance, oxalate may also inhibit liver pyruvate carboxylase as well as pyruvate kinase from muscle, erythrocytes and liver, with inhibition constant values of 6–11 μM [36]. In hepatocytes, the addition of oxalate decreases the Krebs cycle flux owing to an oxaloacetate shortage, as a result of pyruvate carboxylase inhibition [37]. Although it is possible that oxalate may inhibit different enzymes in *Euglena*, it should be noted that in cells grown with glu/mal as the carbon source, oxalate did not affect growth, suggesting a negligible effect on the pathways primarily utilizing pyruvate. Moreover, the activity of the NAD^+-LDH in the cytosolic fraction was not inhibited by 15 mM oxalate (data not shown). However, cells cultured in glu/mal and harvested in the late phase of culture showed glycolytic rates, at 30 °C, of 0.4 and 0.6 nmol of L-lactate per min per 10^7 cells, in the presence and absence of oxalate, respectively. These data suggested that in *Euglena*, oxalate also slightly inhibited enzymes (probably pyruvate kinase and preceding enzymes) involved in the glycolytic pathway, although glycolysis was not apparently required for growth in the early phases, in cells grown in either glu/mal- or lactate.

Oxalate showed a higher inhibitory potency on respiration and ATP levels of lactate-grown cells than of glu/mal-grown cells (Figure 6, Table 2), although in phase III of growth, glu/mal-grown cells showed an increase in oxalate sensitivity. These findings suggested an essential role of iLDH in supplying reducing equivalents for oxidative phosphorylation in cells cultured with lactate as the carbon source. In glu/mal-grown cells, the iLDH relevance was attenuated by the enhanced participation of the respiratory complex I.

Moreover, lactate oxidation by the cytosolic NAD^+-LDH was low (1.5 and 5.5 $nmol \cdot min^{-1} \cdot mg^{-1}$ of cytosolic protein) for 20 mM L- and D-lactate, respectively), whereas the intracellular concentration of pyruvate was determined to be 0.5 ± 0.17 mM ($n = 5$). The K_m value of the NAD^+-LDH for pyruvate was 1.2 ± 0.1 mM with a V_{max} of 120 ± 5 $nmol \cdot min^{-1} \cdot mg^{-1}$ of cytosolic protein ($n = 5$). Therefore, the only way to actively oxidize lactate in *Euglena* appears to be by using mitochondrial iLDHs.

In *S. cerevisae*, oxidation of cytosolic NADH involves the NADH-, glycerol-3-phosphate-, and ethanol-acetaldehyde shuttles [38]. In *Euglena*, our group reported evidence of a functional malate-aspartate shuttle [13], whereas, in the present work, the existence of a novel lactate shuttle is proposed (Scheme I). The lactate shuttle involves the cytosolic NAD^+-LDHs (reducing pyruvate to lactate) and the mitochondrial membrane-bound iLDHs (oxidizing external lactate to pyruvate) which are flavin-linked

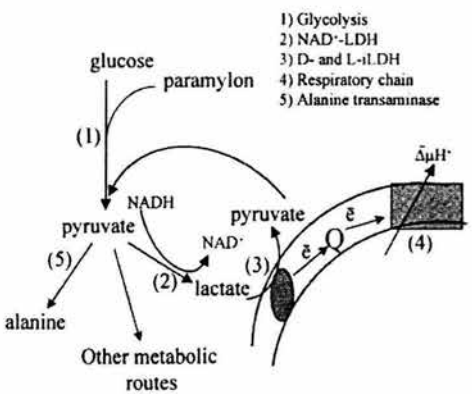

Scheme 1. Lactate shuttle in *Euglena*.

dehydrogenases (R. Jasso-Chávez and R. Moreno-Sánchez, unpublished data). In fact, *Euglena* is the first eukaryotic organism in which this type of metabolic shuttle has been described.

Recently, the existence of lactate oxidation in mammalian mitochondria was reported [39]; however, a transporter was required for the internalization of lactate and subsequent oxidation by soluble intramitochondrial NAD^+-LDH. In both rat heart and liver mitochondria, specific L- and D-lactate/pyruvate antiporters have been described [40]. These authors proposed that the mitochondrial D-lactate oxidation system may account for the removal of cytosolic D-lactate produced by the glyoxalase system, which removes the toxic methylglyoxal formed from triose phosphates, ketone body and threonine metabolism [41]. In *Euglena* mitochondria, a lactate transport reaction is not required because the catalytic site of iLDH is located in the external side of the inner membrane [2]. However, the D-lactate shuttle might have a similar function of removal of toxic by-products. Indeed, it was previously shown [2] that *Euglena* mitochondria exhibited transport of L-lactate, but its rate was not sufficient to support the iLDH activity. Moreover, L-lactate transport was inhibited by mersalyl, while oxalate and oxamate were ineffective; in contrast, iLDH activity was not affected by mersalyl, but instead it was strongly inhibited by oxalate and oxamate.

The inability for aerobe pyruvate oxidation in *Euglena* [4,14] makes evident the advantage of having a lactate shuttle in which a maximal benefit from glycolytic intermediates may be reached through the enhanced efficiencies in the transference of reduced equivalents from the cytosol to the respiratory chain.

Acknowledgements

This work was partially supported by grant 203313 from PAEP, Faculty of Chemistry, UNAM, México.

References

1. Moreno-Sánchez, R., Covián, R., Jasso-Chávez, R., Rodríguez-Enríquez, S., Pacheco-Moisés, F. & Torres-Márquez, M.E. (2000) Oxidative phosphorylation supported by an alternative respiratory pathway in mitochondria from *Euglena*. *Biochim. Biophys. Acta* **1457**, 200–210.
2. Jasso-Chávez, R., Torres-Márquez, M.E. & Moreno-Sánchez, R. (2001) The membrane-bound L- and D-lactate dehydrogenase activities in mitochondria from *Euglena gracilis*. *Arch. Biochem. Biophys.* **390**, 295–303.
3. Ingledew, W.J. & Poole, R.K. (1989) The respiratory chains of *Escherichia coli*. *Microbiol. Rev.* **48**, 222–271.
4. Buetow, D.E. (1989) The mitochondrion. In *The Biology of Euglena*, Vol. IV (Buetow, D.E., ed.) pp. 247–314. Academic Press, New York.
5. Parson, W.W. & Rudney, H. (1965) The biosynthesis of ubiquinone and rhodoquinone from p-hydroxybenzoate and p-hydroxybenzaldehide in *Rhodospirillum rubrum*. *J. Biol. Chem.* **240**, 1855–1860.
6. Erwin, A.L. & Gotschlich, E.C. (1993) Oxidation of D-lactate and L-lactate by *Neisseria mengitidis*: purification and cloning of meningococcal D-lactate dehydrogenase. *J. Bacteriol.* **175**, 6382–6391.
7. Garvie, E.I. (1980) Bacterial lactate dehydrogenases. *Microbiol. Rev.* **44**, 106–139.
8. Allison, N., O'Donell, M.J., Hoey, M.E. & Fewson, C.A. (1985) Membrane-bound lactate dehydrogenases and mandelate dehydrogenases of *Acinetobacter calcoaceticus*. *Biochem. J.* **227**, 753–757.
9. Markwell, J.P. & Lascelles, J. (1978) Membrane-bound, pyridine nucleotide independent L-lactate dehydrogenase of *Rhodopseudomonas sphaeroides*. *J. Bacteriol.* **133**, 593–600.
10. Dailey, H.A. (1976) Membrane-bound respiratory chain of *Spirillum itersonii*. *J. Bacteriol.* **127**, 1286–1291.
11. Somlo, M. (1965) Induction des lactico-cytochrome *c* reductase (D- et L-) de la leuvre aerobie par les lactates (D- et L-). *Biochim. Biophys. Acta* **97**, 183–201.
12. Fischer, R.S., Martin, G.C., Rao, P. & Jensen, R.A. (1994) *Neisseria gonorrhoeae* possesses two nicotinamide adenine dinucleotide-independent lactate dehydrogenases. *FEMS Microbiol. Lett.* **115**, 39–44.
13. Uribe, A. & Moreno-Sánchez, R. (1992) Energy-dependent reactions supported by several substrates in coupled *Euglena gracilis* mitochondria. *Plant Sci.* **86**, 21–32.
14. Inui, H., Ono, K., Miyatake, K., Nakano, Y. & Kitaoka, S. (1985) The physiological role of oxygen-sensitive pyruvate dehydrogenase in mitochondria fatty acid synthesis in *Euglena gracilis*. *Arch. Biochem. Biophys.* **237**, 423–429.
15. Hutner, S.H. & Bach, K.M. (1956) A sugar-containing basal medium for vitamin B12-assay with *Euglena*; application to body fluids. *J. Protozool.* **3**, 101–112.
16. Bergmeyer, H.U. (1983) *Methods of Enzymatic Analysis*, Vol. 3–9 (Bergmeyer, H.U., ed.), Weinheim Verlag Chemie, Germany.
17. González-Moreno, S., Gómez-Barrera, J., Perales, H. & Moreno-Sánchez, R. (1997) Multiple effects of salinity on photosynthesis of protist *Euglena gracilis*. *Physiol. Plant.* **101**, 777–786.
18. Rottenberg, H. (1979) The measurement of membrane potential and ΔpH in organelles and vesicles. *Methods Enzymol.* **55**, 547–569.
19. Weickowski, M.R. & Wojtzak, L. (1998) Fatty acid-induced uncoupling of oxidative phosphorylation is partly due to opening of the mitochondrial permeability transition pore. *FEBS Lett.* **423**, 339–342.
20. Bravo, C., Vargas-Suarez, M., Rodriguez-Enriquez, S., Loza-Tavera, H. & Moreno-Sánchez, R. (2001) Metabolic changes induced by cold stress in rat liver mitochondria. *J. Bioenerg. Biomembr.* **33**, 289–301.
21. Ono, K., Kawanaka, Y., Izumi, Y., Inui, H., Miyatake, K., Kitaoka, S. & Nakano. Y. (1995) Mitochondrial alcohol dehydrogenase from ethanol-grown *Euglena gracilis*. *J. Biochem.* **117**, 1178–1182.
22. Navarro, L., Torres-Márquez, M.E., González-Moreno, S., Devars, S., Hernández, R. & Moreno-Sánchez, R. (1997) Comparision of physiological changes in *Euglena gracilis* during exposure to heavy metals of heterotrophic and autotrophic cells. *Comp. Biochem. Physiol.* **116C**, 265–272.
23. Kempner, E.S. (1982) Stimulation and inhibition of the metabolism and growth of *Euglena gracilis*. *The Biology of Euglena*, Vol. III (Buetow, D.E., ed.), pp. 197–252. Academic Press, New York.
24. Barras, D.R. & Stone, B.A. (1968) Carbohydrate composition and metabolism in *Euglena*. *The Biology of Euglena*, Vol. II (Buetow, D.E., ed.), pp. 149–187. Academic Press, New York.
25. Velazquez, I. & Pardo, J.P. (2001) Kinetic characterization of the rotenone-insensitive internal NADH: ubiquinone oxidoreductase of mitochondria from *Saccharomyces cerevisiae*. *Arch. Biochem. Biophys.* **389**, 7–14.
26. Inui, H., Iyatake, K., Nakano, Y. & Kitaoka, S. (1990) Pyruvate: $NADP^+$ oxidoreductase from *Euglena gracilis*: mechanism of

O_2-inactivation of the enzyme and its stability in the aerobe. *Arch. Biochem. Biophys.* **280**, 292–298.
27. Sumida, S., Ehara, T., Osafune, T. & Hase, E. (1987) Ammonia- and light-induced degradation of paramylum in *Euglena gracilis*. *Plant Cell Physiol.* **28**, 1587–1592.
28. Tomos, A.D. & Northcote, D.H. (1978) A protein-glucan intermediate during paramylon synthesis. *Biochem. J.* **174**, 283–290.
29. Kitaoka, M., Sasaki, T. & Taniguchi, H. (1993) Purification and properties of laminaribiose phosphorylase (EC 2.4 1.31) from *Euglena gracilis*. *Z. Arch. Biochem. Biophys.* **304**, 508–514.
30. Calvayrac, R., Laval-Martin, D., Briand, J. & Farineau, J. (1981) Paramylon synthesis by *Euglena gracilis* photoheterotrophically grown under low O_2 pressure. *Planta* **153**, 6–13.
31. Smillie, R.M. (1968) Enzymology of *Euglena*. *The Biology of Euglena*, Vol. II (Buetow, D.E., ed.), pp. 2–54. Academic Press, New York.
32. Belanger, A.E. & Hatfull, G.F. (1999) Exponential-phase glycogen recycling is essential for growth of *Mycobacterium smegmatis*. *J. Bacteriol.* **181**, 6670–6678.
33. Iuchi, S. & Lin, E.C.C. (1988) *arc* A (dye), a global regulatory gene in *Escherichia coli* mediating repression of enzymes in aerobic pathways. *Proc. Natl Acad. Sci. USA* **85**, 1888–1892.
34. Takenaka, S., Kondo, T., Nazeri, S., Tamura, Y., Tokunaga, M., Tsuyama, S., Miyatake, K. & Nakano, Y. (1997) Accumulation of trehalose as a compatible solute under osmotic stress in *Euglena gracilis*. *Z. J. Eukaryot. Microbiol.* **44**, 609–613.
35. Maggio, A., Miyazaki, S., Veronese, P., Fujita, T., Ibeas, J.I., Damsz, B., Narasimhan, M.L., Hasegawa, P.M., Joly, R.J. & Bressan, R.A. (2002) Does proline accumulation play an active role in stress-induced growth reduction? *Plant J.* **6**, 699–712.
36. Buc, H.A., Augereau, C., Demaugre, F., Moncion, A. & Leroux, J.P. (1983) Influence of oxalate on the rate of tricarboxilic acid cycle in rat hepatocytes. *Biochim. Biophys. Acta* **763**, 220–223.
37. Buc, H.A., Demaugre, F., Moncion, A. & Leroux, J.P. (1982) Effects of oxalate and dichloroacetate on lipogenesis and ketogenesis in rat hepatocytes. *Biochem. Biophys. Res. Commun.* **104**, 1107–1113.
38. Bakker, B.M., Overkamp, K.M., van Maris, A.J.A., Kötter, P., Luttik, M.H.A., van Dijken, J.P. & Pronk, J.T. (2001) Stoichiometry compartmentation of NADH metabolism in *Saccharomyces cerevisiae*. *FEMS Microbiol. Rev.* **25**, 15–37.
39. Brooks, G.A., Dubouchaud, H., Brown, M., Sicurello, J.P. & Butz, C.E. (1999) Role of mitochondrial lactate dehydrogenase and lactate oxidation in the intracellular lactate shuttle. *Proc. Natl Acad. Sci. USA* **96**, 1129–1134.
40. Valenti, D., de Bari, L., Atlante, A. & Pasarella, S. (2002) L-lactate transport into rat heart mitochondria and reconstruction of the L-lactate/pyruvate shuttle. *Biochem. J.* **364**, 101–104.
41. de Bari, L., Atlante, A., Guaragnella, N., Principato, G. & Passarella, S. (2002) D-lactate transport and metabolism in rat liver mitochondria. *Biochem. J.* **365**, 391–403.

2.2. Datos no mostrados en el artículo de investigación.

El aumento en las actividades de la D-iLDH y L-iLDH y de las concentraciones intracelulares de los dos isómeros de lactato, correlacionó estrechamente con la desaparición de la fuente de carbono externa y el inicio de la degradación del paramilo; lo que sugería que el metabolismo del paramilo estaba ligado al aumento del lactato intracelular. Así, la expresión de ambas iLDH no está determinada por la fuente de carbono externa, sino por la concentración intracelular de D-lactato y L-lactato respectivamente, ya que siempre son altas debida a la degradación del paramilo. Precisamente, la inducción de la síntesis de ambas iLDH podría estar relacionada de alguna forma con la degradación de paramilo, más que con la disponibilidad de su sustrato. Para contestar esta pregunta, incubamos células glu/mal de 96 horas de cultivo en presencia de 0.2 M de NaCl durante 2 horas. Esta condición de estrés salino provoca en *Euglena* una degradación activa de paramilo para la síntesis de trehalosa (Takenaka y cols. 1997). Detectamos el mismo porcentaje de degradación de paramilo que el reportado, pero además, un incremento de 3 y 5 veces en las actividades de L- y D-iLDH respectivamente (Figura 5).

En levaduras y bacterias la expresión de la iLDH inducible está sujeta a la disponibilidad de oxígeno (Somlo, 1965; Iuchi y Lin, 1988). En el mismo orden de ideas, nosotros cultivamos a *Euglena* en baja tensión de oxígeno y determinamos la actividad de la D- y L-iLDH en mitocondrias aisladas. En estas condiciones, la cantidad de proteína mitocondrial fue muy semejante a la obtenida para células cultivadas en aerobiosis (55-60 mg de proteína/L de cultivo), pero las actividades de la D- y L-iLDH disminuyeron 9 y 15 veces respectivamente (Tabla 2). Es importante señalar que la actividad de la citocromo *c* oxidasa (TMPDox) también disminuyó en condiciones de baja tensión de oxígeno: Sin embargo, la relación TMPDox/iLDH fue mayor en condiciones de baja tensión de oxígeno que en aerobiosis, lo que sugiere que efectivamente existe una disminución en la cantidad de iLDH en estas mitocondrias.

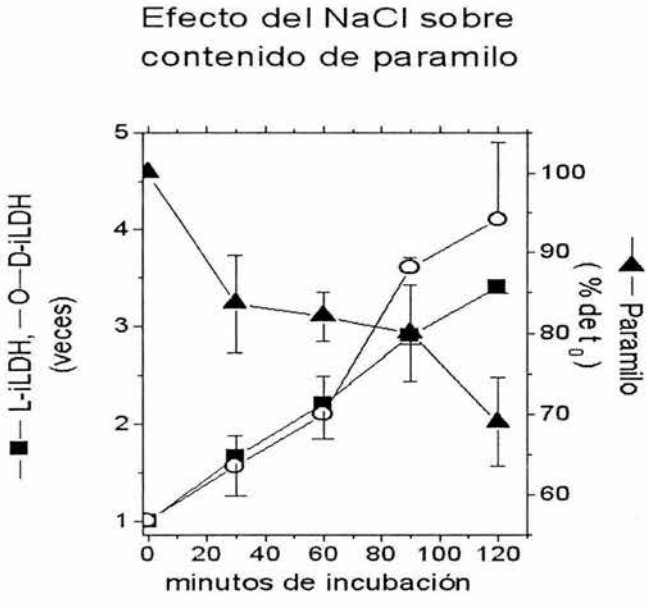

Figura 5. **Efecto del estrés salino sobre el contenido del paramilo**. Las células se incubaron durante diferentes tiempos con 0.2M de NaCl, después se tomó una alícuota de células y se determinó el contenido de paramilo. Para determinar las actividades de iLDH, las células se rompieron con un sonicador de baño durante 30-40 min en presencia de 0.05% de tritón X-100 hasta que la viabilidad fuera menor al 5%. La actividad de enzimática se determinó con 30 mM de L- o D-lactato respectivamente. La actividad de L-iLDH y D-iLDH así como el contenido del paramilo al tiempo cero fueron: 9 ± 2 y 20 ± 2.5 nmoles /min x 10^7 cels., y 0.45 ± 0.08 mg/10^7 cels., respectivamente. Los valores son el promedio de 4 experimentos ± E. S.

Tabla 2. Actividad de las iLDH y TMPD oxidasa en mitocondrias aisladas

	Mitocondrias aeróbicas *	Mitocondrias anaerobias
D-iLDH (mU/mg prot)	340 ± 38	40 (2)
L-iLDH (mU/mg prot)	230 ± 18	15 (2)
TMPD oxidasa (nat O/min x mg prot)	450 ± 35	106 (2)

(n), número de experimentos. * Estos valores fueron tomados de Jasso-Chávez y cols. (2001).

Para evaluar si la D-iLDH y la L-iLDH eran esenciales para obtener la energía requerida para todos los procesos celulares, cultivamos a las células en glu/mal y en lactato en presencia de oxalato, un potente inhibidor de las iLDH y determinamos el efecto sobre el crecimiento celular, la respiración ligada a la fosforilación oxidativa y la cantidad de ATP. Sin embargo, el oxalato puede inhibir a otras enzimas involucradas en la parte baja de la glucólisis y a la piruvato carboxilasa, así como quelar al Ca^{2+} y al Mg^{2+}. Determinamos que el oxalato inhibió la velocidad de glucólisis en *Euglena*, pero sólo a tiempos mayores que los utilizados en los experimentos anteriores, que fueron de 15 minutos (Figura 6). Además, ni las células glu/mal ni las lácticas parecen utilizar a la glucólisis en las fases I y II de los cultivos.

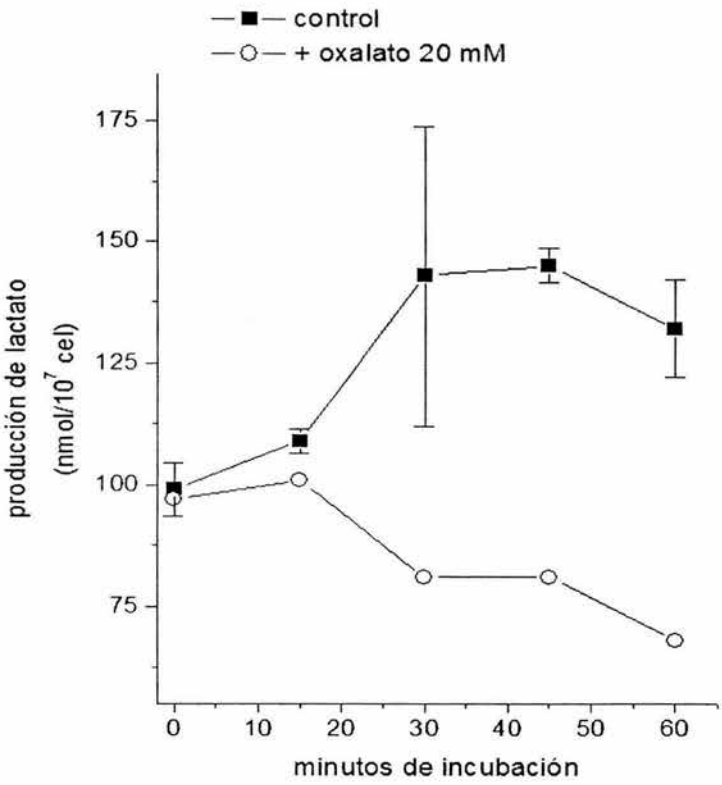

Figura 6. **Efecto del oxalato sobre la velocidad de la glucólisis en *Euglena*.** Las células cultivadas 96 horas en glu/mal, se incubaron a diferentes tiempos en ausencia y en presencia de oxalato, se tomaron alícuotas, se realizaron extractos ácidos y se cuantificó la producción de L-lactato. Los datos mostrados son el promedio ± E. S. de 3 experimentos independientes.

3. Purificación y Caracterización Cinética de los Componentes de la lanzadera de Lactato de *Euglena*

El hecho de que las iLDH de bacterias y *Euglena* funcionalmente presenten similitudes en cuanto a su cinética, su capacidad para reducir quinonas y de estar conectadas a la cadena respiratoria, sugiere que estas enzimas provienen de un origen común. De las enzimas bacterianas secuenciadas, hay entre 40-60% de identidad entre las D-iLDH o L-iLDH, aunque en éstas últimas, son muy pocos los alineamientos que se han realizado por lo difícil de su purificación debido a su labilidad al solubilizarlas en detergentes.

Después de haber concluido los objetivos del proyecto de la tesis y de determinar además, la existencia de una nueva lanzadera de equivalentes reductores a partir de la oxidación de lactato, nos planteamos purificar a los componentes de esta lanzadera, en un intento por determinar las características cinéticas y moleculares de las enzimas que la constituyen. La D-iLDH se ha logrado aislar con un buen grado de pureza. Determinamos que esta enzima, al igual que las bacterianas, tiene una masa molecular de 62 kDa y es una flavoproteína. Tiene la capacidad de reducir quinonas artificiales y es sensible a oxalato y a L-lactato.

La L-iLDH no se logró purificar debido a su labilidad al solubilizarla. Sin embargo, logramos extraerla con cierta actividad utilizando al detergente Lubrol. El solubilizado se pasó por una resina de intercambio iónico fuerte (Mono Q), las fracciones con actividad se colectaron y se hicieron pasar por una columna de afinidad (sefarosa-oxamato); A pesar de su poca retención, se logró obtener una fracción capaz de reducir quinonas y se inhibió con oxalato.

En cuanto a la NAD^+-LDH citosólica de *Euglena* (que es la enzima típica de la glucólisis), Smillie (1968) reportó que la actividad de oxidación de lactato en homogenados de *Euglena*, era 3 veces mayor para el isómero D que para el

isómero L En una fracción concentrada de citosol, encontramos que la reducción de piruvato producía lactato en una proporción de 75% del isómero L y 25% del isómero D. Esto sugiere la existencia de dos entidades moleculares para la producción de cada isómero del lactato. Se determinaron las constantes cinéticas para piruvato y NADH, así como la velocidad máxima de la reacción en el sentido de la reducción de piruvato ya que la velocidad de oxidación de lactato fue entre 15-25 veces más lenta. La NAD^+-LDH mostró una activación alostérica de tipo *K* por la fructosa-1,6-bifosfato (FBP), disminuyendo la K_m por NADH de 3-4 veces y por piruvato de 2 veces, aproximadamente hasta la concentración intracelular de piruvato que determinamos en *E. gracilis*. La concentración intracelular de FBP durante el crecimiento celular aumentó, ya fuera en células cultivadas con lactato o con glutamato/malato como fuente de carbono. Estos cambios en la concentración intracelular de FBP van desde valores por debajo de su $K_{0.5}$ en la fase de latencia, hasta valores por arriba de la $K_{0.5}$ en la fase estacionaria, lo que sugiere que la activación de la NAD^+-LDH puede ser de relevancia para el metabolismo energético de *Euglena*.

Para concluir este trabajo, es necesario identificar la naturaleza de la flavina de la D-iLDH así como terminar la purificación de la NAD^+-LDH citosólica. A continuación se muestra la primera versión del manuscrito en preparación con estos resultados.

The Lactate Shuttle Components from Heterotrophic *Euglena gracilis*

Ricardo Jasso-Chávez[1]*, Israel García-Cano[1], Guillermo Mendoza[2], Álvaro Marín-Hernández[1], Juan Luis Rendón[2], and Rafael Moreno-Sánchez[1].

1. Departamento de Bioquímica, Instituto Nacional de Cardiología
2. Departamento de Bioquímica, Facultad de Medicina, UNAM.

* Correspondence to Ricardo Jasso-Chávez, mail to: rjassoch@aol.com
Departamento de Bioquímica, Instituto Nacional de Cardiología. Juan Badiano #1, Col. Sección XVI, Tlalpan, México, D. F. 14080, México.
Fax: + 52 555 573 0926
Tel: + 52 555 573 2911

ABSTRACT

The structural and kinetic analyses of the components of lactate shuttle from heterotrophic Euglena gracilis were carried out. Mitochondrial membrane-bound, NAD^+-independent D-lactate dehydrogenase (D-iLDH), was purified by using solubilization with CHAPS and a heat treatment. The enzyme was a dimmer with 2 60 kDa (to be confirmed) monomers containing FAD as cofactor. D-iLDH was specific for D-lactate and it was able to reduce quinones with different redox potential values. Oxalate and L-lactate were mixed-type inhibitors of D-iLDH; the *Ki* value (10 mM) for L-lactate suggested that this enzyme could be inhibited by intracellular L-lactate. The mitochondrial L-iLDH did reduce quinones, but it was inactivated when extracted from the membrane by detergents. L-iLDH was inhibited by the specific flavoprotein-inhibitor diphenyleneiodonium, suggesting that L-iLDH was also a flavoprotein. Affinity chromatography revealed that cytosolic fraction from *E. gracilis* contains specific NAD^+-lactate dehydrogenases for the generation of D-lactate and L-lactate, respectively (D-nLDH and L-nLDH). These two enzymes showed an ordered bi-bi kinetic mechanism. The *Vm* and *Km* values for pyruvate and NADH were different in both enzymes. With D-nLDH, the rate of D-lactate oxidation was 40-fold lower than pyruvate reduction, which was inhibited by D-lactate (*Ki* = 15 mM). The L-lactate oxidation by the L-nLDH was not detected. Instead, pyruvate reduction was activated by fructose-1, 6-bisphosphate (FBP), K^+ and NH_4^+. Interestingly, membrane-bound lactate dehydrogenases with quinone reductasa activity and D-nLDH have only described for bacterial systems. Moreover, FBP-activated L-nLDH has only been found in lactic bacteria. Based on their similar kinetic and structural characteristics, a possible common origin among bacterial and *E. gracilis* lactic dehydrogenase enzymes is discussed.

1. INTRODUCTION

The NAD^+-independent lactate dehydrogenases (iLDH) are enzymes widely distributed in bacteria and yeast. Lactate oxidation is coupled to the respiratory chain and hence to the proton gradient formation and ATP synthesis. In bacteria, the quinone pool is the physiologic electron acceptor of iLDH, while in yeast, the acceptor is cytochrome *c*. Localization of the D-iLDH in bacteria, is in the inner cytoplasmic membrane, while in *Sacharomyces cerevisiae* the L-iLDH and D-iLDH are in the mitochondrial intermembranal space [1, 2]. In both kinds of microorganisms, the iLDHs are flavoproteins, but in yeast, D- and L-iLDH have an additional cytochrome b_2. Many of these enzymes have been purified and their molecular characteristics and kinetic constants have been determined. D-iLDH is a 60-66 kDa monomer with one FAD molecule per monomer in both bacteria and yeast [3, 4]; D-iLDH in yeast seems to be mainly associated with the methylglyoxal pathway [4]. On the other hand, the L-iLDH possesses a non-covalently bounded FMN molecule as cofactor. In bacteria, L-iLDH is a 45 kDa monomer, and a 240 kDa homotetramer in yeast [2, 5]. D-iLDH and L-iLDH are inhibited competitively or mixed type by oxamate and/or oxalate with *Ki* values ranging from 3 μM to 2 mM.

Bacteria may express constitutively only one iLDH, in *E. coli*, D-iLDH is present under many growth condition [7], but the L-iLDH is expressed when cells grow aerobically with L-lactate as a carbon source and it is repressed in the presence of glucose [8]. These data suggest that the final predominant product of glycolysis in *E. coli* is D-lactate. In yeast, iLDH expression depends on the availability of both, the lactate isomer and oxygen in the growth medium [9].

Amino acid alignment made between iLDH from bacteria and yeast shows differences among sequences, suggesting a divergent origin for these enzymes [5]. In addition, the alignment between D-iLDH and L-iLDH from bacteria shows that D-

lactate dehydrogenase is a member of the 2-hydroxyacid dehydrogenases family, specific for the D- isomer [6].

Isolated mitochondria from *E. gracilis* cultured under aerobic conditions are unable to oxidize pyruvate for acetyl-coA synthesis. Instead, they have the capacity to coupling the D- and L-lactate oxidation to oxidative phosphorylation by means of isomer-specific lactate dehydrogenases [10, 11]. These enzymes reduce directly the quinone pool, are membrane-bound enzymes and NAD^+-independent (D-iLDH and L-iLDH). They have similar *Km* values for D- and L-lactate respectively, are inhibited competitively by oxamate and in mixed type by oxalate. The D-iLDH is thermo-resistant until 70°C, while L-iLDH is inactivated since 50°C [10]. The D-iLDH and L-iLDH in *E. gracilis* are expressed constitutively, independently of the carbon source and in all phases of growth. Oxygen availability and paramylon catabolism (lineal chain of β-1, 3 glucan) are strongly involved in the increase of the D- and L-iLDH activities. Moreover, we have shown that both iLDH as well as the NAD^+-dependent-cytosolic lactate dehydrogenase (nLDH) perform a lactate shuttle, in which the pyruvate produced from paramylon catabolism by means of glycolysis, is reduced by the cytosolic nLDH to generate lactate that is oxidize by membrane iLDH to produce the reducing equivalents for the oxidative phosphorylation [12].

Then, at least physiologically, both iLDH from *E. gracilis* seem to be similar to the bacterial enzymes. In the present work, we purified and characterized structurally and kinetically the four components of the lactate shuttle. The molecular and kinetic characterization suggested that the lactate shuttle enzymes from *E. gracilis* share a common ancestor with the bacterial membrane-bound and cytosolic lactate dehydrogenases.

2. MATERIAL AND METHODS

Lubrol, D-lactate, and L-lactate were from ICN. Ubiquinone-1 (Q1), dichlorophenol-indophenol (DCPIP), Phenyl-methyl sulfonate fluoride (PMSF), CHAPS, pyruvate, fructose-1, 6- bisphosphate, NAD^+, NADH, diphenyleneiodonium (DPI), FAD, FMN and molecular weight markers were from Sigma. Cyanogen-activated affinity resin coupled to oxamate was from BIO-RAD. The molecular exclusion Sephacryl S-200 resin and the blue-sepharose were from Pharmacia. Tetrachlorohidroquinone (TCHQ) was kindly gift by Dr. E. Escamilla from the IFC, UNAM.

Cell culture and isolation of mitochondrial and cytosolic fractions

Euglena gracilis strain Z was cultured in the dark in presence of 33 mM glutamate and 17 mM malate as carbon source. Isolation of the mitochondrial and cytosolic fractions was made as previously described [10, 12, 13] and kept at -70°C until use.

Determination of metabolites

A 0.9 mL suspension containing 1 x 10^8 washed cells, from different phases of growth was mixed with perchloric acid (PCA, 3% of final concentration). This mixture was centrifuged and the supernatant recovered and neutralized with KOH/Tris. Pyruvate and FBP were determined fluorometrically at 30°C by using standard enzymatic methods [14].

Enzyme assays

D-iLDH activity was determined in 1 mL of a solution of pH 7.5 that contained 20 mM HEPES, 1mM EGTA, 0.2 (w/v) CHAPS, 0.025% (w/v) β-mercaptoethanol, 0.12 % (w/v) Triton X-100 and 0.5 mM PMSF as protease inhibitor (HEC buffer) by measuring the rate of disappearance of either 0.25 mM DCPIP (λ 600nm and ε= 21.3 mM^{-1} cm^{-1}) [15], Q1 (λ 273 nm and ε= 18.1 mM^{-1} cm^{-1}

^{1}) [10], or TCHQ (λ 322 nm and ε= 8.6 mM^{-1} cm^{-1}). The reaction was started by addition of the D-lactate addition. When TCHQ reduction was determined, Tritón-X100 was omitted to avoid interference with the assay. For L-iLDH activity both, CHAPS and Triton were replaced by 0.2 % (w/v) of Lubrol. The reaction was started by addition of 40 mM L-Lactate.

Effect of DPI on L-iLDH activity was determined in 1 mL of HE buffer (without β-mercaptoethanol) previously bubbled with N_2 for 30 min. Mitochondrial protein (0.1 mg) was incubated in the presence of 0.05 mM DCPIP and 0.5 mM L-lactate to maintain the enzyme reduced. After the addition of different DPI concentrations, the mixture was incubated for 5 min under N_2 atmosphere. The activity was determined by measuring the 0.3 mM DCPIP reduction at 600 nm, starting with 30mM L-lactate.

The activity of nLDH was measured in both directions of its reaction; the pyruvate reduction was determined in 1 mL of HEC solution at pH 7.0, but detergents were omitted (HE buffer) by measuring the rate of disappearance of 0.25 mM NADH at λ 340 nm and ε= 6.22 mM^{-1} cm^{-1}. The reaction was started with addition of fresh pyruvate. NAD^+-dependent lactate oxidation was determined in 1 mL of a solution with 400 mM trizine and 500 mM glycine pH 9 by measuring the reduction of 0.8 mM NAD^+. The reaction was started with the addition of 100 mM D-lactate or L-lactate. To determine the D- and L-lactate production by the nLDH, 20-50 μg cytosolic protein was incubated in presence of 150 μM NADH and 0.5 mM pyruvate in 1 mL of HE buffer. After 1-3 min, the reaction was stopped with 3% (v/v) PCA, the mixture centrifuged and the pH of supernatant neutralized. The D- and L-lactate production was determined by using commercial specific NAD^+-dependent D- (ROCHE) and L-lactate dehydrogenases (Sigma) [12].

D-iLDH purification

All steps were made at 4°C. Isolated mitochondria from 90-94h grown cells [10] were diluted at 15-18 mg protein/mL in HE buffer. CHAPS was slowly added until a detergent/protein ratio of 0.7 was reached. The suspension was strongly mixed for 5 min and centrifuged at 40, 000 x *g* for 20 min. The solubilized D-iLDH in the supernatant was incubated in presence of 10 mM oxalate at 60°C for 45-50 min; the heated supernatant was centrifuged at 14,000 x *g* for 10 min. The supernatant was mixed with 50% (v/v) glycerol and stored at -70°C until use. The D-iLDH enrichment throughout the purification steps was monitored by SDS-PAGE and activity measurements.

Partial purification of nLDHs

The cytosolic fraction was mixed with ammonium sulfate up to 30% saturation and incubated for 30 min. The solution was centrifuged at 20,000 x *g* for 20 min.The supernatant was mixed with ammonium sulfate up to 75 % (w/v) saturation and centrifuged. The pellet was resuspended in HE buffer. This last solution was desalted in a Sephadex G-25 minicolumn (2 columns of 0.5 x 5 cm). The desalted solution was loaded on a Blue-sepharose column previously equilibrated with HE buffer. The nLDH was eluted with a 0-1M NaCl gradient in the same buffer, and concentrated in an Amicon ultrafiltration cell, using a MY30 ultrafiltration membrane (Millipore). The concentrated protein was loaded on an oxamate-sepharose column. The oxamate-sepharose resin was prepared according to [23]. The column (1 x 15 cm) was pre-equilibrated with HE buffer containing 0.05 mM NADH and 1 mM FBP. D-lactate dehydrogenase was eluted with the washing buffer, the L-lactate dehydrogenase was eluted with the same buffer but without NADH and FBP.

Molecular weight determinations

The molecular weights of D-iLDH, D-nLDH and L-nLDH from lactate shuttle from *E. gracilis* were evaluated essentially by the use of molecular exclusion

column. The enzymes (1-2.5 mg) were filtered through of a column (56 x 1.7 cm) packed with Sephacryl S-200 and equilibrated against HE buffer. The column was calibrated with molecular standards provided by Pharmacia, blue dextran (2 x 10^6 daltons), horse spleen ferritin (440,000 daltons), bovine liver catalase (232,000 daltons), rabbit muscle aldolase (158,000 daltons), bovine serum albumin (66,000 daltons), bovine pancreas chimotrypsinogen A (25,000), bovine pancreas ribonuclease A (13,700 daltons), and vitamin B12 (1,700 daltons). The distribution coefficient (Kav) was determined with the equation:

Kav = Ve-Vo/ Vt-Vo,

where Ve= elution volume for the protein

Vo= column void volume=elution volume for Blue-dextran (in our case was 59 mL)

Vt= total bed volume (in our case was 127 mL).

The elution volume of each protein was the average of the peak of absorbance at 280 nm of eluted enzymes from the column and was accompanied with the highest activity for each enzyme.

Structural characterization of D-iLDH

An aliquot of the enzyme (5-7.5 μg) was mixed with Laemmli buffer, boiled for 5 min and poured into a 10% acrylamide gel. The gel was stained with silver. The molecular weight was determined by using protein weight markers from 6.5 up to 205 kDa. The extraction of flavine was made with a solution containing 0.5 mg enzyme protein and 10% trichloroacetic acid [16]. After 15 min of incubation at 4°C, the solution was centrifuged at 20,000 x g for 4 min. The supernatant was mixed with another addition of 10% trichloroacetic acid, incubated 15 min and centrifuged again. An aliquot of the last mixture was transferred to a spectrofluorometer cuvette with 2 mL 50 mM citrate pH 3. The fluorescent signal of flavine was measured at 520 nm, with the wavelength set at 450nm. Identification and quantification of flavine was determined by HPLC with reverse phase C18 column (4.6 x 150 mm) 0-20% acetonitrile gradient plus 0.1% trifluoroacetic acid with a flux

of 1mL/min was used. FAD and FMN were used as standards, using a molar extinct coefficient of 12 mM^{-1} cm^{-1}.

3. RESULTS

Purification and structural characterization of D-iLDH

Methodologies reported for bacterial D-iLDH purification are commonly based on enzyme extraction by diverse non-ionic detergents followed by ionic and molecular exclusion chromatography [16, 17, 19]. Our initial attempts to purify the D-iLDH from *E. gracilis* mitochondria were based on similar strategies, like pre-heating of the CHAPS-solubilized mitochondria at 50°C for 20 min at followed by affinity chromatography (oxamate-sepharose). Specific activity rise after each purification step was observed (for instance, from 50 nmol $DCPIP_{red}$/min x mg prot in homogenate up to 2000 nmol $DCPIP_{red}$/min x mg prot after affinity chromatography, data not shown). However, poor enrichment of a protein of 60 kDa was attained (data not shown); this molecular weight is similar at the reported for bacterial D-iLDH [5, 16, 17]. Then, taking advantage of the high thermostability of the D-iLDH [10], the CHAPS-solubilized mitochondrial solution was incubated in presence of 10 mM oxalate as protecting ligand, at 60°C for 45-50 min to denature heat-sensitive proteins. With this rapid and easy method, a highly enriched fraction with a 60 kDa protein was obtained (Fig. 1A) with 80-85% recovering and 29-fold higher D-iLDH activity (Table 1). The 60 kDa protein showed D-iLDH activity in a 10% acrylamide native gel in presence of PMS, NBT and 10 mM D-lactate (Fig.1B). The TCA extract of the D-iLDH showed two excitation peaks at 366 y 450 nm, which are typical of flavines [16, 17, 19] (data not shown). The visible absorption spectrum of the enzyme from *E. gracilis* showed a broad peak around 450 nm and a shoulder at around 488 nm, suggesting a flavoprotein. This result is very similar with the results found to *E.coli* D-iLDH [16, 18]. All bacterial and yeast D-iLDH have a FAD molecule as cofactor [3, 16, 17]. Accordingly, the purified *E. gracilis* D-iLDH exhibited 1.3 ± 0.2 (mean ± S. D., n=4) FAD molecules per D-

iLDH. Surprisingly, molecular exclusion chromatography of D-iLDH showed a 130 kDa of molecular weight, suggesting that this enzyme is a dimmer, unlike at bacterial and yeast enzymes [3, 16, 17].

Kinetic Characterization of D-iLDH and L-iLDH

The *Km* values of the purified D-iLDH for D-lactate, DCPIP, Q1, as well as the *Ki* value for oxalate, were very similar to those previously determined in intact mitochondria [10]. Similar to the *N. meningitidis* enzyme [19], *Euglena* D-iLDH did not oxidize L-lactate (1.5 % of D-lactate oxidation); instead, L-lactate inhibited it. These data suggested that the enzyme from *E. gracilis* is D-lactate specific and that L-lactate may physiologically modulate its activity, depending on the growth phase and culture conditions. The enzyme was able to reduce Q1 as well as TCHQ, a quinone with a redox potential value of -8 mV [41] (Table 2). Similar to the *E. coli* enzyme, *Euglena* D-iLDH was activated by 0.12% (w/v) Triton X-100. The ability of D-iLDH to reduce quinones of high and low redox potential implied that ubiquinone-9 (+ 100 mV) and rhodoquinone-9 (-65 mV), quinones with high and low redox potential respectively [20] present in the mitochondrial quinone pool of *E. gracilis*, may be both its physiological substrates.

Several works have determined that bacterial L-iLDH inactivates when membranes are solubilized by detergents [5, 19]. We previously described that 11 mM β-octyl glucopyranoside (50% of detergent critical micellar concentration, CMC), solubilized 30% of total L-iLDH activity but activity disappear after a few hours [10]. Solubilization of mitochondria with detergent at its CMC (22 mM), the enzyme inactivated almost completely after a few min (data not shown), suggesting a key role of membrane lipids for the enzyme functionality. However, in a soluble extract with Lubrol (0.98% w/v), the L-iLDH activity did not change and was stable a pH values of 7.6-9 for 60 min and able to reduce Q1 in an oxalate-sensitive reaction (data not shown). Diphenyleneiodonium chloride (DPI) has been used as

a specific irreversible flavoenzyme inhibitor since it reacts with the flavines to form irreversible adducts [37]. The L-iLDH activity in isolated mitochondria was 85% inhibited by 4 mM DPI and with an IC_{50}= 2mM (data not shown). These kinetic and structural data suggests that both mitochondrial iLDH from *Euglena* may share a common ancestor with the bacterial enzymes, in agreement with the classification of lactate and mandelate dehydrogenases established by Fewson and coworkers whom based on structure and identity sequence of the enzymes, proposed that L-iLDH and D-iLDH from bacteria belong to specific categories and evolved separately of yeast enzymes [5].

Metabolic role of nLDH

Smille showed that in crude extracts of *E. gracilis*, the D-lactate oxidation by nLDH was 3-fold faster than L-lactate oxidation [21]. In our hands, the nLDH activity in a cytosolic fraction of *E. gracilis* was 6 and 2 nmol/min x mg prot., for D- and L-lactate oxidation, respectively [12]. Remarkably, these activities were 50-100 folds lower than pyruvate reduction activity (Table 3). Similar to L-nLDH from some hetero fermentative bacteria [22-28], nLDH from *E. gracilis* was activated by FBP following a michaelis-menten kinetics. FBP was a non-essential activator which diminished the *Km* values for both, NADH and pyruvate. In contrast to the cooperative bacterial FBP-dependent L-nLDH [25], the enzyme from *E. gracilis* was competitively inhibited by oxamate (Table 3), a classic inhibitor of mammalian nLDH. Oxalate (20 mM) did not affect nLDH activity (data not shown).

In an attempt to elucidate whether the FBP activation on nLDH might have physiological relevance, the intracellular concentration of FBP in cells cultured in glutamate/malate or lactate as carbon source was determined. In general, the intracellular concentration of FBP was similar in both cultures, although it's changed with the progress of the growth curve, from 0.2 mM in the first 20 hours of culture up to 0.8 mM in the stationary phase (96 h). The $K_{0.5}$ value of L-nLDH for FBP was 0.3 mM (Table 3), which suggested that in *Euglena*, the L-nLDH

activation by FBP was significant in the logarithmic and stationary phases. FBP activation diminished the *Km* value for pyruvate from 1.1 a 0.47 mM, latter, being this latter value the intracellular concentration of pyruvate in *Euglena* [12]. We have previously showed that lactate formation in the cytosol strongly depends on paramylon catabolism, and that lactate oxidation mediated by mitochondrial lactate shuttle is essential in *E. gracilis* bioenergetics when external carbon sources are scarce. Then, the activation of the glycolytic nLDH by FBP warrants a constant flux toward lactate production for ATP synthesis (Scheme 1). To stimulate glycolysis in the hetero fermentative bacteria *Lactobacillus casei*, the culture medium was supplemented with substrates that lead to the formation of high FBP concentrations which in turn activates L-nLDH [22].

Kinetic characterization of nLDH

In some hetero fermentative bacteria, L-nLDH may show either hyperbolic or cooperative saturation kinetic with pyruvate as substrate. FBP, Co^{2+} and Mn^{2+} activate the enzyme [23, 24, 26, 28, 29], but the activation depends on the organism and pH of the reaction. Thus, we analyzed the pH optimum of nLDH from *Euglena* in absence or in presence of activators. The pH optimum for nLDH activity was 6.5-7.0. The enzymatic activity in presence of 2 mM Mn^{2+} was ~33% higher than basal activity only at pH values of 7.7-8.5. FBP (0.8 mM) displaced the optimum pH value to 8.0 and induced a 40% increase in the basal nLDH activity. These data suggested that the activators give stability at the *E. gracilis* nLDH as proposed for the *Bifidibacterium longum* enzyme [26] in which FBP stabilizes the dimmer with a concomitant decrease in *Km* values. Like *Streptococcus faecalis* [24], the *Euglena* enzyme showed a hyperbolic saturation kinetic, and it was FBP activated in a non-essential manner in which *Km* values for pyruvate and NADH decreased, but in contrast, *E. gracilis* nLDH did not show Mn^{2+} activation at acidic pH values.

Steps of nLDH purification are shown in Table 4. The nLDH activity was measured in the pyruvate reduction direction. The nLDH profile after passing the cytosolic fraction through the blue-sepharose column showed 2 peaks of activity, the first eluting with the washing buffer (blue$^-$) (and which was not further examined), whereas the second was eluted with a 0-1M NaCl gradient (blue$^+$). The concentrated blue$^+$ fractions were loaded onto oxamate-sepharose column previously equilibrated with buffer supplemented with NADH in accord with an ordered the kinetic mechanism as reported for bacterial enzymes, and 1mM FBP, to increase the affinity for insoluble oxamate [23]. Similar to the elution profile of a cell extract from *Lactobacillus planatarum* which contains variable proportions of both, D- and L-specific nLDHs [23], the blue$^+$ showed two peaks of activity (Fig. 2), the specific D-lactate dehydrogenase activity (D-nLDH), that eluted with the washing buffer, and the specific L-lactate dehydrogenase activity (L-nLDH), which remained strongly adsorbed to the resin but eluted when NADH in the buffer was discontinued (Fig. 2, Table 4). These two nLDH activities were determined in the direction of pyruvate consumption (Table 4). SDS-PAGE of both D- and L-nLDH enriched fractions showed a 35 kDa protein, which was accompanied by significant amounts of other contaminating proteins (data not shown). Exclusion molecular chromatography showed molecular weights of approximately 130 kDa suggesting a tetramer for both enzymes (data not shown) as reported by bacterial D- and L-LDH [24, 29]. The kinetic parameters (*Km* values for pyruvate and NADH) of the partially purified *E. gracilis* D- and L-nLDH (Table 5) were similar to those of bacterial nLDHs [23, 26, 28]. In this preparation, the NAD^+-dependent L-lactate oxidation was negligible (Table 5). The intersecting pattern for both substrates in a double reciprocal plot for *E. gracilis* L-nLDH fitted well with a steady-state bi-bi ordered mechanism but also with a rapid equilibrium random mechanism (Fig. 3). However, L-nLDH was adsorbed to the sepharose-oxamate column only in the presence of NADH; this observation was consistent with a steady-state bi-bi order mechanism (Scheme 2), in agreement with other bacterial FBP-activated nLDHs [23, 24]. The *E. gracilis* L-nLDH showed a 2- and 3-fold activation by 30 mM K^+ and 150 mM NH_4^+, respectively (data not shown). Activation by K^+ and NH_4^+ has been reported

for many other enzymes in which a cation is very important to maintain the three-dimensional structure of the protein [38-40].

The semi-purified D-nLDH showed different *Km* values for both NADH and pyruvate in comparison to L-nLDH (Table 5). D-lactate exerted a mixed-type inhibition (Fig. 4) on D-nLDH with a relatively high *Ki* value (Table 5). Similar to D-nLDH from bacteria, *E. gracilis* enzyme showed a bi-bi ordered mechanism (data not shown). These data suggested that D-nLDH and L-nLDH are unidirectional enzymes and that the former may be inhibited by its product, depending on the cell growth conditions. In agreement with all bacterial D-nLDH [22], the enzyme from *Euglena* did not show activation by either FBP or cations (data not shown).

4. DISCUSSION

The energy metabolism in *E. gracilis* seems to be closely linked to the mitochondrial lactate oxidation which relies on the functioning of a lactate shuttle constituted by D- and L-iLDH, and by D- and L-nLDH. The molecular weight, cofactor nature, flavine/enzyme ratio, and substrate specify determined for the *E. gracilis* D-iLDH were almost identical to those reported for bacterial and yeast enzymes [4, 16]. However, the ability to reduce quinones strongly suggested a common origin for *Euglena* and bacterial D-iLDH [16, 17, 19]. *E. gracilis* L-iLDH was inhibited by diphenyleneiodonium suggesting a flavine as cofactor. Similar to the bacterial enzymes [19], *E. gracilis* L-iLDH was inactivated by detergent solubilization suggesting that both, *Euglena* and bacterial L-iLDH require lipids for keeping the three dimensional structure and function.

Previously, we determined milimolar intracellular concentrations of L- and D-lactate in *Euglena* [12]. In all organisms, L-lactate is produced exclusively by the cytosolic NAD^+-dependent lactate dehydrogenase from pyruvate and NADH. In *E. coli* and other bacteria, D-lactate is the final product of glycolysis as well the

methylglyoxal pathway; in eukaryotic organisms, D-lactate is produced exclusively by enzymes located in the methylglyoxal pathway (Glyoxylase I and II). In this work, the existences of different nLDHs specific for the D- and L-lactate production were described. FBP and divalent cations-activated L-nLDH are widespread in homo and hetero fermentative bacterial systems [22-28], Regardless the a high identity percentage among the amino acid sequences of bacterial L-nLDH has been found (until 66%), profound differences in the enzyme kinetics of the FBP-activated L-nLDH have been described. FBP activation can be essential [22, 25, 26, 29] or non-essential [21, 23, 24, 27, 28]; the enzyme may show hyperbolic or sigmoidal kinetic pattern respect to pyruvate [25, 26]. These observations are indicative that probably these enzymes diverged recently [30]. In this work we found that heterotrophic *Euglena* have specific enzymes for both, the production (nLDHs) and the oxidation (iLDHs) of D- and L-lactate for enzymes that only found in bacterial systems. The preservation of the iLDH enzymes in a eukaryotic organism like *Euglena* may have originated with the absence of a pyruvate dehydrogenase to oxidize pyruvate in aerobic conditions [32]. In contrast, the FBP-activated L-nLDH does not a characteristic feature even among bacteria, suggesting that the enzyme in *Euglena* was probably, a lateral gene transfer event which appears to be common in this protist [33-35]. *Trypanosoma sp.*, the most closely phylogenetic relative of *Euglena*, produces D-lactate by glyoxylase II only, because D-nLDH does not exist in this parasite [31]. The presence of D-nLDH does not exclude that *E. gracilis* may produce D-lactate by means of the methylglyoxal pathway due to methylglyoxal is toxic and its produced during high rates of glycolysis, which appears to be usual in *Euglena* when paramylon catabolism has started; although these remains to be elucidated.

REFERENCES

1. Ingledew, W. J., and Pool, R. K. (1984) The respiratory chains of *Escherichia coli*. *Microbiol. Rev.* **48**, 222-271.

2. Daum, G., Ovni, P. C., and Schatz G. (1982) Import of proteins into mitochondria. Cytochrome b_2 and cytochrome *c* peroxidase are located in the intermembrane space of mitochondria. *J. Biol. Chem.* **257**, 13028-13033.
3. Garvie, E. I. (1980) Bacterial lactate dehydrogenases. *Microbiol. Rev.* **44**, 106-139.
4. Lodi, T., and Ferrero, Y. (1993) Isolation of the DLD gene of *Saccharomyces cerevisiae* encoding the mitochondrial enzyme D-lactate ferricytochrome *c* oxidoreductase. *Mol. Gen. Genetic* **238**, 315-324.
5. Fewson, C. A., Baker, D. P., Chalmers, R. M., Keen, J. N., Hamilton, I. D., Scott, A. J., and Yasin, M. (1993) Relationships amongst some bacterial and yeast lactate and mandelate dehydrogenases. J. *Gen. Microbiol.* **139**, 1345-1352.
6. Taguchi, H., and Ohta, T. (1991) D-lactate dehydrogenase is a member of the D-isomer-specific 2-hydroxyacid dehydrogenase family. *J. Biol. Chem.* **266**, 12588-12594.
7. Haugaard, N. (1968) D- and L-lactic acid oxidase of *E. coli*. *Biochim. Biophys. Acta* **31**, 66-72.
8. Iuchi, S., Lin E. C. C. (1988) *arc* A (dye), a global regulatory gene in *Escherichia coli* mediating repression of enzymes in aerobic pathways. *Proc. Natl. Acad. Sci. USA* **85**, 1888-1892.
9. Somlo, M. (1965) Induction des lactico-cytochrome *c* reductase (D- et L-) de la leuvre aerobie par les (D- et L-). *Biochim. Biophys. Acta* **97**, 183-201.
10. Jasso-Chávez, R., Torres-Márquez M. E., and Moreno-Sánchez, R. (2001) The membrane-bound L- and D-lactate dehydrogenase activities in mitochondria from *Euglena gracilis*. *Arch. Biochem. Biophys.* **390**, 295-303.
11. Moreno-Sánchez, R. Covián, R., Jasso-Chávez, R. Rodríguez-Enríquez, S., Pacheco-Moisés, F., and Torres-Márquez, M.E. (2000) Oxidative phosphorylation supported by an alternative respiratory pathway in mitochondria from *Euglena*. *Biochim. Biophys. Acta* **1457**, 200-210.

12. Jasso-Chávez, R. and Moreno-Sánchez, R. (2003) Cytosol-mitochondria transfer of reducing equivalents by a lactate shuttle in heterotrophic *Euglena*. *Eur. J. Biochem.* **270**, 4942-4951.
13. Moreno-Sánchez, R. and Raya, J. C. (1987) Preparation of coupled mitochondria from *Euglena* by sonication. *Plant Sci.* **48**, 151-157.
14. Bergmeyer, H. U. (1983) Methods of Enzymatic Analysis, 3-9 (Bergmeyer, H. U., ed.), Weinheim Verlag Chemie, Germany.
15. Armstrong, J. M. (1964) The molar extinction coefficient of 2, 6-dichlorophenol indophenol. *Biochim. Biophys. Acta* **86**, 194-197.
16. Futai, M. (1973) Membrane D-lactate dehydrogenase from *Escherichia coli*. Purification and properties. *Biochemistry* **12**, 2468-2474.
17. Allison, N., O´Donell, M. J., Hoey, M. E., and Fewson, C. A. (1985) Membrane-bound lactate dehydrogenase and mandelate dehydrogenase of *Acinetobacter calcoaceticus*. *Biochem. J.* **231**, 407-416.
18. Pratt, E. A., Fung, L. W-M., Flowers, J. A., and Ho C. (1979) Membrane-bound D-lactate Dehydrogenase from *Escherichia coli*: purification and propierties. *Biochemistry* **18**, 312-316.
19. Erwin, A. L., and Gotschlich, E. C. (1993) Oxidation of D-lactate and L-lactate by *Neisseria meningitidis*: Purification and cloning of meningococcal D-lactate dehydrogenase. *J. Bacteriol.* **175**, 6382-6391.
20. Buetow, D. E. (1989) The mitochondrion. In The Biology of *Euglena*, Vol. IV (Buetow, D. E., ed) pp 247-314. Acad. Press, New York.
21. Smillie, R. M. (1968) Enzymology of *Euglena*. In The Biology of *Euglena*, Vol. II (Buetow, D. E., ed), pp. 2-54, Acad. Press, New York.
22. Hensel, R., Mayr, U., Stetter, K. O., and Kandler, O. (1977) Comparative studies of lactate dehydrogenases in lactic acid bacteria: Amino-acid composition of an active-site region and chemical properties of the L-lactate dehydrogenase of *Lactobacillus casei*, *Lactobacillus curvatus*, *Lactobacillus plantarum*, and *Lactobacillus acidophilus*. *Arch. Microbiol.* **112**, 81-93.
23. Kelly, N., Delaney, M., and O´Carra, P. (1978) Affinity Chromatography of bacterial Lactate dehydrogenases. *Biochem. J.* **171**, 543-547.

24. Hardman, M. J., Pritchard, G. G. (1987) Kinetics of activation of L-lactate dehydrogenase from *Streptococcus faecalis* by fructose 1, 6-bisphosphate and by metal ions. *Biochim. Biophys. Acta* **912**, 185-190.

25. Iwata, S., and Ohta, T. (1993) Molecular basis of allosteric activation of bacterial L-lactate dehydrogenase. *J. Mol. Biol.* **230**, 21-27.

26. Fushinobu, S., Kamata, K., Iwata, S., Sakai, H., Ohta, T., and Matsuzawa, H. (1996) Allosteric activation of L-lactate dehydrogenase analyzed by hybrid enzymes with effector-sensitive and insensitive subunits. *J. Biol. Chem.* **271**, 25611-25616.

27. Wyckoff, H. A., Chow, J., Whitehead, T. R., Cotta, M. A. (1997) Cloning, sequence, and expression of L-(+) lactate dehydrogenase of *Streptococcus bovis*. *Curr. Microbiol.* **34**, 367-373.

28. Arai, K., Kamata, T., Uchikoba, Y., Fushinobu, S., Matsuzawa, H., Taguchi, H. (2001) Some *Lactobacillus* L-lactate dehydrogenases exhibit comparable catalytic activities for pyruvate and oxaloacetate. *J. Bacteriol.* **183**, 397-400.

29. Arai, K., Hishida, A., Ishiyama, M., Kamata, T., Uchikoba, H., Fushinobu, S., Matsuzawa H., and Taguchi, H. (2002) An absolute requirement of fructose 1, 6-bisphosphate for the *Lactobacillus casei* L-lactate dehydrogenase activity induced by a single amino acid substitution. *Prot. Eng.* **15**, 35-41.

30. Taguchi, H., and Ohta, T. (1992) Unusual amino acid substitution in the anion-binding site *Lactobacillus plantarum* non-allosteric L-lactate dehydrogenase. *Eur. J. Biochem.* **209**, 993-998.

31. Cazzullo, J. J. (1992) Aerobic fermentation of glucose by trypanosomatids. *FASEB J.* **6**, 3153-3161.

32. Inui, H., Miyatake, K., Nakano, S., and Kitaoka, S. (1985) The physiological role of oxygen-sensitive pyruvate dehydrogenase in mitochondria fatty acid synthesis in *Euglena gracilis*. *Arch. Biochem. Biophys.* **237**, 423-429.

33. Palmer, J. D., and Delwiche, C. F. (1996) Second-hand chloroplasts and the case of the disappearing nucleus. *Proc. Natl. Acad. Sci. USA* **93**, 7432-7435.

34. Figge, R. M., Schubert, M., Brinkmann, H., and Cerff, R. (1999) Glyceraldehyde-3-phosphate dehydrogenase gene diversity in eubacteria and eukaryotes: evidence for intra- and inter-kingdom gene transfer. *Mol. Biol. Evol.* **16**, 429-444.

35. Matsui, K., Ishii, N., Kawabata, Z. (2003) Release of extracellular transformable plasmid DNA from *Escherichia coli* co cultivated with algae. *Appl. Environ. Microbiol.* **69**, 2399-2404.

36. Segel, Y. H. (1975) Enzyme Kinetics, John Wiley & Sons, Inc. New York.

37. Chakraborty, S., and Massey, V. (2002) Reaction of reduced flavins and flavoproteins with diphenyliodonium chloride. *J. Biol. Chem.* **277**, 41507-41516.

38. Beet G. F., Poole, P. L., Springham, M. G., and Bostran K. A. (1979) Kinetic and spectroscopic evidence of cation-induced conformation changes in yeast K^+-activated aldehyde dehydrogenase. *Biochem. J.* **183**, 633-646.

39. Xiang, B., Taylor, J. C., Markham, G. D. (1996) Monovalent cation activation and kinetic mechanism of inosine 5' monophosphate dehydrogenase. *J. Biol. Chem.* **271**, 1435-14440.

40. Valenzuela-Soto, E. M., Velasco-García, R., Mujica-Jimenez, C., Gaviria-Gonzalez, L. L., and Muñoz-Clares, R. A. (2003) Monovalent cations requirements for the stability of betaine aldehyde dehydrogenase from *Pseudomonas aueruginosa*, porcine kidney and amaranth leaves. *Chem. Biol. Interac.* **143-144**, 139-148.

41. Kim, J., Chung, T. D., and Kim, H. (2001) Determination of biologically active acid based on the electrochemical reduction of quinone in acetonitrile + water mixed solvent. *J. Electroanalytical Chem.* **499**, 78-84.

Figure legends.

Figure 1. **Purification of mitochondrial D-iLDH from *E. gracilis*.** A) D-iLDH purification by heat treatment. 5 μg protein were loaded in a 10 % acrylamide gel and stained with silver. Lane 1, molecular weight markers; lane 2, mitochondria; lane 3, solubilized mitochondria; and lane 4, heat treatment. B) 5 μg protein was electrophorased in a native 7.5% acrylamide gel. Activity was revealed with 0.001% PMS, 0.001% NBT and 10 mM D-lactate. Right lane was stained with silver.

Figure 2. **Elution profiles of nLDH from affinity chromatography**. A) Blue-sepharose chromatography. Buffer (Buffer HE) flux was1.5 mL/min. Dashed line shows the 0-1 M NaCl gradient. B) Sepharose-oxamate chromatography. Buffer flux was 1 min/mL. HE buffer was supplemented with 50 μM NADH and 1mM FBP. Dashed line shows when NADH and FBP were omitted in the washing buffer. The volume of the fractions was 6 mL (□) Absorbance at 280 nm, (•) pyruvate reductase activity.

Figure 3. **Kinetic mechanism of the L-nLDH**. Activity was measured at room temperature in HE buffer pH 7.0 supplemented with 1mM FBP and 15-20 μg protein of partially purified enzyme. A) The nLDH activity was determined at different pyruvate concentrations: 0.2 (■), 0.5 (•), 0.75 (▲), 1 (▼) and 5 mM (♦). B) Double reciprocal plot at different NADH concentrations: 5 (■), 10 (•), 20 (▲), 40 (▼) and 80 μM (♦). Straight lines derived for nonlinear regression analysis of the experimental points fitted to the equation for a steady-state bi-bi ordered mechanism [36].

Figure 4. **Inhibition of D-nLDH pyruvate reduction by D-lactate.** A) Activities were measured at room temperature in HE buffer pH 7.0, varying the pyruvate concentrations at a fixed concentration of 0.25 mM NADH in absence (□), or presence of 6 mM (○), 10 mM (Δ), 15 mM (▽), and 30 mM (◊) D-lactate. B) Double reciprocal plot. The straight lines shown were derived from nonlinear regression analysis of the experimental points fitted to a mixed-type inhibition [36]:

$v = S \times Vm/ [1+ (I/(\alpha \times Ki)]/ [Km \times ((1+ (I/Ki))/ (1+ (I/(\alpha \times Ki))) + S]$,

where *v* is the velocity; S is the pyruvate concentration; *Vm* is the maximal velocity, I is D-lactate concentration, *Km* is the Michaelis-Menten constant, *Ki* is the inhibition constant, and α is the factor by which the substrate and inhibitor dissociation constants are affected when enzyme is in presence of the inhibitor.

Table 1. **Purification of the D-iLDH from *E. gracilis***

	Total protein (mg)	**Specific activity nmol/min x mg Prot**	**Total Activity nmol/min**	**Times of purification**	**Yield (%)**
Mitochondria	51 ± 8	210 ± 82	10, 700 ± 2190	1	100
Solubilized mitochondria	21 ± 2.0	510 ± 100	10, 710 ± 180	2.4	100
60°C 45´ supernatant	1.57 ± 0.25	6000 ± 1400	9450 ± 1500	29	88 ± 6

Values showed are the mean ± SE at least 4 mitochondria preparations.

Table 2. **Kinetic parameters of the D-iLDH from *E. gracilis***

	E. gracilis **D-iLDH**	***E.gracilis*** **Mitochondria ***	***E. coli*** **D-iLDH ****
Km D-lactate (mM)	2.0 ± 0.8	2.7 ± 0.3	1.0
Km DCPIP (μM)	10	35 ± 5	----
Vm (nmol DCPIP/min x mg)	6000 ± 1400	480 ± 40	15,000
Km Q1 (μM)	8.1	18.5 ± 5	8.5
Vm (nmol Q1/min x mg)	7000	0.62 ± 0.07	-----
Km TCHQ (μM)	21	30	-----
Vm (nmol TCHQ/min x mg)	1480	310	-----
Ki oxalate (mM)	0.14 (Mixed type)	0.09 (Mixed type)[b]	0.001
Ki L-lactate (mM) [a]	10 (Mixed type)	19 (Competitive)	16 (Substrate)
$K_{0.5}$ Triton X-100 (%)	0.005	Non effect	0.003

* Data obtained with freshly prepared mitochondria [10]. ** Data reported by Futai [16]. [a] This parameter was determined in CHAPS-solubilized mitochondria. [b] The global linear regression analysis of the oxalate inhibition data best fitted to a mixed-type inhibition (see legend fig. 4 for equation). The factor α was 7 and 4 for oxalate and L-lactate, respectively.

Table 3. **Kinetic parameters of nLDH from *E. gracilis***

Parameters were determined in a cytosolic fraction at room temperature (27°C) in HE buffer. Values shown are the mean ± S. E. of 4 different preparations.

	- FBP	**+ 0.8 mM FBP**
V_m (nmol NADH ox/min x mg prot)	135 ± 5	154 ± 20
$K_{m\ pyruvate}$ (mM)	1.1 ± 0.1	0.47 ± 0.03
$K_{m\ NADH}$ (μM)	82 ± 9	24 ± 3
$K_{i\ oxamate}$ (mM)	1.2 (competitive)	---------

* $K_{0.5}$ value for FBP in the presence of 0.25 mM NADH and 0.5 mM pyruvate was 0.22 ± 0.03 mM and the nLDH activity in the absence of FBP was 26 ± 9 nmol $NADH_{ox}$ /min x mg cytosolic prot.

Table 4. **Separation of the cytosolic D-nLDH and L-nLDH from *E. gracilis***

Enzymatic activity was measured in HE buffer plus 0.15 M ammonium sulfate. Concentration of NADH and pyruvate were 0.25 and 5 mM, respectively.

	Total Protein (mg)	Specific activity (nmol NADH $_{ox}$ /min x mg prot)	Total activity (nmoles /min)	Times of purification	Yield (%)
nLDH					
Homogenate	22,472	15	337,080	1	100
Cytosol	4,240	75	318,000	5	94
70% saturation $(NH_4)_2SO_4$	512	276	141,400	18.5	42
L-nLDH *					
Blue-seph	5.2	9,025	46,930	601	14
Oxamato-seph	2.0	11,401	22,802	760	6.8
D-nLDH**					
Oxamato-seph$^-$	16.4	4,380	70,550	292	21

* Oxamate-sepharose pooled fractions produced 3350 nmol L-lactate/ min x mg prot., and did not produce D-lactate. ** Oxamate-seph$^-$ pooled fractions (enzyme activity did not bind to the resin) produced 4,350 nmol D-lactate / min x mg prot., but did not produce L-lactate (see the text). Times of purification were calculated using the increment of specific activity in each step/specific activity in homogenate.

Table 5. **Kinetic parameters of the semi purified D-nLDH and L-nLDH**

L-nLDH activity was measured in the presence of 1 mM FBP.

	D-NAD^+-LDH	L-NAD^+-LDH
Km $_{Pyruvate}$ **(mM)**	0.15	0.44
Km $_{NADH}$ **(μM)**	41	8
Vm **(nmol** $NADH_{ox}$ **/min x mg prot)**	4200	4500
Vm **(nmol** $NADH_{red}$ **/min x mg prot)**	20	1
Kia $_{NADH}$ **(μM)**	-------	28
Ki $_{D\text{-}lactate}$ **(mM)**	15 (mixed type) α= 4.5	--------

Kia and *Ki* $_{D\text{-}lac}$ are the dissociation constants for NADH and D-lactate respectively.

Figure 1

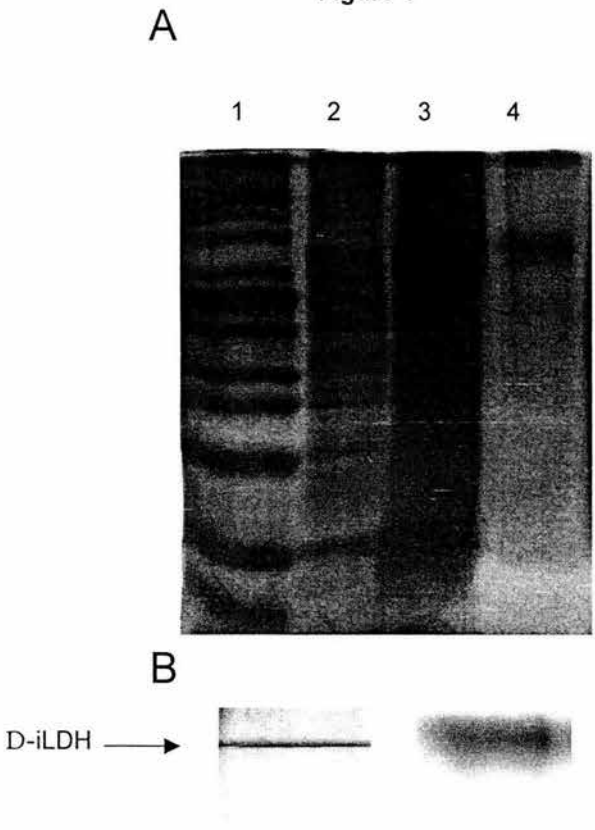

Figure 2

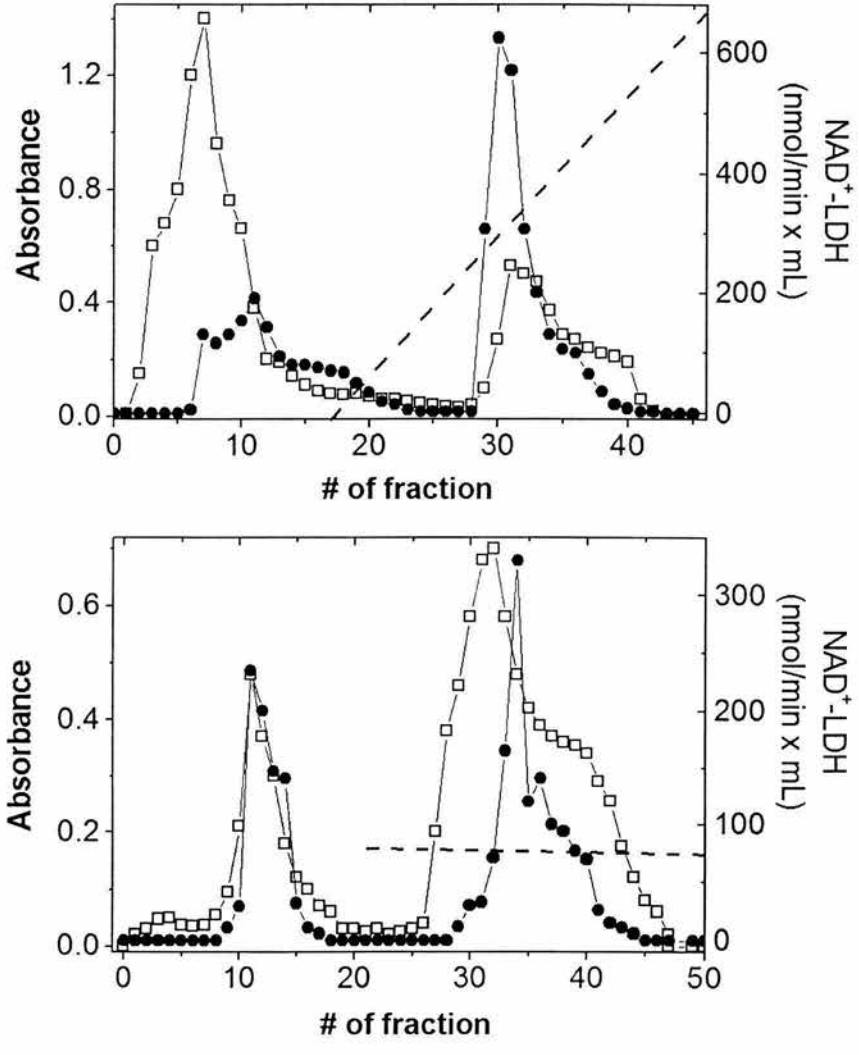
Absorbance
NAD+-LDH (nmol/min x mL)
# of fraction
Absorbance
NAD+-LDH (nmol/min x mL)
# of fraction

Figure 3

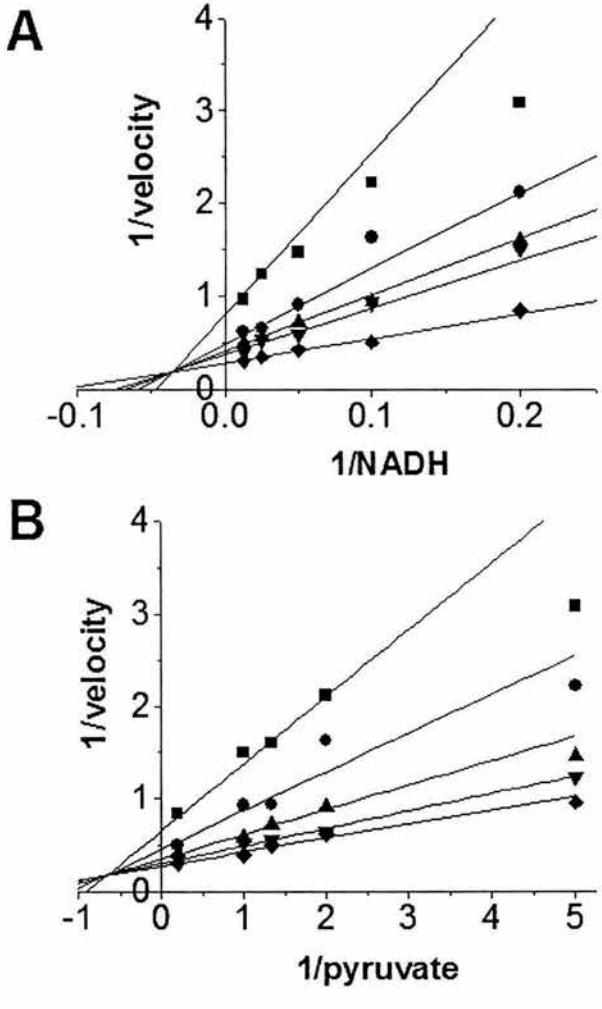
A
1/velocity
4
3
2
1
0
-0.1
0.0
0.1
0.2
1/NADH
B
1/velocity
4
3
2
1
0
-1
0
1
2
3
4
5
1/pyruvate

Figure 4

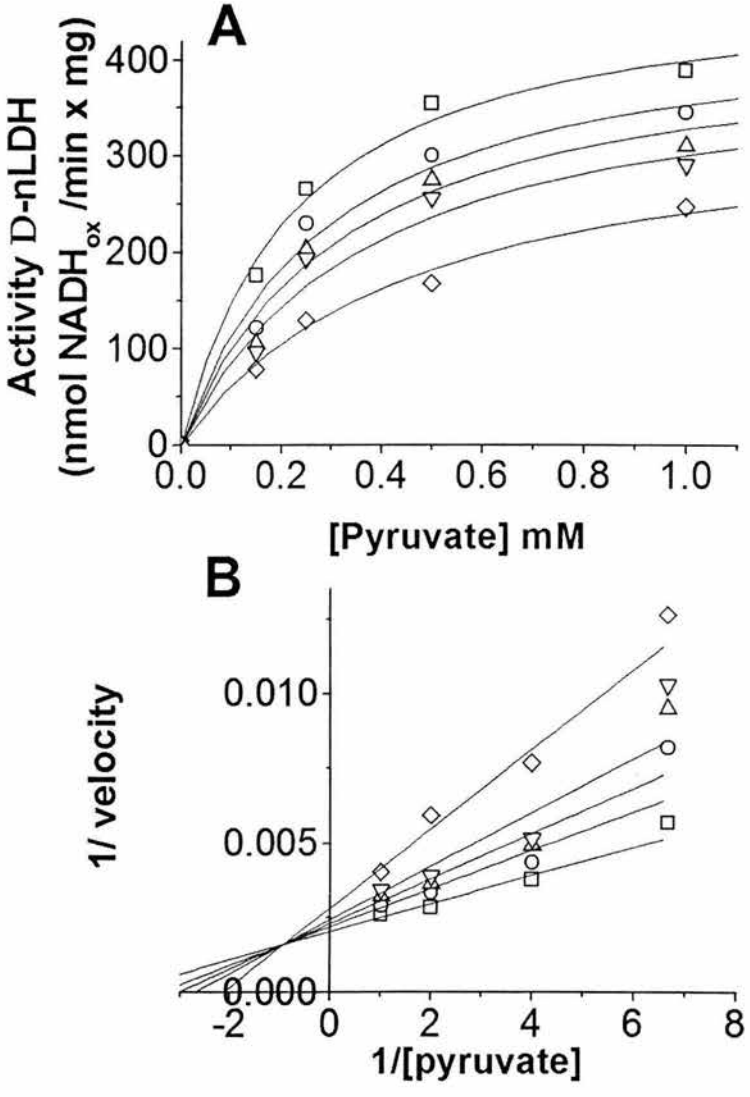
A
Activity D-nLDH
(nmol NADH$_{ox}$ /min x mg)
400
300
200
100
0
0.0
0.2
0.4
0.6
0.8
1.0
[Pyruvate] mM
B
1/ velocity
0.010
0.005
0.000
-2
0
2
4
6
8
1/[pyruvate]

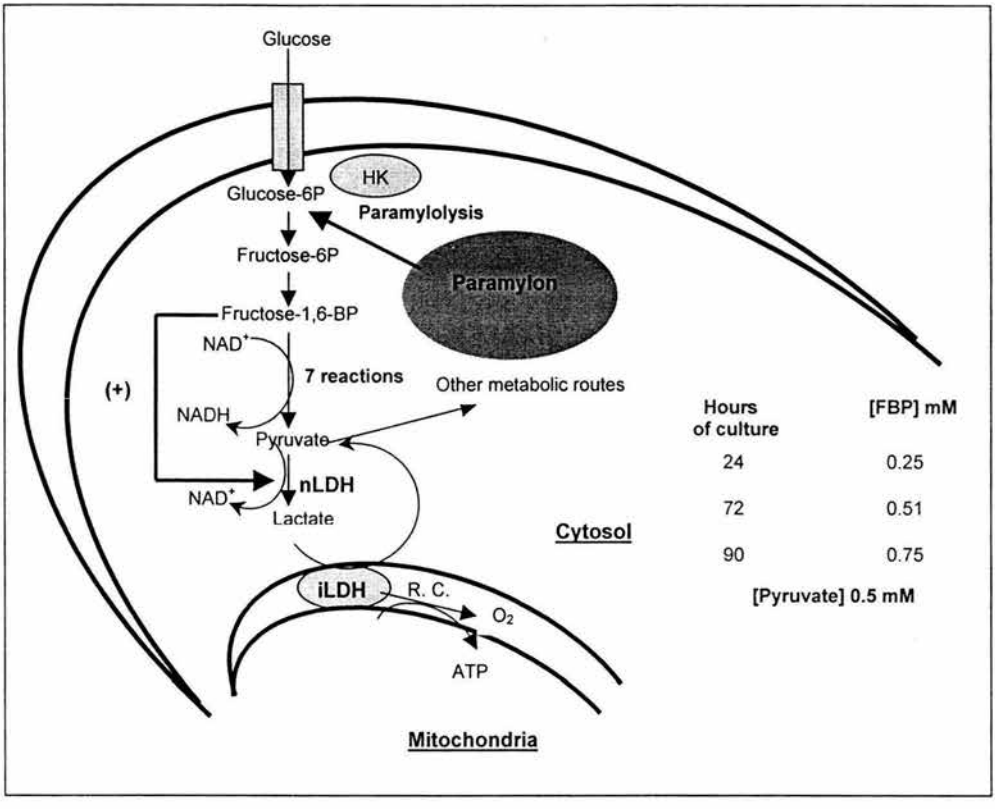

Scheme 1. **Effect of FBP over L-lactate production in *E. gracilis***. Catabolism of paramylon starts when external carbon source has been exhausted (~72 hours) and bringing about the elevation of the glucose-6-phosphate intracellular concentration (from 7 up to 15 mM). In parallel, the intracellular concentration of FBP continuously increases, which may stimulate the rate of glycolysis yielding a higher L-lactate production, and consequently an enhanced ATP synthesis [12]. HK, hexokinase; nLDH, cytosolic lactate dehydrogenase; iLDH, mitochondrial membrane-bound NAD^+- independent lactate dehydrogenase; R. C., respiratory chain. Other metabolic routes: malic enzyme, pyruvate decarboxylase, alanin transaminase, glycolate pathway.

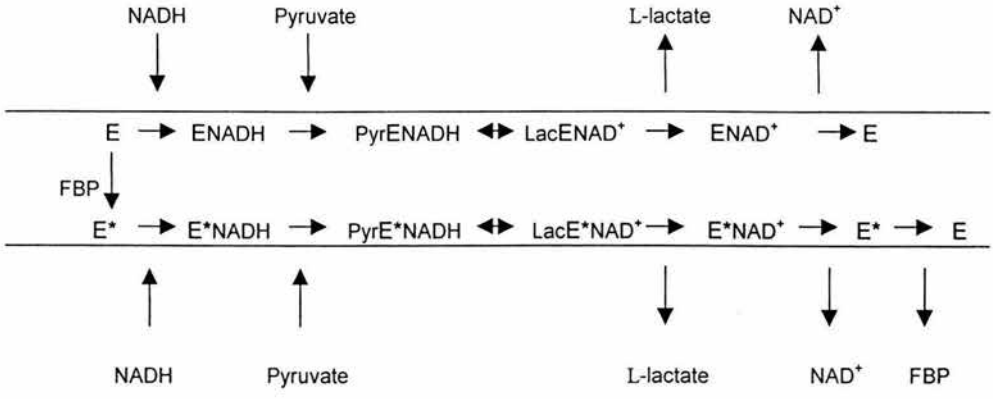

Scheme 2. **Cleland diagram showing the steady-state bi-bi ordered kinetic mechanism of the *E. gracilis* L-nLDH from.** E, free enzyme; E*, free enzyme activated by FBP; FBP, fructose-1, 6-bisphosphate; Pyr, pyruvate; Lac, L-lactate.

Hubo algunos en la primera versión de este trabajo que no se mostraron. Sin embargo, es importante mencionarlos en la tesis y se discuten a continuación:

Con las preparaciones de actividad específica alta de la D-iLDH determinamos algunos parámetros cinéticos de la D-iLDH los cuales mostramos en la Tabla 1 del trabajo. Asimismo, determinamos por fluorescencia que la D-iLDH es una flavoproteína, ya que la enzima mostró 2 máximos de excitación a 366 y 450 nm y un máximo de emisión a 520, característicos de las flavinas (Fig. 7).

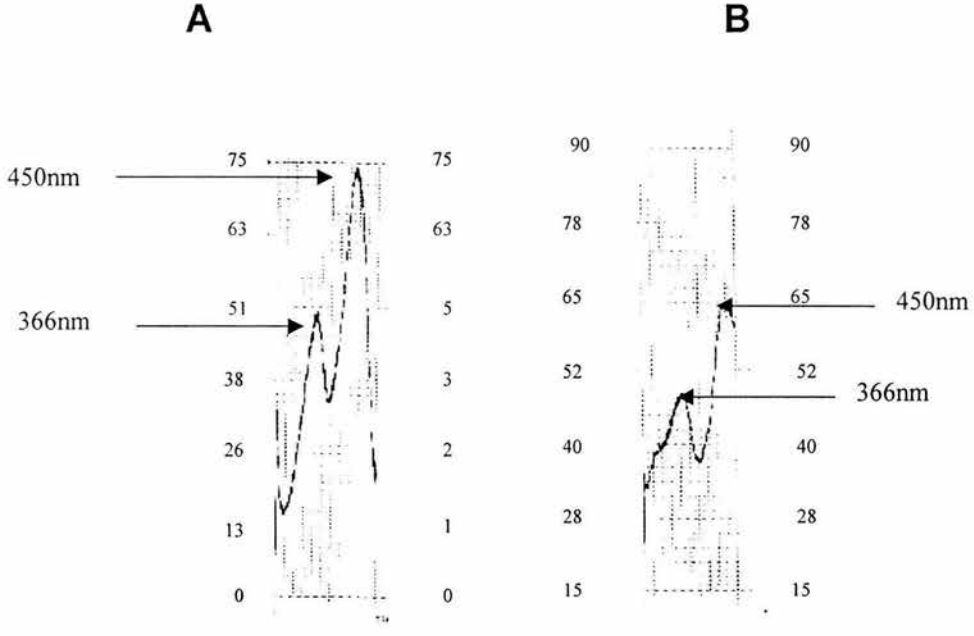

Figura 7. **Espectros de fluorescencia de la D-iLDH de *Euglena gracilis***. A) Se adicionaron 5 nmoles de riboflavina en 2 mL de una solución de citratos 50 mM a pH de 3.5, y en B) 0.7 mg de mitocondrias solubilizadas con CHAPS, la señal se registró a una λ de emisión fija de 520 nm y se varió la λ de excitación.

En cuanto a NAD^+-L-LDH citosólica, determinamos que a diferencia de algunas de las enzimas bacterianas activadas por FBP, la enzima de *Euglena* no se activó por Mn^{2+} o Co^{2+}. Sorprendentemente, esta enzima se activó por cationes monovalentes; dos veces por K^+ 30 mM y tres veces por NH_4^+ 150 mM. El efecto del K^+ y del NH_4^+ se ha reportado en muchas otras deshidrogenasas en las cuales la presencia de K^+ es muy importante para mantener la estructura tridimensional de la enzima (Bett y cols, 1979; Xiang y cols, 1996; Valenzuela-Soto y cols, 2003). La NAD^+-D-LDH de *Euglena* pudo oxidar D-lactato a una velocidad de 20 nmoles NAD^+_{red}/ min x mg, no fue activada por FBP ni por metales mono y divalentes al igual que las enzimas bacterianas.

V

DISCUSIÓN GENERAL

A diferencia de la cadena respiratoria de mamíferos, las de los microorganismos presentan ramificaciones en cuanto a deshidrogenasas y oxidasas terminales se refiere (Covián, 2002). En los sistemas bacterianos las deshidrogenasas que alimentan la cadena respiratoria son muy variadas y diferentes a las de mamíferos. Sustratos como NADH, etanol, metanol, fumarato, orotato, succinato y lactato son algunos ejemplos de la gran variedad de metabolitos oxidables en bacterias. Esta gran cantidad de deshidrogenasas y demás enzimas conectadas con la cadena respiratoria, confieren a los microorganismos una ventaja para sobrevivir y duplicarse en condiciones adversas. *Euglena* es un protista de vida libre capaz de duplicarse en muchas condiciones tanto silvestres como de laboratorio, y esto se debe muy probablemente a la gran variedad de deshidrogenasas y de enzimas múltiples que le permiten obtener ATP para duplicarse aún en presencia de inhibidores biológicos como cianuro, peróxido de hidrógeno, mixotiazol, antimicina y metales pesados (Moreno-Sánchez y cols., 2000; Castro-Guerrero y cols, 2004; Mendoza-Cózatl y cols., 2002). Así, la descripción de deshidrogenasas específicas para la oxidación del D- y L-lactato en la cadena respiratoria tuvo dos aportaciones: la primera fue el avance en el esclarecimiento de la cadena respiratoria de *Euglena* y la segunda que estableció que este protista es el único eucarionte de vida libre que posee constitutivamente ambas iLDH con las mismas características (participación fisiológica, localización celular, aceptor de electrones, sensibilidad a los mismos inhibidores, termoestabilidad, peso molecular y cofactor) que sus contrapartes bacterianas (Futai, 1970; Markwell y Lascelles, 1978; Garvie, 1980). Esto último sugiere que estas enzimas comparten un origen común, mientras que las iLDH de las levaduras, son totalmente diferentes en cuanto a su localización, estructura, aceptor de electrones e incluso, en su participación fisiológica (Lodi y Ferrero, 1993; Somlo, 1963).

Para poder determinar la participación de la D-iLDH y L-iLDH en el metabolismo energético de *Euglena*, se determinó la actividad de estas enzimas a lo largo del crecimiento celular y su aporte a la producción de ATP para la duplicación celular. También se determinó la concentración de los dos isómeros del lactato, sus variaciones durante el crecimiento celular y la relación de éstos y otros metabolitos con el aporte energético celular. Los resultados fueron muy interesantes en cuanto a que ambas iLDH se expresaron constitutivamente sin importar la fase de crecimiento ni la fuente de carbono externa, característica que en bacterias y levaduras no existe, ya que la expresión de estas enzimas depende de la presencia de lactato en el medio de cultivo y de la disponibilidad de oxígeno (Iuchi y Lin, 1997; Somlo, 1965). En *Euglena* la expresión de las iLDH no dependió de la fuente externa de carbono debido a las altas concentraciones intracelulares de D- y L-lactato, pero sí dependió de la disponibilidad de oxígeno y estuvo fuertemente ligada a la degradación de paramilo. Uno de los resultados más importantes fue el determinar una vía de utilización del lactato no reportada previamente en ningún otro organismo. Este modelo propone la participación de cuatro enzimas; la D- y L-lactato deshidrogenasas citosólicas dependientes de NAD^+, que reducen al piruvato producido en la glucólisis debido a una intensa degradación del paramilo, y produce D- y L-lactato. El lactato es entonces oxidado por ambas iLDH, las cuales ceden directamente los equivalentes reductores a la cadena respiratoria para llevar a cabo la síntesis de ATP. En parásitos como *Trypanosoma* y *Leishmania*, así como en mamíferos, el D-lactato se produce exclusivamente en la vía del metil-glioxal, un metabolito tóxico producido en la parte media de la glucólisis cuando ésta se encuentra muy activa (Cazzulo, 1992; Bari y cols., 2002). Reportamos que al final de la curva de crecimiento en *Euglena* hay una degradación intensa de paramilo para producir glucosa-6-fosfato, la cual es metabolizada en la glucólisis. La acumulación de glucosa en forma de paramilo es 120 veces mayor que la glucosa que pueden acumular otros microorganismos como *Leishmania donovani* (Keegan y Blum, 1992). Esta degradación intensa de paramilo mantiene a la vía glucolítica muy activa (1.6 nmol L-lactato /min x 10^7 cel., y se mantiene constante al menos por 45

minutos), por lo que muy probablemente también produzca metil-glioxal. Así, aún queda por determinar si *Euglena* produce D-lactato por 2 vías, la glucolítica (por la NAD+-D-LDH citosólica) y por la vía del metil-glioxal (por la glioxilasa II).

Recientemente se han propuesto otros modelos de lanzadera de lactato en mamíferos, que incluye la participación de un transportador de L-lactato para su oxidación en la mitocondria. Al parecer esta lanzadera tiene relevancia fisiológica cuando el individuo se encuentra en un estado de ejercicio intensivo (Brook y cols., 2000). El caso del metabolismo del D-lactato en mamíferos es diferente (de Bari y cols., 2003). El D-lactato no necesita ingresar a la mitocondria para ser oxidado y proponen que existe una enzima en a la membrana externa que se encarga de oxidarlo (Bari y cols., 2002).

Una vez identificada la lanzadera de lactato, nos enfocamos al estudio de la cinética y la estructura de los componentes de la lanzadera de lactato. Cinéticamente, la D-iLDH de *Euglena* resultó ser muy similar a las enzimas bacterianas. Además, el peso molecular y la naturaleza del cofactor (Ingledew y Poole, 1989; Futai, 1970) también fueron similares a los de las enzimas bacterianas. Sin embargo, otros aspectos estructurales fueron diferentes. Por ejemplo, la D-iLDH de *E. coli* es una deshidrogenasa periférica membranal, la cual se encuentra unida por un dominio de superficie electropositiva con lisinas y argininas que interactúan con las cargas negativas de los fosfolípidos de la membrana; por esta razón, la D-iLDH de *E. coli* puede solubilizarse utilizando soluciones concentradas de KCl (Dym y cols., 2000). Esto no sucede con la enzima de *Euglena* que requiere necesariamente de detergentes para su extracción de la membrana. La L-iLDH de *Euglena* se inactivó al extraerla de la membrana al igual que las enzimas de bacterias (Erwin y Gotschlich, 1993). A pesar de ello, su pH óptimo alcalino y su capacidad para reducir quinonas son otras similitudes entre esta enzima presente en *Euglena* y las de bacterias.

En esta última parte del proyecto se realizó también la caracterización cinética del componente citosólico de la lanzadera de lactato. Esta enzima realiza la reducción del piruvato casi 200 veces más rápido que la reacción de oxidación del lactato, lo que sugiere que en *Euglena* heterotrófica la única forma de utilizar lactato es por medio de las iLDH. Esta fracción citosólica mostró la existencia de enzimas específicas para la producción de los dos isómeros del lactato, un hecho sólo documentado en las bacterias. Sin embargo, lo más interesante fue que la NAD^+-L-LDH se activó por fructosa-1,6-bifosfato a una concentración intermedia de la concentración intracelular de FBP, la cual varió y alcanzó su máximo al final del cultivo, lo que sugiere que esta activación puede ser relevante durante la fase estacionaria (cuando la célula está sujeta a una restricción en la fuente de carbono y se prepara para enquistarse). La activación de la NAD^+-L-LDH de *Euglena* por FBP apoya la propuesta de una participación esencial de la utilización del lactato para el metabolismo energético de este protista, esto es, un flujo glucolítico continuo hacía la formación del lactato para garantizar así la síntesis de ATP mitocondrial para la duplicación celular (Uribe y Moreno-Sánchez, 1992). La NAD^+-L-LDH también por cationes monovalentes como el K^+ y $(NH_4)^+$, pero aún queda por determinarse si esta activación tiene una razón fisiológica. El hecho de que esta enzima se inhibió por oxamato la hace diferente a la enzima de *Bifidibacterium longum*, la cual muestra una cinética cooperativa y un sitio homotrópico para el piruvato, por lo que su análogo el oxamato es capaz de activarla (Fushinobu, *et al.*, 1996).

Enzimas activadas por FBP como la NAD^+-L-LDH de *Euglena* son comunes en algunas bacterias que llevan a cabo un metabolismo homofermentativo. Estas enzimas presentan diferencias entre ellas mismas, como su cinética, activación por metales divalentes y en algunos casos la activación esencial por FBP, lo que sugiere que estas enzimas aunque muestran un porcentaje de identidad alto (hasta 60%), variaron a su vez por las diferencias en el medio ambiente particular de cada bacteria. De esta forma, la NAD^+-L-LDH de *Euglena* podría compartir un origen común con las enzimas de bacterias. Sin embargo, se requiere purificar a la

enzima y secuenciar el extremo amino terminal para sustentar experimentalmente esta hipótesis.

CONCLUSIONES

1) Las mitocondrias de *Euglena gracilis* poseen enzimas estereo-específicas para la oxidación del D- y L-lactato.
2) El lactato no se internaliza a la mitocondria para su oxidación.
3) La D- y L-iLDH son capaces de reducir quinonas de diferente potencial redox
4) La D- y L-iLDH de *Euglena* se expresan de manera constitutiva sin importar la fuente de carbono y la fase de crecimiento. Sin embargo, su expresión parece estar ligada a la presencia de oxígeno y a la degradación de paramilo.
5) La D- y L-iLDH junto con las NAD^+-LDH del citosol conforman una lanzadera de lactato
6) La D-iLDH es una flavoproteína similar a la de bacterias y probablemente la
   L-iLDH también lo sea.
7) *Euglena* posee deshidrogenasas lácticas específicas para la producción de L- y D-lactato.
8) La NAD^+-L-LDH de se activa por FBP al igual que las enzimas de bacterias homofermentativas.

PERSPECTIVAS

El estudio inicial de la cinética y estructura de los componentes de la lanzadera de lactato de *Euglena* ha originado datos interesantes. Hemos demostrado la existencia de dos enzimas citosólicas que producen D- y L-lactato y dos enzimas mitocondriales acopladas a la cadena respiratoria que los oxidan para la producción de ATP. La D-iLDH es la enzima más estudiada al momento; sin embargo, aún queda por determinar con certeza si su cofactor es FAD o FMN además de poder secuenciar el extremo amino terminal y compararlo con el de las enzimas bacterianas para poder analizar su origen filogenético. La purificación de esta enzima nos da la posibilidad de poder generar anticuerpos y con la ayuda de éstos podríamos determinar la presencia de esta enzima en muchas otras condiciones de cultivo y aun en condiciones de estrés como lo sería cultivar a las células en presencia de inhibidores respiratorios y de metales pesados. Otra vertiente de la investigación que se podría generar con la obtención de anticuerpos anti-D-iLDH, sería el determinar la existencia de esta enzima en los organismos más cercanos filogenéticamente a *Euglena*, como los Tripanosomas y las Leishmanias (Cazzulo, 1997), las cuales producen D-lactato por la vía del metil-glioxal y en donde no se ha caracterizado una D-iLDH.

Con respecto a las deshidrogenasas citosólicas que producen específicamente D- y L- lactato, su caracterización se encuentra en sus inicios y queda mucho por estudiar. Lo primordial es lograr purificar a homogeneidad ambas enzimas, ya que sólo hemos logrado enriquecerlas. En este nuevo proyecto, hemos determinado algunas constantes cinéticas de las NAD^+-L-LDH como la *Km* y *Ki* por sus sustratos y por el oxamato, respectivamente; así como el efecto de la FBP, Mn^{2+}, K^+ y $(NH_4)^+$ sobre su actividad. También se encontró que el mecanismo cinético de reacción se ajusta a un modelo bi-bi ordenado. Falta determinar aún la *Ka* por FBP y otros análogos de la fructosa así como el efecto por otros cationes divalentes y monovalentes (Mg^{2+}, Co^{2+}, Na^+, Li^+ y Cs^+). En las enzimas bacterianas alostéricas, el mecanismo de activación por FBP puede ser

de dos formas, por desplazamiento del equilibrio de la enzima libre inactiva a la forma de la enzima-FBP activa o la inducción de la tetramerización a partir de dos dímeros. En el caso de la NAD^+-L-LDH de *Euglena*, la forma de activación de la FBP se determinará haciendo geles nativos de actividad en presencia y ausencia de FBP y K^+ para determinar si la adición de estos activadores induce un complejo de mayor peso molecular con respecto a la actividad de la enzima sin activadores.

La NAD^+-D-LDH de *Euglena* fue detectada por actividad (en el sentido de la reducción de piruvato) en la fracción que no se unió a la resina de afinidad de sefarosa-oxamato y que se determinó producía D-lactato. Así, aún queda por determinar su pH óptimo, especificidad de sustratos y el mecanismo cinético de reacción, aunque todas las deshidrogenasas productoras de D-lactato muestran un mecanismo cinético bi-bi ordenado, en el cual el NADH es el primer sustrato en unirse a la enzima.

Finalmente, en cuanto a la L-iLDH, ahora sabemos que será muy difícil purificarla debido a que se inactiva durante el proceso de purificación que utilizamos, que toma entre 3 y 4 días. Sin embargo, por medio de la biología molecular podríamos lograr su sobre expresión para facilitar su purificación y poder esclarecer la naturaleza de su flavina, su masa molecular y su secuencia primaria. De hecho, con la ayuda de una biblioteca genómica de *Euglena* hecha con cDNA, la cual hemos conseguido recientemente, pensamos lograr la sobre expresión de los cuatro componentes de la lanzadera para obtener cantidades altas de proteína y así poder avanzar en su estudio. La obtención de las enzimas puras nos dará nuevamente la posibilidad de generar anticuerpos que podrían ser muy útiles para determinar la expresión de estas enzimas en condiciones variadas, por ejemplo; nosotros demostramos que la actividad de la D- y L-iLDH era entre 9 y 15 veces menor en mitocondrias aisladas de células cultivadas en condiciones de baja tensión de oxígeno. Sin embargo, falta determinar si este cambio es debido a una disminución de la cantidad de mitocondrias o a la disminución en la expresión de éstas enzimas. Así mismo faltaría esclarecer si las

deshidrogenasas lácticas del citosol están reguladas también por la disponibilidad de oxígeno y cambian su actividad, expresión o su sensibilidad a activadores. Con la ayuda de la biblioteca genómica de *Euglena* podríamos también buscar la secuencia de bases que codifique para la vía del metil-glioxal, la cual aún no ha sido reportada en *Euglena*. Esto sería importante porque así podríamos proponer dos vías de producción de D-lactato en *Euglena*, la vía glucolítica y la vía del metil-glioxal.

De esta forma, con la biblioteca genómica podremos clonar, purificar y caracterizar las enzimas de la lanzadera de lactato para avanzar en el conocimiento del metabolismo energético de *E. gracilis*, el cual le permite vivir y reproducirse en ambientes tan variados y adversos.

BIBLIOGRAFÍA

Allison, N., O'Donell, M. J., and Fewson, C. A. (1985) Membrane-bound lactate and mandelate dehydrogenases of Acinetobacter calcoaceticus. *Biochem. J.* **231**, 407-416.

Barquera, B., Zhou, W., Morgan, J. E., and Gennis, R. B. (2002) Riboflavin is a component of the Na^+-pumping NADH-quinone oxidoreductase from *Vibrio cholerae*. *Proc. Natl. Acad. Sci. USA* 99, 10322-10324.

Beet G. F., Poole, P. L., Springham, M. G., and Bostran K. A. (1979) Kinetic and spestroscopic evidence of cation-induced conformation changes in yeast K^+-activated aldehyde dehydrogenase. *Biochem. J.* **183**, 633-646.

Buetow, D. E. (1989) in *The Biology of Euglena* (Buetow, D. E. Ed.), **Vol. IV**, pp. 247-314, Academic Press, New York.

Castro-Guerrero, N. A., Krab, K., and Moreno-Sánchez, R. (2004) *J. Bioenerg. Biomembr.* En prensa.

de Bari, L., Atlante, A., Guaragnella, N., Principato, G., and Pasarella, S. (2002) D-lactate transport and metabolism in rat liver mitochondria. *Biochem. J.* **365**, 391-403.

Díez-Gonzalez, F., Rusell, J. B., and Hunter, J. B. (1997) NAD^+-independent Lactate and butyryl-CoA dehydrogenase of *Clostridium acetobutylicum* P262. *Curr. Microbiol.* **34**, 162-166.

Erwin, A. L. and Gotschlich, E. C. (1993) Oxidation of D-lactate and L-lactate by *Neisseria meningitidis*: Purification and cloning of meningococcal D-lactate dehydrogenase. *J. Bacteriol.* **175**, 6382-6391.

Fewson,C. A., Baker, D. P., Chalmers, R. M., Keen, J. N., Hamilton, I. D., Scott, A. J., and Yasin, M. (1993) Relationship amongst some bacterial and yeast lactate and mandelate dehydrogenases. *J. Gen. Genet.* **139**, 1345-1352.

Fushinobu, S., Kamata, K., Iwata, S., Sakai, H., Ohta, T., and Matsuzawa, H. (1996) Allosteric activation of L-lactate dehydrogenase analyzed by hybrid enzymes with effector-sensitive and insensitive subunits *J. Biol. Chem.* **271**, 25611-25616.

Garvie, E. I. (1980) Bacterial lactate dehydrogenases. Microbiol. Rev. **44**, 106-139.

Gondry, M., and Lederer, F. (1996) Functional properties of the histidine-aspartate ion pair of flavocytochrome b_2 (L-lactate dehydrogenase): substitution of Asp282 with asparagines. *Biochemistry* **35**, 8587-8594.

Inui, H., Ono, K., Miyatake, K., Nakano, Y., and Kitaoka, S. (1985) The physiological role of oxygen-sensitive pyruvate dehydrogenase in mitochondria fatty acid synthesis in *Euglena gracilis*. *Arch. Biochem. Biophys.* **280**, 292-298.

Iuchi,S., and Lin, E. C. C. (1988) arc A (dye), a global regulatory gene in *Escherichia coli* mediating repression of enzymes in aerobic pathways. *Proc. Natl. Acad. Sci. USA* **85**, 1888-1892.

Jasso-Chávez, R., Torres-Márquez, M. E. and Moreno-Sanchez, R. (2001) The membrane-bound L- and D-lactate dehydrogenase activities in

mitochondria from *Euglena gracilis*. *Arch. of Biochem. and Biophys.* **390**, 295-303.

Kaback, H. R., and Millner, L. S. (1970) Relationship of a membrane-bound D-(-)-Lactic dehydrogenase to amino acid transport in isolated bacterial membrane preparations. *Biochemistry* **66**, 1008-1015.

Kim, J., Chung, T. D., and Kim, H. (2001) "Determination of biologically active acids based on the electrochemical reduction of quinone in acetonitrile + water mixed solvent" *J. Electroanal. Chem.* **499**, 78-84.

Linton, E. W., Hittner, D., Auld, T., and Triemer, R. E. (1999) A molecular study of euglenoid phylogeny using small subunit rDNA. *J. Euk. Microbiol.* **46**,217-223.

Lodi, T., and Ferrero, Y. (1993) Isolation of the DLD gene of *Saccharomyces cerevisiae* encoding the mitochondrial enzyme D-lactate ferricytochrome oxidoreductase. Mol. Gen Genet. **235**, 315-324.

Lord, J. M., and Merret, M. J. (1971) The intracellular localization of glicollate oxidoreductase in *Euglena gracilis*. *Biochem. J.* **124**, 275-281.

Markwell, J. P. and Lascelles, J. (1978) Membrane-bound, pyridine nucleotide-independent L-lacatte dehydrogenase of *Rhodopseudomonas sphaeroides*. *J. Bacteriol.* **133**, 593-600.

Matsushita, K., and Kaback, H. R. (1986) D-lactate oxidation and generation of the proton electrochemical gradient in membrane vesicles from *Escherichia coli* GR19N and in proteoliposomes reconstituted with purified D-lactate dehydrogenase and cytochrome *o* oxidase. *Biochemistry* **25**, 2321-2327.

Mendoza-Cózatl, D., Devars, S., Loza-Tavera, H., and Moreno-Sánchez R. (2002) Cadmium accumulation in the chloroplast of *Euglena gracilis*. *Physiol. Plant.* **115**, 276-283.

Moreno-Sánchez, R., Covián, R., Jasso-Chávez, R., Rodríguez-Enríquez, S., Pacheco-Moisés, F., and Torres-Márquez, M. E. (2000) Oxidative phosphorylation supported by an alternative respiratory pathway in mitochondria from *Euglena*. *Biochim. Biophys. Acta* **1457,** 200-210.

Müller, M. and Martin W. (1999) The genome of *Rickettsia prowazekii* and some thoughts on the origin of mitochondria and hydrogenosomes. *BioEssays* **21**,377-381.

Nordnes, S., Graus, S., and Johansen, T. (1994) cDNA sequence of zebrafish (*Brachydanio rerio*) translation elongation factor-1α: molecular phylogeny of eukaryotes based on elongation factor-1α protein sequences. *Biochem. Biophys. Acta* **1219**, 529-532.

Reed, D. W., and Hartzell, P. L. (1999) The *Archaeoglobus fulgidus* D-lactate dehydrogenase is a Zn^{2+} flavoprotein. *J. Bacteriol.* **181**, 7580-7587.

Smillie, R. M. (1968) Enzymology of *Euglena*, en: The Biology of *Euglena*, **Vol. II** (Buetow, D. E., ed) pp 2-54. Academic Press, New York.

Somlo, M. (1965) Induction des lactico-cytochrome c reductase (D- et L-) de la leuvre aerobie par les lactates (D- et L-). *Biochim. Biophys. Acta* **97**, 183-201.

Takenaka, S., Kondo, T., Nazeri, S., Tamura, Y., Tokunaga, M.,Tsuyama, S., Miyatake, K., and Nakano, Y. (1997) Accumulation of trehalose as a compatible solute under osmotic stress in *Euglena gracilis* Z. *J. Eukariot. Microbiol.* **44**, 609-613.

Tielens, A. G. M., and Van Hellemond, J. J. (1998) The electron transport chain in anaerobically functioning eukaryotes. *Biochim. Biophys. Acta* **1365**, 71-78.

Uribe, A., and Moreno-Sánchez, R. (1992) Energy-dependent reactions supported by several substrates in coupled *Euglena gracilis* mitochondria. *Plant Sci.* **86**, 21-32.

Valenti, D., de Bari, L., Atlante, A., and Pasarella, S. (2002) L-lactate transport into rat heart mitochondria and reconstruction of the L-lactate/pyruvate shuttle. *Biochem. J.* **364**, 101-104.

Valenzuela-Soto, E. M., Velasco-García, R., Mujica-Jimenez, C., Gaviria-Gonzalez, L. L., and Muñoz-Clares, R. A. (2003) Monovalent cations requirements for the stability of betaine aldehyde dehydrogenase from Pseudomonas aueruginosa, porcine kidney and amaranth leaves. *Chem. Biol. Interac.* **143-144**, 139-148.

Xiang, B., Taylor, J. C., Markham, G. D. (1996) Monovalent cation activation and kinetic mechanism of inosine 5' monophosphate dehydrogenase. *J. Biol. Chem.* **271**, 1435-14440.

Yokota, A., and Kitaoka, S. (1979) Occurrence of glycolate dehydrogenase in mitochondria and microsomas in streptomycin bleached mutant of *Euglena gracilis*. *Agric. Biol. Chem.* **43**, 855-857.

Zboril, P. and Wernerová, V. (1996) The isolation and some propierties of the membrane-bound lactate dehydrogenase of *Paracoccus denitrificans*. *Biochem. Biol. Int.* **39**,595-605.

LACTATO DESHIDROGENASAS ACOPLADAS A LAS CADENAS RESPIRATORIAS

Ricardo Jasso-Chávez[1,2], María Eugenia Torres Márquez[1] y Rafael Moreno Sánchez[2]. Departamentos de Bioquímica, [1]Facultad de Medicina, UNAM y [2]Instituto Nacional de Cardiología "Ignacio Chávez". Juan Badiano No. 1, Delegación Tlalpan, C. P. 14080, México, D. F. Tel.: 5573-2911 Ext. 1422 Fax: 5573-0926. Correo electrónico: rjasso@hotmail.com

Recibido: 6 de junio de 2000. Aceptado: 19 de septiembre de 2000.

RESUMEN

Las enzimas más conocidas que oxidan al lactato son las lactato deshidrogenasas dependientes de los piridín nucleótidos. Sin embargo, en los organismos unicelulares se han encontrado enzimas que son independientes de los piridín nucleótidos (iLDH). En las bacterias las iLDH son membranales y funcionan como quinona reductasas, mientras que en las levaduras se encuentran en el espacio intermembranal de la mitocondria y funcionan como citocromo c reductasas. Las iLDH mitocondriales de *Euglena gracilis* comparten con las de las bacterias, la característica de reducir a las quinonas. En esta revisión se describen y se comparan las características cinéticas y estructurales de las iLDH reportadas para *E. gracilis* , bacterias y levaduras.

PALABRAS CLAVE: iLDH, *Euglena gracilis*, bacterias, levaduras, FMN, FAD.

ABSTRACT

The NAD-dependent lactate dehydrogenase are the best known enzymes that oxidize lactate. However, in unicellular organisms there have also been found pyridine nucleotide-independent forms of the enzyme (iLDH). iLDH are membrane-bound and quinone reductases in bacteria, whereas in yeast they are located within the intermembrane mitochondrial space and have as electron acceptor cytochrome c. In *E. gracilis* mitochondria, iLDH have been found, which reduce quinones. In this review, we describe and compare the kinetic and structural characteristics of the iLDH, the iLDH reported for *E. gracilis*, bacteria and yeast.

KEY WORDS: iLDH, *Euglena gracilis*, bacteria, yeast, FMN, FAD.

INTRODUCCIÓN

En eucariotes superiores la cadena respiratoria de la mitocondria puede oxidar diversos substratos como NADH + H^+, glicerol-3-fosfato, succinato y ácidos grasos, por medio de las deshidrogenasas que son quinonas reductasas, siendo la NADH deshidrogenasa y la succinato deshidrogenasa las más abundantes.

En la cadena respiratoria de las bacterias existen deshidrogenasas cuya especificidad por los substratos es diferente a los que utilizan las mitocondrias de eucariotes superiores. Entre estos substratos están el formato, dihidroorotato, glicerol, mandelato, metanol, piruvato y L- y D-lactato (1). La actividad de dichas deshidrogenasas está asociada en la mayoría de los casos a la reducción de quinonas.

Lactato deshidrogenasas independientes de los piridín nucleótidos en los procariotes.

El lactato es también oxidado en una gran variedad de bacterias por una deshidrogenasa diferente a la que participa en la glucólisis; esta enzima no utiliza NAD^+/NADH + H^+ como coenzima, por lo que se conocen como lactato deshidrogenasas independientes de piridín nucleótidos (iLDH); éstas transforman al lactato en piruvato con la reducción de una flavina como cofactor, sin embargo, no hay estudios acerca de que la reacción opuesta ocurra *in vivo* o *in vitro* (2). Las iLDH pueden existir en forma soluble (3) o particulada (4) y en muchos casos el aceptor natural de los electrones se desconoce. Cuando son membranales, forman parte de la cadena respiratoria y pueden tener afinidad por los dos isómeros del lactato o ser esteroespecíficas.

La iLDH más estudiada es la D-iLDH de *Escherichia coli*. Esta enzima es constitutiva sin importar cuál fuente de carbono hay en el medio, mientras que

la L-iLDH se induce bajo condiciones aeróbicas en presencia de lactato (5); asimismo, se ha reportado el consumo de oxígeno acoplado a la oxidación de D-lactato, además de que el sitio activo de la D-iLDH se encuentra orientado hacia el citoplasma.

La D-iLDH de *E. coli* está asociada a la membrana y se ha utilizado para el estudio de las interacciones proteína-lípidos. La enzima purificada presenta una baja actividad en ausencia de detergentes y lípidos. Se ha reportado que la actividad enzimática se incrementa 5 veces en presencia de Tritón X-100 y 10 veces por los fosfolípidos de *E. coli* o por lisolecitina. La preincubación de la enzima con los lípidos de *E.coli* o la lisolecitina por 10 minutos a 37°C, incrementa la actividad y la K_m (6). En su estado nativo esta enzima se encuentra rodeada predominantemente por fosfatidilglicerol y fosfatidilserina, los cuales están presentes en baja concentración en la membrana plasmática de *E. coli* (7). Campbell y col. (8) clonaron el gen estructural de la D-iLDH de *E. coli*; el marco de lectura predijo que el polipéptido consistía de 571 aminoácidos (incluyendo el residuo de inicio, la metionina) con una masa relativa de 64,613 Da. La polaridad de la proteína (47%) es alta con respecto a algunas proteínas membranales. En la enzima hay una pequeña región de baja hidrofobicidad que contiene una repetición idéntica en la secuencia de los residuos de los aminoácidos SVIG (residuos 140-143 y 150-153), la cual es homóloga con la cadena H de la lactato deshidrogenasa de cerdo; esta secuencia se repite después de dos residuos de los cuales el segundo es una cisteína. De manera interesante, esta cisteína es esencial ya que su modificación puede impedir el cambio conformacional requerido para la catálisis. Mutaciones específicas en la D-iLDH con la incorporación del 5-fluorotriptofano indicaron que en la estructura secundaria el sitio posible de enlace de la flavina se encuentra en el carboxilo terminal de la enzima.

Las predicciones de estructura de la hechas a partir de los datos de resonancia magnética nuclear con ^{19}F y de algunas deshidrogenasas citosólicas, han mostrado dos regiones en las iLDH comunes con las LDH citosólicas; una es el dominio de unión al substrato y la otra el dominio de unión al cofactor. En el caso de la D-iLDH de *E. coli*, el dominio de unión al cofactor es de 200 residuos de aminoácidos y se encuentra en el extremo del carboxilo terminal, mientras que en el extremo del amino terminal se encuentra el dominio de unión al substrato. Además, la D-iLDH parece tener una pequeña región necesaria para su fijación a la membrana y para acoplarse a los acarreadores de electrones lipofílicos, delimitada por los residuos de aminoácidos 226 al 384. Esta última región, no esta totalmente inmersa o anclada en la membrana, sugiriendo que la D-iLDH se fija a la membrana por fragmentos separados estructuralmente, como se muestra en la figura 1 (9).

Generalmente en *E. coli* como en otras bacterias, la solubilización de las iLDH se lleva a cabo con detergentes aniónicos, preferentemente el Tritón X-100. Con este detergente incluso se activan las iLDH de *E. coli* y de *Neisseria gonorrhoeae*. El pH óptimo para las iLDH varía desde 5.5 para la L-iLDH de *Lactobacillus casei*, hasta 8 y 9 en la L- y D-iLDH de *N. meningitidis* y *E.coli* (2).

Los alineamientos realizados entre las iLDH bacterianas muestran una gran similitud en la secuencia de los residuos de los aminoácidos de las D-iLDH y las L-iLDH, respectivamente. Las secuencias de las D-iLDH y de algunas mandelato deshidrogenasas que también son independientes de los piridín nucleótidos, muestran regiones homólogas entre sí. Asimismo, en las secuencias de al-

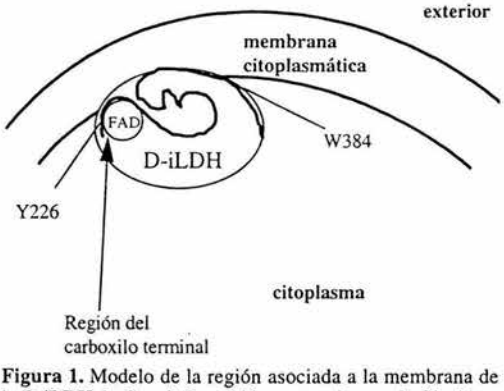

Figura 1. Modelo de la región asociada a la membrana de la D-iLDH de *E. coli*. La región necesaria para la fijación a la membrana (línea negra) y para acoplarse a los acarreadores de electrones lipofílicos, está delimitada por los residuos de aminoácidos 226 al 384. Esta región no está totalmente inmersa o anclada en la membrana (Modificado de 9).

gunas L-iLDH bacterianas se aprecia una secuencia (SNHGGRQ) muy conservada entre las α-hidroxiácido deshidrogenasas y las oxidasas que contienen mononucleótidos de flavina como la L-lactato oxidasa de *Streptococcus iniae* y de *Aerococcus viridans*.

Con respecto a la especificidad de las iLDH bacterianas, éstas pueden oxidar exclusivamente a su substrato como la L-iLDH de *Rhodopseudomonas sphaeroides* y la D-iLDH de *Megasphaera elsdenii*, o pueden oxidar al enantiómero opuesto además de otros substratos, como el α-DL-hidroxibutirato y la D-treonina para la D-iLDH de *E. coli*; y la L-treonina, la fenilalanina, el L-β-fenil lactato y el 4-hidroxifenil lactato para la L-iLDH de *Neisseria gonorrhoeae*, sin embargo, tienen muy poca afinidad y una velocidad de oxidación menor al 10 % en comparación con su verdadero substrato.

Los parámetros cinéticos de las iLDH bacterianas son variables entre especies. La Tabla I muestra que la afinidad por L- o D-lactato (K_m) es similar ya que se encuentra en concentraciones milimolares, mientras que la velocidad máxima es diferente, siendo mayor para las D-iLDH. El efecto de algunos inhibidores es distinto en cuanto al tipo de inhibición y K_i.

Las iLDH en eucariotes.

Las iLDH de los eucariotes, específicamente en levaduras, son significativamente distintas a las encontradas en las bacterias. En las levaduras éstas se localizan en el espacio intermembranal de la mitocondria. Las iLDH de *Saccharomyces cerevisiae* y *Hansenula anomala* son flavocitocromos b_2 y fisiológicamente tienen la actividad de L-iLDH que transfiere los electrones directamente al citocromo *c*. Estructuralmente son tetrámeros idénticos, cada uno de los monómeros contiene dos dominios diferentes. El dominio del citocromo b_2 está en el extremo del amino terminal y se relaciona con el citocromo b_5 de los mamíferos, mientras que el dominio que contiene al FMN y a la actividad de la deshidrogenasa se encuentran en el extremo carboxilo terminal.

Todas estas enzimas son de masa molecular muy semejante y las secuencias del amino terminal, que es donde se encuentra el dominio del citocromo b_2, indican que son homólogas; el dominio del carboxilo terminal que contiene el FMN (con protoporfirina IX), pertenece a la familia de las L-2-hidroxiácido deshidrogenasas las cuales presentan un mecanismo catalítico muy similar para la oxidación del substrato, aunque varían considerablemente en la selectividad del mismo. Este tipo de enzimas se han encontrado en las plantas, los animales y las bacterias; como la glicolato oxidasa peroxisomal de las plantas, la L-mandelato deshidrogenasa de *Pseudomonas putida* y de *Rhodotorula graminis* y la lactato mono-oxigenasa de *Mycobacterium smegmatis* (10); las cuales tienen substratos que difieren en el tamaño, la naturaleza química y su participación metabólica. Los alineamientos de algunas L-iLDH y otras enzimas también independientes de los piridín nucleótidos de diversos organismos, forman parte de una superfamilia de flavoproteínas con la actividad de 2-hidroxiácido deshidrogenasa y oxidasa.

La levadura *Saccharomyces cerevisiae* presenta una D-iLDH mitocondrial unida a la membrana. La D-iLDH consta de un solo polipéptido y no presenta ninguna homología con la L- iLDH presente en el mismo organismo (11). El alineamiento de secuencias de la iLDH entre las bacterias y las levaduras no mostró regiones de similitud. Del mismo modo, al intentar alinear secuencias entre las L- y las D-iLDH, tampoco se encontraron similitudes. Se ha sugerido que existe una familia de 2-hidroxiácido deshidrogenasas específicas para el isómero D (12).

En la Tabla II se presentan algunas características de las enzimas bacterianas y de las levaduras. Se incluyen algunas L- y D-mandelato deshidrogenasas cuya relación estructural y propiedades de purificación con las iLDH son muy similares (10). El mandelato, que es una molécula de lactato modificada, es oxidado por la mandelato deshidrogenasa a fenilglioxilato que, por medio de la vía de la 3-oxoadipato y con la salida de succinato, termina en la síntesis de acetil-CoA.

La iLDH en *Euglena gracilis*.

Se ha reportado en el protista *E. gracilis* una actividad de D-iLDH, que se encuentra en la fracción particulada de la mitocondria, es dependiente de zinc e independiente de los piridín nucleótidos. El L-lac-

TABLA I

PARÁMETROS CINÉTICOS DE ALGUNAS ILDH BACTERIANAS

Organismo	Enzima	P.M. [a] (KDa)	Aceptor de e^-	K_m [c] para lactato (mM)	V_m [d]	Inhibidor [b]	K_i (mM)
Escherichia coli.[1]	D-iLDH (FAD)	74	DCPIP o MTT- PMS	1.4 -2.2	——	Oxamato (C) Oxalato (C)	0.0033 0.0009
Acinetobacter calcoaceticus [2]	D-iLDH (FAD)	62.8	DCPIP-PMS	0.264	——	Oxalato (C) Reactivos de grupos -SH	———
Neisseria meningitidis [3]	D-iLDH	70	MTT-PMS	5.1	0.5	Oxamato Piruvato	——— ———
N. meningitidis	L-iLDH	——	MTT-PMS	14	0.06	———	———
Megasphaera elsdenii [4]	D-iLDH (FAD)	55	——-	——-	——-	Oxalato D-lactato	——-
Rhodopseudo-monas sphaeroides [5]	L-iLDH	107	DCPIP-PMS	0.5	——-	Oxamato (NC) Oxalato (NC) D-lactato. (C)	0.96 0.03 22
Neisseria gonorrhoeae [6]	D-iLDH	———	MTT-PMS	0.2	——	———	———
Paracoccus denitrificans [7]	D-iLDH	54	DCPIP-PMS	0.81	——-	Tenoiltrifluo-roacetona (NC)	2.2
Selenomonas ruminantium [8]	D-iLDH	——	DCPIP	0.5	——	———	——-
Clostridium acetobutylicum [9]	D-iLDH	55	DCPIP o MTT	3.5	13[d]	———	———
C. acetobutylicum[9]	L-iLDH	55	DCPIP o MTT	0.7	0.3[d]	———	——-

Determinado por SDS-PAGE, [b]C inhibidor competitivo, NC inhibidor no competitivo, [c]Los valores fueron obtenidos de extractos crudos, [d]µmoles de metasulfato de tetrazolio (MTT), metasulfato de fenazina (PMS) o diclorofenolindofenol (DCPIP) reducido min^{-1} mg $proteína^{-1}$. [1](4); [2]Allison N, O´Donnell M J, Hoey M E y Fewson C A (1985) Biochem. J *227*:753-757; [3]Erwin A L y Gotschlich E C (1993) J Bacteriol *175*:6382-6391; [4]Olson S T y Massey V (1979) Biochemistry *18*:4714-4724; [5]Markwell J P y Lascelles J (1978) J Bacteriol *133*:593-600; [6]Fischer R S, Martin G C, Rao P y Jensen R A (1994) FEMS Microbiol *115*:39-44; [7]Zboril P y Wernerová V (1996) Biochem and Mol Biol Int *39*:595-605; [8]Gilmour M, Harry J F, Wilfrid J M (1994) Microbiol *140*:2077-2084; [9](3).

tato también se oxida pero a velocidades más bajas (13). La oxidación del lactato se encontró acoplada a la fosforilación oxidativa, los electrones de la oxidación del D- y L-lactato entran a la cadena respiratoria de la mitocondria de *Euglena* al nivel de la ubiquinona. Además, la oxidación del L- y D-lactato presenta entre 50 y 90 % de resistencia a la antimicina, por lo que se propuso que una fracción de la oxidación del lactato procede a través de una cadena transportadora de electrones alterna e independiente al citocromo bc_1 (14).

En este protista se ha determinado cinéticamente que la oxidación del lactato se lleva a cabo por dos enzimas estereoespecíficas y, a diferencia de todos los organismos reportados que presentan a la iLDH, las dos se expresan cuando las células se cultivan en medios sin glucosa o lactato. El sitio activo de la L-iLDH está orientado hacia la cara externa de la membrana interna mitocondrial. Además, ambas enzimas son resistentes a altas temperaturas cuando se encuentran en mitocondrias intactas, siendo la D-iLDH la más resistente. El pH óptimo de las iLDH de *E. gracilis* se encuentra entre 7.3-7.6 (15).

Se han utilizado varios aceptores artificiales de electrones para llevar a cabo estudios cinéticos de estas enzimas. El aceptor artificial más utilizado ha sido el diclorofenolindofenol (DCPIP) debido a su alto potencial redox. Al igual que la D-iLDH de *E. coli*, las iLDH de *E. gracilis* también pueden ceder los electrones a las quinonas (Fig. 2), lo que hace suponer que las iLDH de estos organismos tuvieron un origen común, ya que *E. gracilis* es de los eucariotes más primitivos con mitocondrias (16).

Los inhibidores clásicos de las lactato deshidrogenasas dependientes de $NAD^+/NADH + H^+$, como el oxamato y oxalato, también inhiben a las iLDH (Tablas I y III). En cuanto al mecanismo cinético de reacción, se ha reportado para *S. cerevisiae* un modelo que involucra dos estados distintos de la enzima durante la reacción (Fig. 3A). De forma similar, nosotros hemos identificado que el mecanismo de reacción para las isoenzimas mitocondriales de *E. gracilis*, es de tipo ping-pong (Fig. 3B).

Cofactores de las iLDH

Los cofactores de las iLDH son flavinas unidas o no de forma covalente. Sin importar el organismo en

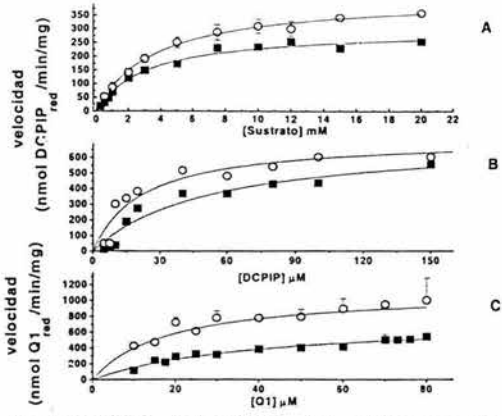

Figura 2. Cinética de la oxidación de L- y D-lactato en las mitocondrias de *Euglena. gracilis*. A, oxidación de L- y D-lactato. B, oxidación del lactato con DCPIP como aceptor de los electrones. C, oxidación del lactato con Q1 (quinona artificial con un solo grupo isoprenoide en la posición 5 del anillo) como aceptor de electrones. (■) L-lactato, (○) D-lactato (Tomado de 15).

estudio para todas las L-iLDH el cofactor es siempre FMN, mientras que para las D-iLDH el cofactor es siempre FAD. Esta diferencia entre los grupos prostéticos y en los alineamientos de las secuencias entre las L- y D-iLDH hacen suponer que son familias totalmente distintas. Sin embargo las L- y D-iLDH son muy parecidas con otras deshidrogenasas enantiómero-específicas (Tabla II).

Lactato deshidrogenasas asociadas a las membranas celulares en los mamíferos.

No se ha descrito la existencia de la lactato deshidrogenasa en las mitocondrias de los mamíferos. Se ha supuesto que las actividades de la lactato deshidrogenasa que se han encontrado en las preparaciones mitocondriales, eran contaminaciones por enzimas del citosol, ya que éstas no eran preparaciones puras. Sin embargo, recientemente se reportó una actividad de lactato deshidrogenasa dependiente de $NAD^+/NADH + H^+$ acoplada a un consumo de oxígeno, sensible a oxamato y N-etilmaleimida, lo que sugiere que el lactato se internaliza a la mitocondria para ser oxidado. Isoformas de estas enzimas se han identificado en el corazón, hígado y músculo (17).

Importancia de las iLDH en microorganismos patógenos.

Las iLDH son muy importantes en el metabolismo

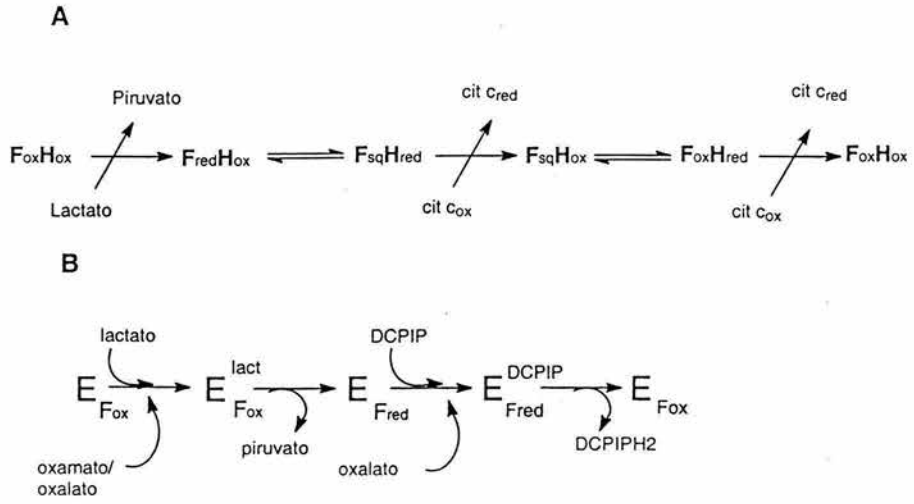

Figura 3. A, representación lineal del ciclo catalítico del flavocitocromo b2 de *S. cerevisiae*. Los estados redox del citocromo c (cit c), el hemo (H) y la flavina (F) del flavocitocromo b_2 están indicados por los suscritos "ox" y "red" para sus formas oxidadas y reducidas respectivamente. (Modificado de 22); **B.** Esquema del mecanismo de reacción propuesto para la L-iLDH y la D-iLDH mitocondriales de *E. gracilis* (Tomado de 15).

energético de las bacterias así como de algunas levaduras y protistas. Su importancia radica principalmente en que pueden utilizar ambos isómeros del lactato durante su crecimiento y desarrollo en condiciones aeróbicas.

Algunas bacterias patógenas como *Neisseria gonorrhoeae* expresan la L- y la D-iLDH. La L-iLDH participa en el metabolismo de los aminoácidos aromáticos de la bacteria, ya que puede convertir al fenil-lactato a fenilalanina y al 4-hidroxi-fenil-lactato a tirosina. Se ha asociado a esta enzima en el mecanismo de patogénesis, en donde el lactato del hospedero es oxidado por el gonococo, con el consecuente aumento en el consumo de oxígeno y transporte electrónico; de forma similar a lo que se ha sugerido para el 4-hidroxi-fenil-lactato, un metabolito disponible en el hospedero humano (18).

Neisseria meningitidis posee también a las L- y D-iLDH. El L-lactato es producido por las células del mamífero, mientras que el D-lactato puede ser detectado en la sangre humana, tal vez absorbido del intestino, aunque su concentración es sólo el 5% de la del L-lactato. El D-lactato puede ser producido en la oxidación de la glucosa por algunas bacterias lácticas, o bien por *E. coli*, la cual habita en la superficie de la mucosa intestinal, que es el sitio donde también coloniza *Neisseria* (19)

En *Haemophilus influenza* se ha demostrado la existencia de una D-iLDH asociada a membrana. Su importancia estriba en que esta enzima puede utilizar al D-lactato que se encuentra en pequeñas cantidades en el hospedero (20). La incubación de *H. influenzae* en lactato incrementa su resistencia contra el suero humano. El mecanismo de este fenómeno no se conoce pero aparentemente está relacionado a la expresión de lipopolisacáridos.

CONCLUSIÓN

Los microorganismos presentan una diferencia importante en la variedad de sustratos oxidables que pueden utilizar para sintetizar ATP con respecto a organismos superiores. La presencia de las lactato deshidrogenasas acopladas a la cadena transportadora de los electrones, puede representar una ventaja para el metabolismo de estos organismos. En sistemas bacterianos los electrones de la oxidación del lactato, que es producto de la glucólisis anaerobia, entran directamente a la cadena respiratoria que promueve la generación de un gradiente de protones necesario para la síntesis de ATP y para el transporte de azúcares y aminoácidos. En el caso de algunos protis-

TABLA II

TIPOS DE LACTATO DESHIDROGENASA Y SU RELACIÓN CON ALGUNAS MANDELATO DESHIDROGENASAS (MDH) Y OTRAS 2-HIDROXIÁCIDO DESHIDROGENASAS INDEPENDIENTES DE LOS PIRIDÍN NUCLEÓTIDOS

ORGANISMO	ENZIMA	LOCALIZACIÓN
Dependientes de FMN, Mr ≅ 44000. Procariotes		
Pseudomonas putida [a]	L-MDH	Membranal
Acinetobacter calcoaceticus [b]	L-MDH	Membranal
A. calcoaceticus [c]	L-LDH	Membranal
Escherichia coli [d]	L-LDH	Membranal
Dependientes de FMN (flavocitocromos), Mr ≅ 59000. Eucariotes		
Espinaca [e]	Glicolato oxidasa	Peroxisoma (soluble)
Mycobacterium smegmatis [f]	L-Lactato monooxigenasa	Soluble?
Sacharomyces cerevisiae [g]	L-LDH	Mitocondria (soluble)
Rhodotorula graminis [a, f]	L-MDH	Mitocondria (soluble)
Hansenula anomala [a]	L-LDH	Mitocondria (soluble)
Dependientes de FAD, Mr ≅ 60000. Procariotes		
A. calcoaceticus [b]	D-LDH	Membranal
A. calcoaceticus [h]	D-MDH	Membranal
E. coli [h]	D-LDH	Membranal
Paracoccus denitrificans [i]	D-LDH	Membranal
Megasphaera elsdenii [j]	D-LDH	Membranal
Dependientes de FAD (flavocitocromos), Mr ≅ 64040		
Sacharomyces cerevisiae [k]	D-LDH	Membranal

[a] (10); [b] Allison N, O'Donnell M J, Hoey M E y Fewson C A (1985) Biochem. J *227*:753-757; [c] (10); [d] (5); [e] Volokita M y Somerville C R (1987) J Biol Chem *262*:15825-15828; [f] Illias R M, Sinclair R, Robertson D, Neu A, Chapman S K y Reid G A (1998) Biochem J *333*:107-115; [g] Daum G, Böhni P C y Schatz G (1982) J Biol Chem *257*:13028-13033; (10); [h] Futai M (1973) Biochemistry *12*:2468-2474; (2); [i] Zboril P y Wernerová A (1996) Biochem and Mol Biol Int *39*:595-605; [j] Olson S T y Massey V (1979) Biochemistry *18*:4714-4724; [k] (11)

tas como *Euglena* y *Leishmania*, el gradiente de protones puede ser utilizado para la producción de ATP. Este hecho puede ser de suma importancia ya que estos organismos presentan deficiencias en el ciclo de Krebs, lo que podría tener consecuencias en la producción de ATP.

Las iLDH bacterianas y de la mitocondria de *Euglena* son membranales, acopladas a la cadena respiratoria y ceden los electrones de la oxidación del lactato a las quinonas. Estas semejanzas hacen pensar que estas enzimas pueden presentar un origen común. Además, *Euglena* que es de los organismos más primitivos con mitocondrias, es el único eucariote que posee iLDH con las mismas características que las de bacterias, hecho que apoya la teoría de la temprana adquisición de mitocondrias por *Euglena*. Las diferencias entre las iLDH encontradas en los procariotes y las levaduras pueden deberse a un proceso evolutivo, el cual haría mas eficiente la utilización del lactato sin que sus electrones tengan que pasar por la poza de quinonas sino directamente al citocromo c.

Sin importar la forma en que se encuentren las iLDH, solubles, membranales o que se localicen en el espacio intermembranal de la mitocondria, por ser de las primeras deshidrogenasas en la cadena respiratoria son esenciales para los microorganismos que las poseen, ya sea para la producción de ATP, para el transporte de los metabolitos esenciales o para poder colonizar e invadir a un organismo hospedero. Las iLDH tienen una participación esencial en el metabolismo, por lo que es de relevancia conocer más acerca de estas enzimas y las vías metabólicas en las que están involucradas.

TABLA III

PARÁMETROS CINÉTICOS DE LAS iLDH DE ALGUNOS EUCARIOTES

ORGANISMO	ENZIMA	P.M. (KDa)	ACEPTOR DE e^-	K_m PARA LACTATO (mM)	V_m	INHIBIDORES	K_i (mM)
Saccharomyces cerevisiae[a]	L-iLDH flavocitocromo	240 tetrámero	ferricianuro citocromo c	0.49 0.29	0.27 0.155	Sulfito (C) D-lactato (C) Piruvato (C,NC) Oxalato (M)*	0.0014 1.4 3.3 0.3
S. cerevisiae[b]	D-iLDH flavocitocromo	64 monómero	ferricianuro citocromo c	—— ——	—— ——	—— ——	—— ——
Euglena gracilis[c]	L-iLDH	——	DCPIP-PMS	2.6	0.28	Oxamato (C) Oxalato (M)*	0.84 0.25
E. gracilis[c]	D-iLDH	——	DCPIP-PMS	2.8	0.42	Oxamato (C) Oxalato (M)*	0.54 0.14

Las observaciones son las mismas que las de la Tabla I.* (M) inhibidor tipo mixto; [a]Gondry M y Lederer F (1996) Biochemistry *35*:8587-8594; [b](11); [c](15).

AGRADECIMIENTOS

La elaboración de este trabajo fue apoyada por los donativos de CONACyT 25274M y 25465N.

REFERENCIAS

1. Ingledew W J y Poole R K (1984) The respiratory chains of *Escherichia coli.* Microbiol Rev *48*:222-271.

2. Garvie E I (1980) Bacterial lactate dehydrogenases. Microbiol Rev *44*:106-139.

3. Diez-Gonzalez F, Rusell J B y Hunter J B (1997) NAD-independent lactate and butyryl-CoA dehydrogenases of *Clostridium acetobutylicum* P262. Curr Microbiol *34*:162-166.

4. Kohn L D y Kaback H R (1973) Mechanisms of active transport in isolated bacterial membrane vesicles. J Biol Chem *248*:7012-7017.

5. Haugaard N (1959). D- and L-Lactic acid oxidases of *E. coli.* Biochim Biophys Acta *31*:66-72.

6. Fung L W-M, Pratt E A y Ho C (1979) Biochemical and biophysical studies on the interaction of a membrane-bound enzyme, D-lactate dehydrogenase from *Escherichia coli* with phospholipids. Biochemistry *18*:317-324.

7. Kovatchev S, Vaz Winchill L C y Eibl H (1981) Lipid dependence of the membrane-bound D-lactate dehydrogenase of *Escherichia coli.* J Biol Chem *256*: 10369-10374.

8. Campbell H D, Rogers B L y Young I G (1984) Nucleotide sequence of the respiratory D-Lactate dehydrogenase gene of *Escherichia coli.* Eur J Biochem *144*:367-373.

9. Sun Z-Y, Truong H-T N, Pratt E A, Sutherland D C, Kulig C E, Homer R J, Groetsch S F, Hsue P Y y Ho C (1993) A ^{19}F-NMR study of the membrane-binding region of D-lactate dehydrogenase of *Escherichia coli.* Prot Sci 2:1938-1947.

10. Fewson C A, Baker D P, Chalmers R M, Keen J N, Hamilton I D, Scott A J y Yasin M (1993) Relationship amongst some bacterial and yeast lactate and mandelate dehydrogenases. J Gen Microbiol *139*:1345-1352.

11. Lodi T y Ferrero Y (1993) Isolation of the DLD gene *Saccharomyces cerevisiae* encoding the mitochondrial enzyme D-lactate ferricytochrome c oxidoreductase. Mol Gen Genet *238*:315-324.

12. Taguchi H y Ohta T (1991) D-lactate dehydrogenase is a member of the D-isomer specific 2-hydroxyacid dehydrogenase family. J Biol Chem *266*:12588-12594.

13. Price C A (1961) A zinc-dependent lactate dehydrogenase in *Euglena gracilis*. Biochem J *82*:61-66.

14. Moreno-Sánchez R, Covián R, Jasso-Chávez R, Rodríguez S, Pacheco F y Torres-Márquez M E (2000) Oxidative phosphorylation supported by alternative respiratory pathway in mitochondria from *Euglena*. Biochim Biophys Acta *1457*:200-210.

15. Jasso Chávez R (2000) Caracterización cinética y Termodinámica de la L- y D-Lactato deshidrogenasas mitocondriales de *Euglena gracilis*. Tesis de Maestría. Facultad de Química, UNAM. México. pp 40-69.

16. Linton E W, Hittner D, Auld T, y Triemer R E (1999) A molecular study of euglenoid phylogeny using small subunit rDNA. J Eukariot Microbiol *46*:217-223.

17. Brooks G A, Dubouchaud H, Brown M, Sicurello J P y Butz C E (1999) Role of mitochondrial lactate dehydrogenase and lactate oxidation in the intracellular lactate shuttle. Proc Natl Acad Sci USA *96*:1129-34.

18. Bhatnagar R K, Hendry A T, Shanmugan K T y Jensen R A (1989) The broad-specifity, membrane-bound lactate dehydrogenase of *Neisseria gonorrhoeae*: ties to aromatic metabolism. J Gen Microbiol *135*:353-360.

19. Erwin A L y Gotschlich E C (1996) Cloning of a *Neisseria meningitidis* gene for L-Lactate dehydrogenase (L-LDH): Evidence for a second meningococcal L-LDH with different regulation. J Bacteriol *178*:4807-4813.

20. Denicola-Seaone A y Anderson B M (1990) Purification and characterization of *Haemophilus influenza* D-lactate dehydrogenase. J Biol Chem *265*:3691-3696.

21. Sharp R E, Chapman S K y Reid GA (1996) Modulation of flavocytochrome b2 intraprotein electron transfer via an interdomain hinge region. Biochem J *316*:507-513.

Archives of Biochemistry and Biophysics
Vol. 390, No. 2, June 15, pp. 295–303, 2001
doi:10.1006/abbi.2001.2353, available online at http://www.idealibrary.com on IDEAL®

The Membrane-Bound L- and D-Lactate Dehydrogenase Activities in Mitochondria from *Euglena gracilis*

Ricardo Jasso-Chávez,*,† M. Eugenia Torres-Márquez,* and Rafael Moreno-Sánchez†,[1]

Departamento de Bioquímica, Facultad de Medicina, UNAM, and †Departamento de Bioquímica, Instituto Nacional de Cardiología, 14080 México, DF, Mexico

Received January 18, 2001, and in revised form March 12, 2001; published online May 24, 2001

The activity of the pyridine nucleotide-independent lactate dehydrogenase (iLDH) was characterized in mitochondria isolated from the protist *Euglena gracilis*. The dissociation constants for L- and D-lactate were similar, but the V_{max} was higher with the D isomer. A ping-pong kinetic mechanism was displayed with 2,4-dichlorophenol-indolphenol (DCPIP), or coenzyme Q_1, reacting as the second substrate with the modified, reduced enzyme. Oxamate was a competitive inhibitor against both L- and D-lactate. Oxalate exerted a mixed-type inhibition regarding L- or D-lactate and also against DCPIP. The rate of L-lactate uptake was partially inhibited by mersalyl and lower than the rate of dehydrogenation, which was mersalyl-insensitive. These data suggested that the active site of L-iLDH was orientated toward the intermembrane space. The following observations indicated the existence of two stereo-specific iLDH enzymes in the inner membrane of *Euglena* mitochondria: a greater affinity of the D-iLDH for both inhibitors, D-iLDH thermo-stability at 70°C and denaturation of L-iLDH, opposite signs in the enthalpy change for the association reaction of the isomers to the enzyme, differential solubilization of both activities with detergents, and different molecular mass. © 2001 Academic Press

Key Words: **respiratory chain; lactate dehydrogenase; stereo-specific enzymes; NAD⁺-independent dehydrogenation.**

Mitochondria isolated from the free-living protist *Euglena gracilis* oxidize a variety of substrates, including succinate, 2-oxoglutarate, glutamate, malate, external NADH, and metabolites such as succinate semialdehyde, γ-amino-butyric acid and lactate, not commonly used by other kinds of mitochondria (1–7). However, these mitochondria do not readily oxidize pyruvate since they lack the pyruvate dehydrogenase complex (6). Pyruvate can be transformed to acetyl-CoA by the pyruvate/NADP⁺ oxidoreductase which is inactivated by O_2 (8). Then, to obtain a maximal benefit (ATP^2 synthesis) from glycolytic intermediates, *Euglena* may have developed, in their mitochondria, an active oxidation pathway for external lactate.

Indeed, the largest rates of electron transport and ATP^2 synthesis in *Euglena* mitochondria occur with lactate as substrate (7–10). Lactate oxidation is initiated by a dehydrogenase that transfers electrons from lactate to the inner mitochondrial membrane quinone pool; in turn, quinol can be oxidized by either the cytochrome b–c_1 complex, an antimycin-resistant cytochrome c reductase, or a cyanide-resistant oxidase (9).

Pyridine nucleotide-independent lactate dehydrogenase (iLDH) is widely distributed in bacterial respiratory systems (for a review see Ref. 11). Price (10) originally described the existence of the iLDH activity in *Euglena* cells. This activity has been associated with the mitochondrial fraction in *Euglena* (12, 13). Several groups (12, 14, 15) described the existence of iLDH activity only for the D-isomer in cell extracts, whereas Yokota and Kitaoka (13) found activity with both isomers in *Euglena* mitochondria. In bacterial systems,

[1] To whom correspondence should be addressed at Instituto Nacional de Cardiología, Departamento de Bioquímica, Juan Badiano No. 1, Col. Sección XVI, Tlalpan, México, D.F. 14080, Mexico. Fax: 525-573-0926. E-mail: morenosanchez@hotmail.com.

[2] Abbreviations used: ATP, adenosine triphosphate; iLDH, pyridine nucleotide-independent lactate dehydrogenase; PMS, phenazine methosulfate; Q_1, ubiquinone 1; Q_2, ubiquinone 2; DBQ, decylbenzoquinone; NBT, nitroblue tetrazolium; Chaps, 3-[(3-cholamidopropyl)-dimethylammonio]-1-propanesulfonic acid; SMP, submitochondrial particle; DCPIP, 2,4-dichlorophenol-inophenol; Mops, 4-morpholinopropanesulfonic acid; ADP, adenosine 5′-diphosphate; BSA, bovine serum albumin; TMPD, *N,N,N′,N′*-tetramethyl-*p*-phenylenediamine.

0003-9861/01 $35.00

one iLDH may oxidize both isomers with different catalytic efficiency or different molecular iLDH entities oxidize each isomer (11, 16–22).

Isomer-specific iLDH activity can be constitutive or inducible in bacteria and yeast (11, 16, 17, 19, 22, 23). In *Neisseria gonorrhoeae* and *N. meningitidis* (20, 21) both iLDH activities are constitutive. iLDHs activities may be induced by culture in either L- or D-lactate as carbon source (11, 19) or by aerobiosis (24), while they are repressed by culture in glutamate or succinate (19) or by anaerobiosis (24). These data suggest that iLDHs participate in the aerobic oxidation of lactate. In contrast, the physiological role of the D-iLDH activity in yeast is not the catabolism of lactate but it rather seems involved in the methylglyoxal metabolism at the level of lactylglutathione (23).

Degradation of paramylon (glucose chain with $\beta[1 \rightarrow 3]$ glycosidic bonds), the main energy storage in *Euglena* (25), yields glucose which, through the glycolytic pathway, produces pyruvate (26). In turn, pyruvate can be reduced by NAD^+-dependent lactate dehydrogenase to either L- or D-lactate (27). Thus, the presence of both iLDH activities in mitochondria may allow the oxidation of both lactate isomers and, hence, catalyze an optimal transfer of reduced equivalents from the cytosol to the respiratory chain. In this work, we examined the kinetic and some structural properties of the iLDH activity in mitochondria isolated from dark-grown *Euglena*, to determine whether these mitochondria have a single iLDH with catalytic ability to transform either isomer or two different stereo-specific iLDH enzymes.

MATERIALS AND METHODS

Phenazine methosulfate (PMS), 2,6 dichlorophenol indophenol (DCPIP), ubiquinone-1 (Q_1), ubiquinone-2 (Q_2), decylbenzoquinone (DBQ), L-lactate, D-lactate, nitroblue tetrazolium (NBT), and bovine serum albumin were from Sigma. Oxalic acid and oxamic acid were from Merck. [^{14}C]L-lactate, 3-[(3-cholamidopropyl)-dimethylammonio]-1-propanesulfonate (Chaps), β-D-octylpyranoside, and silicone oil were from ICN.

Culture of *E. gracilis* strain Z and preparation of mitochondria were carried out as previously described (9). Submitochondrial particles (SMPs) were prepared by sonication of the mitochondrial suspension. Approximately 15–25 mg mitochondrial protein/ml were sonicated three times for 15 s at 60% of maximal output with 1 min rest, in a Branson sonicator with a probe tip of 0.5 cm diameter in an ice bath. The sonicate was centrifuged twice at 17,370*g* for 5 min to remove unbroken mitochondria. The supernatant was centrifuged at 105,000*g* for 40 min at 4°C to obtain submitochondrial particles.

The activity of iLDH was determined at 30°C in 1 ml of 120 mM KCl, 20 mM Mops, 0.5 mM EGTA, pH 7.6 (KME buffer), 0.2 mM PMS, 0.2 mM DCPIP, and 0.03–0.05 mg mitochondrial protein. The reaction was started by addition of L- or D-lactate, and the rate of DCPIP reduction was determined by measuring the absorbance change at 600 nm and using an extinction coefficient of 21.3 mM^{-1} cm^{-1} at pH 7.6 (28). The succinate dehydrogenase activity was also determined using DCPIP and 10 mM succinate as electron acceptor and donor, respectively. When the electron acceptor used was Q_1 instead of DCPIP, mitochondria were previously incubated with 1 mM ADP, 1 mM $MgCl_2$, and 0.2% (w/v) fatty acid-free bovine serum albumin (BSA) for 15–20 min at 25°C to deplete endogenous substrates. The rate of quinone reduction at 273 nm was measured under the same above-mentioned conditions with 10 mM azide also added to the assay medium. The activity of the cytochrome c oxidase was measured by following the rate of oxygen consumption. Mitochondria were incubated in KME buffer and in the presence of 10 mM ascorbate, freshly prepared, and 2 μM antimycin; the reaction was started by addition of 2 mM TMPD and the rate was corrected for the oxygen uptake resistant to 20 mM azide (29).

Uptake of [^{14}C]L-lactate was carried out according to Wanders *et al.* (30). *Euglena* mitochondria (1.5–3 mg protein) were incubated with 0.6 ml KME buffer and 1 mM [^{14}C]L-lactate (100 cpm/nmol) at 15°C. After 20 s, the reaction mixture was withdrawn and carefully layered into a microfuge tube that contained, from bottom, 0.3 ml 30% (v/v) perchloric acid and 0.3 ml silicone oil (density of 1.028 g/ml). The reaction was stopped by rapid centrifugation at 14,000*g* for 2 min at 4°C. The perchloric acid phase was collected to measure the radioactivity in a liquid scintillation counter.

Extraction of iLDH activity was done by treatment with detergents at several different detergent/protein ratios. The concentration of protein was adjusted to the desired dilution (7 mg protein/0.25–0.3 ml) with KME buffer. The mixture was placed in a microfuge tube of 1.5 ml, strongly stirred in a vortex, set at maximal speed for 3 min in ice. The mixture was centrifuged at 14,000*g* for 3 min at 4°C. The supernatant was used to determine the solubilization of iLDH activity.

The identification of the iLDH activity in SDS–PAGE gels was performed by using submitochondrial particles (0.3–0.5 mg protein) mixed with 10% (v/v) mercaptoethanol, 4% (w/v) sodium dodecyl sulfate (SDS), 20% (v/v) glycerol, 0.005% (w/v) bromophenol blue, in 125 mM Tris, pH 6.8 (31). This mixture was boiled for 5 min. Samples of 50 μg were poured into a 7.5% acrylamide gel that also contained 0.5 mM L- or D-lactate. After electrophoresis, the gel was subjected to a renaturable enzyme activity assay as described by Marshall and Leevers (32) with some modifications. The gel was incubated for 30 min at room temperature, twice, in 50 mM Tris, pH 7.5, 0.5 mM mercaptoethanol. Then, a second incubation was carried out in the last buffer with 6 M guanidine for 20 min. Finally, to renature the proteins, the gel was incubated in the Tris/mercaptoethanol buffer with 0.02% (v/v) Tween 20 and 0.5% (v/v) Nonidet P-40 for 14–18 h at 4°C. The "in gel" iLDH activity was identified by incubating at 35°C in 50 mM Tris, pH 8.5, 2 mM $MgCl_2$, 5 μM PMS, and 10 μM NBT; the reaction was stopped with 3% (v/v) acetic acid.

RESULTS

Enrichment of the iLDH Activity in the Mitochondrial Fraction

Yokota and Kitaoka (13) reported iLDH activity with both isomers in mitochondria and in the microsomal fraction. However, the degree of cross-contamination between both fractions was significant. Then, to further assess whether iLDH is in fact located in the mitochondrial fraction, we followed its activity through the cell fractionation by sonication and differential centrifugation (Table I). The enrichment of the iLDH activity was associated with increases in the succinate dehydrogenase and cytochrome c oxidase activities, which are respiratory chain enzymes of the inner mitochondrial membrane.

TABLE I

Subcellular Location of the iLDH Activity

Cell fraction	D-iLDH	L-iLDH	SDH	Cyt c oxidase
Homogenate	1.0	1.0	1.0	1.0
Mitochondrial + microsomal	1.68 ± 0.16 (9)	0.83 ± 0.1 (3)	1.36 ± 0.16 (9)	0.63 ± 0.19 (3)
Mitochondrial	6.24 ± 0.92 (9)	4.9 ± 0.5 (3)	4.44 ± 0.65 (6)	5 ± 1.2 (3)
Microsomal	0.69 ± 0.08 (9)	0.46 ± 0.07 (3)	0.54 ± 0.11 (9)	0.38 ± 0.07 (3)
SMP	9.15 ± 1.61 (5)	ND	ND	ND

Note. Euglena cells were disrupted by gentle sonication to obtain the homogenate, which was subjected to consecutive centrifugation steps for 10 min at 280*g* and 8000*g* at 4°C. The supernatant of the first centrifugation was labeled "mitochondrial + microsomal" fraction; the pellet of the second centrifugation was the "mitochondrial" fraction and the supernatant was the "microsomal" fraction. The enzyme activities were measured as described under Materials and Methods after the addition of 5 mM D-lactate, 10 mM L-lactate, 10 mM succinate (succinate dehydrogenase, SDH), or 2 mM TMPD (cytochrome c oxidase), respectively. The absolute rates were, in the homogenate, 54 ± 6 (9), 46.6 ± 2 (3), 16 ± 2 (9) nmol DCPIP/(min × mg protein) for D-iLDH, L-iLDH, and SDH, respectively, and 89 ± 7 (3) ng atoms oxygen/(min × mg protein) for cytochrome c oxidase. In the mitochondrial fraction the rates were 336 ± 38 (10) and 230 ± 18 (3) nmol DCPIP/(min × mg protein) for D-iLDH and L-iLDH, respectively. The data shown represent the mean ± the standard error of the mean (SE), with the number of different preparations assayed between parentheses. ND, not determined.

Kinetics of the iLDH Activity

The rate of dehydrogenation in *Euglena* mitochondria of both lactate isomers followed a Michaelis–Menten kinetics pattern. The dissociation constants (K_s) for both isomers were similar, but the V_{max} was higher with D-lactate (Table II), when using either DCPIP or Q_1 as electron acceptor. The enzyme affinity for Q_1 was different with each isomer ($P < 0.05$), whereas the V_{max} was 1.6 (L-lactate) and 1.3 (D-lactate) times higher with Q_1 than with DCPIP. Substitution of Q_2 or DBQ for Q_1 yielded lower V_{max} values for D-lactate dehydrogenation, although the catalytic efficiencies (V_{max}/K_s; min^{-1} mg^{-1} ml) were rather similar: 34.3 ± 4.5, 34 ± 7, and 17 ± 6 for Q_1, Q_2, and DBQ, respectively (mean ± SD of three different preparations). The catalytic efficiency for DCPIP reduction was slightly lower (13.6) with D-lactate (Table II).

Oxamate competitively inhibited iLDH activity with both isomers, whereas oxalate exerted a mixed-type inhibition (Table III). It should be noted, however, that the dehydrogenation of D-lactate was two times more sensitive to both inhibitors and that the K_i values were three times lower for oxalate than for oxamate. The inhibition exerted by oxalate when varying DCPIP was also of the mixed-type with K_i of 0.9 ± 0.1 mM ($n = 3$) for 10 mM D-lactate and 5.9 ± 0.7 mM ($n = 4$) for 10 mM L-lactate.

A set of parallel straight lines was obtained in the double-reciprocal plot of different concentrations of DCPIP versus activity, at different fixed concentrations of L- or D-lactate (Fig. 1). This kinetic behavior is typical of a double-displacement kinetic (ping-pong) mechanism (33). The non-linear regression fitting of the experimental points also supported the same conclusion: the variability of the values for K_{lac}, K_{DCPIP}, and V_{max} was significantly lesser in the fitting to the ping-pong mechanism than in that to the random or the ordered mechanisms. Similar sets of parallel straight lines, although less reliable because of higher variability, were also obtained with different concentrations of Q_1 (data not shown).

The iLDH activity showed a maximum at pH values of 7.3–7.6 (data not shown). The activity was constant when mitochondria were preincubated for 5 min at pH values from 7 to 8 and the activity assayed at pH 7.6. At lower or higher pH values, the activity with both isomers gradually decayed, reflecting lower enzyme stability.

Thermostability of the iLDH Activity

Exposure of mitochondria to increasing temperatures above 45°C induced a concomitant diminution in iLDH activity with both isomers, following a first-order exponential decay kinetics (data not shown). The slope

TABLE II

Kinetic Parameters for the Dehydrogenation of L- and D-Lactate in *Euglena* Mitochondria

	L-Lactate	D-Lactate
K_s (mM)	2.45 ± 0.3 (17)	2.7 ± 0.3 (15)
V_{max} (nmol DCPIP/(min × mg protein))	268 ± 31 (17)	477 ± 44 (15)*
K_{DCPIP} (μM)	35 ± 10 (6)	35 ± 5 (6)
K_{Q1} (μM)	41 ± 7 (3)	18.4 ± 5 (3)*
V_{max} (nmol Q_1/(min × mg protein))	427 ± 35 (3)	617 ± 70 (3)*

Note. The K_s values for D- and L-lactate, using Q_1 as electron acceptor, were very similar to those found with DCPIP as acceptor. The data shown represent the mean ± standard error of the mean (SE) of the number of preparations assayed shown between parentheses.

* $P < 0.05$ versus L-lactate.

TABLE III

Oxamate and Oxalate Inhibition Constants of the iLDH Activity

	L-Lactate	D-Lactate
$K_{OXAMATE}$ (mM) (competitive)	1.2 ± 0.2 (7) (Dixon plot) 0.95 ± 0.2 (7) (Nonlinear regression)	0.51 ± 0.1 (8) (Dixon plot) 0.38 ± 0.09 (6) (Nonlinear regression)
$K_{OXALATE}$ (mM) (mixed-type)	0.36 ± 0.07 (10) (Dixon plot) 0.26 ± 0.08 (11) (Nonlinear regression) α = 5 ± 1.5	0.15 ± 0.02 (11) (Dixon plot) 0.09 ± 0.1 (11) (Nonlinear regression) α = 1.3 ± 0.2

Note. The rates of iLDH activity were obtained in the presence of 0.2 mM DCPIP, at different concentrations (1–10 mM) of L- or D-lactate, and in the presence of five different concentrations of oxamate or oxalate. The rates were fitted by linear regression to the Dixon plot or by nonlinear regression to the Michaelis-Menten equation for competitive, noncompetitive, and mixed-type inhibition. The equation for mixed-type inhibition used was [33]

$$V = \frac{V_{max_{ap}} S}{Ks_{ap} + S} \text{ where } V_{max_{ap}} = \frac{V_{max}}{1 + I/\alpha K_i} \text{ and } K_{s_{ap}} = K_S \frac{1 + I/K_i}{1 + I/\alpha K_i}.$$

of the semilogarithmic plot of activity versus time (Fig. 2) yielded the inactivation rate constant (k_{inac}) for each temperature. The plot of k_{inac} versus temperature showed that the denaturation of the L-iLDH activity, in the absence of ligands, was accelerated above 50°C (Fig. 3A). The addition of ligands, either inhibitors, the D isomer, or the substrate itself, protected the L-iLDH activity from thermal inactivation, bringing about stability at temperatures up to 65°C. In turn, the D-iLDH activity was thermoresistant at 75°C in the absence or in the presence of ligands (Fig. 3B).

The activation energies for thermal inactivation were 44 and 55.7 kcal mol^{-1} for the L- and D-iLDH activities in the range of 50–70°C and 80–90°C, respectively. For comparison, the activation energies in the range of 20–35°C were 9.5 ± 0.1 (n = 4) and 9.4 ± 0.06 (n = 3) kcal mol^{-1} for the L- and D-iLDH activities, respectively.

Taking advantage of the greater thermostability of the D-iLDH activity, mitochondria were incubated at 70°C to abolish the L-iLDH activity. A large inactivation of L-iLDH occurred after 2 min exposure at 70°C, without affecting the D-iLDH (Fig. 4A). The subsequent determination of the kinetic parameters of the D-iLDH activity, in these 70°C-treated mitochondria (Fig. 4B), revealed the preservation of the enzyme structure, since the K_s for D-lactate (2 ± 0.4 mM; n = 3) and V_{max} (574 ± 92 nmol/(min × mg protein)) were very similar to those from control mitochondria (Table II). The iLDH activity with 2 mM D-lactate in the heat-treated mitochondria was 23 ± 3% (n = 3) inhibited by 15 mM L-lactate. With 300 mM L-lactate, the inhibition was only 28%, probably due to either a significant residual L-iLDH activity, to some transformation of L-lactate by D-iLDH, or to unspecific effects by the high ionic strength.

Assuming that the reaction catalyzed by the iLDH establishes a rapid equilibrium for the substrate association, the dissociation constant obtained at different temperatures was used to calculate the thermody-

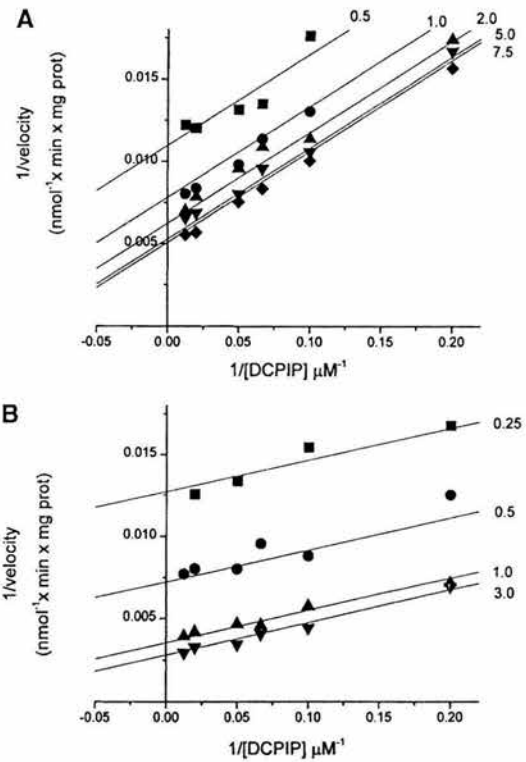

FIG. 1. Kinetic mechanism of the iLDH activiy. *Euglena* mitochondria freshly prepared (0.03–0.05 mg protein/ml) were incubated at 30°C as described under Materials and Methods. The reaction was started with the indicated (mM) L-lactate (A) or D-lactate (B) concentrations at variable DCPIP concentrations. From the nonlinear regression analysis (solid lines), V_{max} (nmol DCPIP/(min × mg protein)) of 347 ± 65 (n = 6) and 577 ± 70 (n = 8), and K_{LAC} (mM) of 3.3 ± 1 (n = 6) and 3.1 ± 0.4 (n = 8) were derived for L- and D-lactate, respectively.

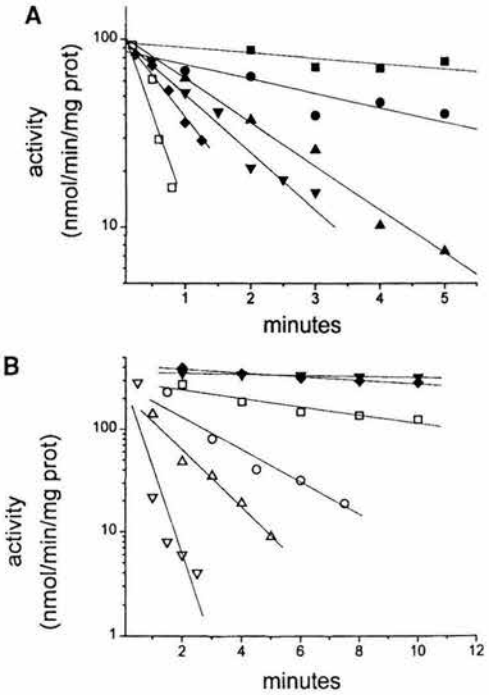

FIG. 2. Inactivation of the iLDH by temperature. Mitochondria (5–10 mg protein) were preincubated at different temperatures for the indicated times. (A) 45°C (squares), 50°C (circles), 55°C (triangles), 60°C (inverted triangles), 65°C (diamonds), and 70°C (open squares). (B) 60°C (inverted triangles), 65°C (diamonds), 70°C (open squares), 75°C (open circles), 80°C (open triangles), and 85°C (inverted open triangles). Then, an aliquot of 10 μl (50–100 μg protein) was transferred to a cuvette thermostated at 30°C for measurements of the DCPIP reduction in 1 ml medium for about 1 min with 20 mM L-lactate (A) or 20 mM D-lactate (B).

namic parameters of the reaction for each isomer (Fig. 5), using the equation (33)

$$\log K_s = -\frac{\Delta H^\circ}{2.303RT} + \frac{\Delta S^\circ}{2.303R}$$

The straight lines with slopes of different sign for each isomer (Fig. 5C) indicated that the dissociation of L-lactate was an endothermic process with an increase in entropy, whereas that of D-lactate was an exothermic reaction with a decrease in entropy. The resulting positive change in Gibbs free energy for the dissociation at 30°C was essentially identical for both isomers and indicated that the association was thermodinamically favored.

L-Lactate Uptake

The transport of [^{14}C]L-lactate into mitochondria was determined in an attempt to establish the orientation of the iLDH catalytic site. The rate of uptake was linear for 45 s at 15°C and with 1 mM [^{14}C]L-lactate (data not shown); the control rate was 11.2 ± 1 nmol/(min × mg protein) (mean ± SD; n = 3). The effect of either 2 mM oxalate, 5 mM oxamate, 0.2 mM *N*-ethylmaleimide, 0.1 mM α-cyano-4-hydroxycinnamate, 0.5 nmol stigmatellin, or 30 mM D-lactate on the uptake rate was negligible; in contrast, 40 nmol mersalyl/mg protein exerted a strong inhibitory effect of 48 ± 6% (n = 3). At 15°C and with 1 mM L-lactate, oxamate, and oxalate inhibited the L-iLDH activity of 61 ± 8 nmol/(min × mg protein) (n = 4) by 85 and 60%, respectively; mersalyl did not affect the L-iLDH activity. However, preincubation of mitochondria with mer-

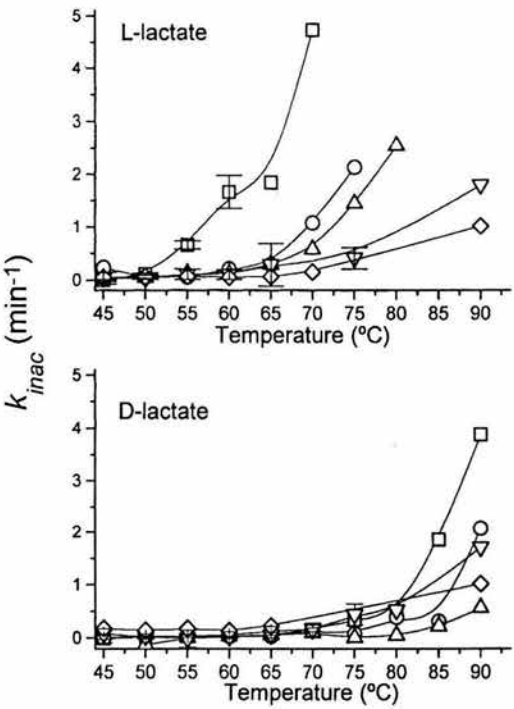

FIG. 3. Ligand protection against thermal inactivation. Mitochondria were preincubated in the absence (squares) or in the presence of the different ligands and temperatures to obtain inactivation curves as shown in Fig. 2. The concentrations of the ligands were 5 mM oxamate (circles), 5 mM oxalate (triangles), 5 mM opposite ligand (inverted triangles), and 5 mM substrate (diamonds). The inactivation constant (k_{inac}, min^{-1}) was estimated from the slope in the plot of log activity versus time (see Fig. 2). The data shown represent the mean ± SD of three different mitochondrial preparations assayed.

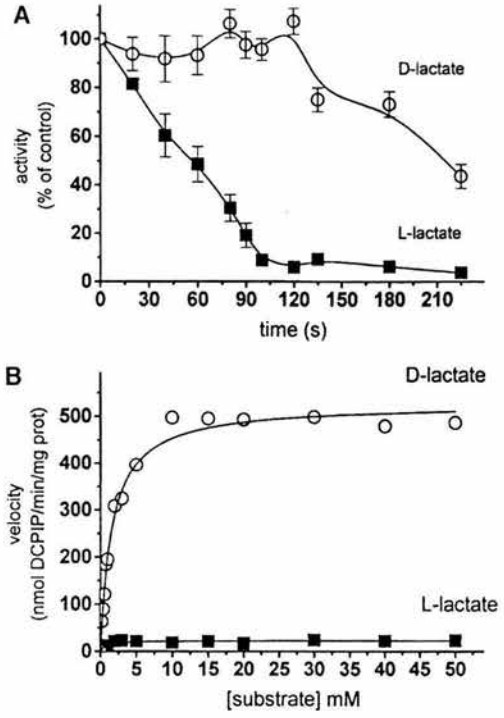

FIG. 4. Specific thermal inactivation of L-iLDH at 70°C. (A) Mitochondria (5–10 mg protein) were incubated at 70°C for the indicated times; aliquots of 10–15 μl (0.05–0.1 mg protein) were transferred to 1 ml medium thermostated at 30°C to determine the rate of lactate dehydrogenation with the corresponding isomer. The data shown are means ± SD of 14 different preparations. (B) The rate of iLDH activity was determined at 30°C and different lactate concentrations in mitochondria previously incubated at 70°C for 2 min. The solid line represents the best fit to the Michaelis–Menten equation.

salyl for 2 min prompted a 60% inhibition of L-lactate transport and 47% inhibition of dehydrogenation.

Solubilization of iLDH

Treatment of *Euglena* mitochondria with Chaps, in a detergent/protein ratio of 0.7 (2% (w/v) final detergent concentration; 7 mg mitochondrial protein), resulted in a maximal solubilization of the D-iLDH activity (75.5 ± 10% of initial activity; 4.18 ± 1.3 mg protein solubilized; n = 16). Lower or higher ratios yielded a lower solubilized activity (data not shown). Other detergents such as β-octyl-pyranoside, Lubrol, Triton X-100, Tween 20, and sodium deoxycholate, yielded lower solubilization of D-iLDH. Addition of 0.02% (w/v) Chaps, concentration reached in the activity assay of the solubilized samples, to intact mitochondria increased the D-iLDH activity by 10–12%; concentrations of Chaps of 0.01 or 0.04% did not affect the activity. Addition of 0.05% Lauryl-maltoside, β-octyl-pyranoside, or Lubrol strongly inhibited the D-iLDH activity by 75–81%. The solubilization of the D-iLDH activity by Chaps, from that originally present in intact mitochondria, was almost complete since only 5% of total initial activity was found in the pellet.

Solubilized D-iLDH activity exhibited similar kinetic parameters (K_s for D-lactate, V_{max}, K_i for oxalate, K_i for oxamate, and type of inhibition exerted by oxalate and oxamate) to those observed in intact mitochondria (data not shown). To examine the L-lactate inhibition on the D-iLDH activity, without the interference of residual L-iLDH activity, the solubilized D-iLDH was heated at 70°C for 2 min. In this latter preparation, the D-iLDH activity was preserved (V_{max} = 532 nmol/(min × mg protein); K_s for D-lactate = 2.9 mM) and inhibited, competitively, by L-lactate with a K_i of 39.3 mM (n = 2) (data not shown).

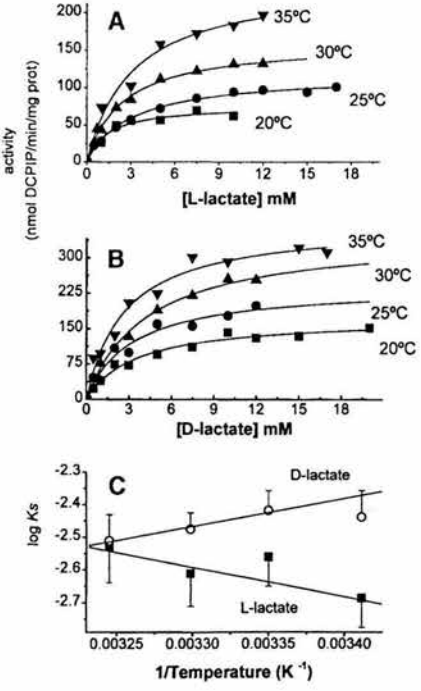

FIG. 5. Thermodynamic parameters for substrate association. Dehydrogenation of L-lactate (A) and D-lactate (B) was measured at the indicated temperatures in the conditions described under Materials and Methods. The dissociation constant were derived from fitting the experimental points to the Michaelis–Menten equation at each temperature by nonlinear regression analysis. The data shown represent the mean ± SD of four different mitochondrial preparations.

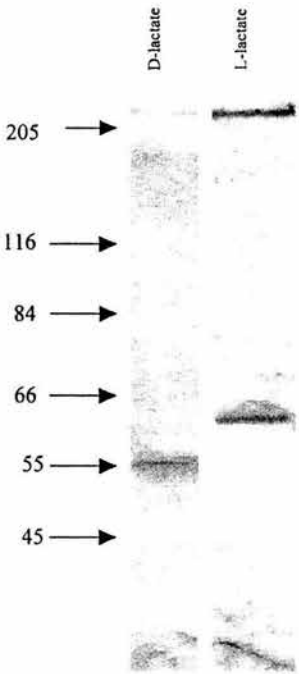

FIG. 6. Molecular weight of the iLDH. Analyses of enzyme activities in SMP (50 μg per lane) were carried out after separation, on a continuous 7.5% SDS–PAGE, and renaturation, as described under Materials and Methods.

None of the above-mentioned detergents was useful for solubilization of the L-iLDH activity, except for β-octyl-pyranoside, which was somewhat successful in extracting and preserving some activity (30 ± 15%; 3.7 ± 1.3 mg protein solubilized; $n = 14$). However, a 19% of total initial activity was still found in the pellet. Note that only half of total L-iLDH was recovered after the solubilization procedure. This apparent labile nature of *Euglena* L-iLDH is in agreement with similar behavior found for the same enzyme from *Neisseria meningitidis* (20) and *Acinetobacter calcoaceticcus* (34).

Molecular Weight of the iLDH

To estimate the molecular mass of the mitochondrial proteins with iLDH activity, submitochondrial particles were subjected to "in gel" dehydrogenase assay electrophoresis (32), in which proteins were renatured and assayed for activity using the artificial electron acceptors PMS and NBT. A discrete band of approximately 55 kDa was obtained when gels were supplemented with D-lactate, whereas another band of 60 kDa was revealed with L-lactate (Fig. 6).

DISCUSSION

Kinetics

The affinity of the iLDH activity, and its kinetic behavior, for both lactate isomers and DCPIP in *Euglena* mitochondria was similar to that described for bacterial systems (17, 20, 22). We recently described that isooctane-treated *Euglena* mitochondria, to extract endogenous quinones, showed a severe diminution in the lactate oxidase activity (even in the presence of an excess of cytochrome c), which could be recovered by addition of exogenous quinones (9). The bacterial membrane-bound iLDHs have quinones as natural acceptors (35), whereas the yeast iLDH transfers electrons directly to cytochrome c (36). Our mitochondrial preparations showed a higher V_{max} with Q_1 as acceptor than with DCPIP. These data strongly suggest that iLDH in *Euglena* mitochondria transfers electrons directly to the quinone pool, as occurs in the bacterial enzymes (35).

The different affinity for oxamate and oxalate when using L- and D-lactate suggests that different molecular entities catalyze the dehydrogenation of each isomer. Similarly, the effect of oxamate and oxalate on bacterial iLDH varies. A competitive inhibition of oxamate on D-iLDH from *Escherichia coli* has been reported (37), although the K_i was much lower (3.3 μM); the L-iLDH from *Rhodopseudomonas sphaeroides* was noncompetitively inhibited by oxamate with a K_i of 0.96 mM (17). On the other hand, oxalate competitively inhibited the D-iLDH from *E. coli* (37) and noncompetitively the L-iLDH from *R. sphaeroides* (17) with K_i values of 0.9 and 30 μM, respectively. It should be noted that these authors (17, 37) used double-reciprocal plots to determine the inhibition type and the K_i values. To diminish the distortion in the error distribution when the experimental data are analyzed by linear regression (38), in this work we applied a nonlinear regression analysis to obtain the kinetic parameters.

The ping-pong kinetic mechanism for iLDH described here is in agreement with previous reports describing the same mechanism for other respiratory dehydrogenases (39, 40). Although we have not yet examined the nature of the prosthetic group, it is conceivable that, by analogy with other flavin-dehydrogenases such as succinate (40, 41), α-glycerophosphate (42), and acylCoA (43) dehydrogenases, the electrons from the dehydrogenation of lactate reduce the flavin, which in turn reduces the quinone. The mixed-type inhibition exerted by oxalate, when varying the lactate concentration, suggests that this inhibitor may bind to both the free (with the prosthetic group oxidized F, which could be FMN or FAD; see Scheme I) and the modified, reduced (FH_2) enzyme form. Binding of oxalate to the free, oxidized enzyme in the lactate site, together with binding to the modified, reduced enzyme in the pyruvate or quinone site, would explain the observed

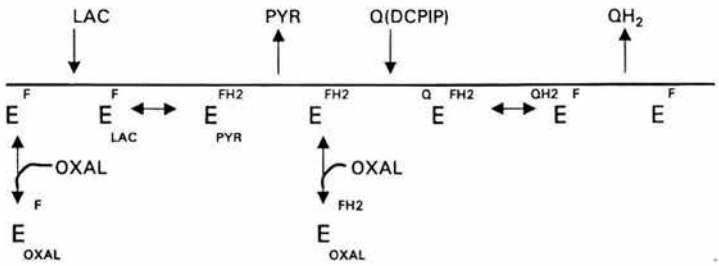

SCHEME I

mixed-type inhibition. The mixed-type oxalate inhibition when varying the DCPIP concentration supports the notion that this inhibitor binds to both the oxidized and the reduced enzyme species (see Scheme I); however, oxalate should preferentially bind to the free enzyme due to a higher affinity ($K_{i(lactate)} < K_{i(DCPIP)}$).

Thermostability

The high iLDH resistance to the inactivation by temperature was unexpected since *Euglena* is highly sensitive to temperatures above 34°C (44). The D-iLDH from the sulfate-reducing thermophylic archeobacterium *Archaeoglubus fulgidus* is indeed stable at 80°C (45), and also that from *E. coli* at 60°C for 1 h (46). The different sensitivity to the temperature inactivation for the iLDH activity, depending on the isomer used, indicated, clearly, that different stereo-specific enzymes were involved in the dehydrogenation of each lactate isomer. Since the opposite isomer protected from the temperature inactivation, it was thought that both isomers may bind to both iLDH, but that the D-iLDH only oxidizes the D isomer. The preservation of the kinetic properties of the D-iLDH activity after an incubation of 2 min at 70°C supported the last interpretation. Moreover, the different activation energies for denaturation of both isomers provided further support to the proposal of two stereo-specific iLDH in *Euglena* mitochondria. Since the opposite isomer protected from thermal inactivation, and L-lactate competitively inhibited the D-iLDH activity in the solubilized and heated preparation, it is evident that D-iLDH is specific for the D isomer, but may bind the L isomer without being able to transform it. The higher affinity (14-fold) of the *Euglena* D-iLDH for the D isomer (K_s for D-lactate = 2.9 mM; K_i for L-lactate = 39.3 mM) has also been observed in the *E. coli* (16) and *N. gonorrhoeae* (21) purified D-iLDHs (30- and 60-fold, respectively).

Despite the high dispersion of the experimentally determined K_s, a linear relationship with the inverse of the temperature could be established. However, the completely opposite pattern obtained for each isomer indicated again that different enzymes catalyzed the dehydrogenation of L- and D-lactate.

General Aspects

The rate of L-lactate uptake was five times lower than the rate of dehydrogenation. Moreover, the sensitivity of both reactions to oxalate, oxamate, and mersalyl was completely opposite. In consequence, these data suggest that the transport of L-lactate into mitochondria is not required for its dehydrogenation to occur; hence, the catalytic site of the L-iLDH is very likely located facing the intermembrane space. The presence of a slow transport of L-lactate in *Euglena* mitochondria which is mersalyl-sensitive suggests that an unspecific transport system, perhaps the dicarboxylate or the monocarboxylate carrier, is involved in this reaction. The external orientation of the catalytic site fits well with a function for the L-iLDH as the final acceptor of glycolytic L-lactate from paramylum degradation, which ensures full oxidation and generation of a maximal profit (ATP synthesis by oxidative phosphorylation instead of only by glycolysis).

Since the NADH-dependent D-lactate dehydrogenase belongs to the glycolytic pathway in *Euglena* (27), it is expected that the catalytic site of the mitochondrial D-iLDH is also orientated toward the intermembrane space. The D-iLDH in *E. coli* is located on the inner face of the cytoplasmic membrane (47). However, it has been recently reported that the intracellular concentration of L-lactate in *Euglena* cells, grown on glutamate plus malate and harvested in the early stationary growth phase, was 3.8 mM, whereas that of D-lactate was negligible (9). It is unknown whether the L-lactate concentration varies with the growth phase and the carbon source and that of D-lactate becomes significant.

The apparent molecular mass of several bacterial D-iLDH and L-iLDH is around 60 and 45 kDa, respectively (48), although the D-iLDH from *Archaeglobus fulgidus* exhibited a molecular mass of 50 kDa (45) and that of yeast L-iLDH of 60 kDa (48). These molecular mass values are within the range found in this work for

the proteins with L- and D-iLDH activities in *Euglena* mitochondria.

The activity of iLDH was not detected in mitochondria isolated from *Polytomella, Phaseolus vulgaris,* alfalfa, *Vicia faba, Crithidia,* and *cysticerci* (data not shown). However, this activity was apparent in *Trypanosoma cruzi* mitochondria and in membranes from several bacteria such as *E. coli, Paracoccus denitrificans, Bacillus subtilis, B. cereus,* and *B. stearothermophillus,* in agreement with previous reports (11, 48). *Trypanosoma* and *Euglena* belong to the most primitive eukaryotic phyla with cells containing mitochondria (49). Then, the presence of iLDH activity suggests a close phylogenetic relationship between the respiratory chains of bacteria and *Euglena.*

In conclusion, the following data support the existence of two different stereo-specific iLDH in *Euglena* mitochondria. Different affinity for oxamate and oxalate, different thermo-stability, different thermodynamic parameters for substrate binding and thermal denaturation, different solubilization with detergents, and different apparent molecular weight.

ACKNOWLEDGMENTS

The authors thank Drs. R. Muñoz-Clares and G. MacCarthy for their critical reading of the manuscript. The present work was partially supported by grants 25274-M and 25465-N from CONACyT-Mexico.

REFERENCES

1. Buetow, D. E., and Buchanan, P. J. (1965) *Biochim. Biophys. Acta* **96,** 9–17.
2. Sharpless, T. K., and Butow, R. A. (1970) *J. Biol. Chem.* **245,** 50–57.
3. Sharpless, T. K., and Butow, R. A. (1970) *J. Biol. Chem.* **245,** 58–70.
4. Tokunaga, M., Nakano, Y., and Kitaoka, S. (1976) *Agric. Biol. Chem.* **40,** 1439–1440.
5. Moreno-Sánchez, R., and Raya, J. C. (1987) *Plant Sci.* **48,** 151–157.
6. Buetow, D. E. (1989) *in* The Biology of *Euglena* (Buetow, D. E., Ed.), Vol. IV, pp. 247–314, Academic Press, New York.
7. Uribe, A., and Moreno-Sánchez, R. (1992) *Plant Sci.* **86,** 21–32.
8. Inui, H. (1984) *J. Biochem.* **96,** 931–934.
9. Moreno-Sánchez, R., Covian, R., Jasso-Chávez, R., Rodríguez-Enríquez, S., Pacheco-Moisés, F., and Torres-Márquez, M. E. (2000) *Biochim. Biophys. Acta* **1457,** 200–210.
10. Price, C. A. (1961) *Biochem. J.* **82,** 61–66.
11. Garvie, E. I. (1980) *Microbiol. Rev.* **44,** 106–139.
12. Collins, N., and Merrett, M. J. (1975) *Biochem. J.* **148,** 321–328.
13. Yokota, A., and Kitaoka, S. (1979) *Agric. Biol. Chem.* **43,** 855–857.
14. Nelson, E. B., and Tolbert, N. E. (1970) *Arch. Biochem. Biophys.* **141,** 102–110.
15. Lord, J. M., and Merrett, M. J. (1971) *Biochem. J.* **124,** 275–281.
16. Futai, M. (1973) *Biochemistry* **12,** 2468–2474.
17. Markwell, J. P., and Lascelles, J. (1978) *J. Bacteriol.* **133,** 593–600.
18. Olson, S. T., and Massey, V. (1979) *Biochemistry* **18,** 4714–4724.
19. Allison, N., O'Donell, M. J., Hoey, M. E., and Fewson, C. A. (1985) *Biochem. J.* **227,** 753–757.
20. Erwin, A. L., and Gotschlich, E. C. (1993) *J. Bacteriol.* **175,** 6382–6391.
21. Fischer, R. S., Martin, G. C., Rao, P., and Jensen, R. A. (1994) *FEMS Microbiol.* **115,** 39–44.
22. Zboril, P., and Wernerová, V. (1996) *Biochem. Mol. Biol. Int.* **39,** 595–605.
23. Lodi, T., and Ferrero, I. (1993) *Mol. Gen Genet.* **238,** 315–324.
24. Somlo, M. (1965) *Biochim. Biophys. Acta* **97,** 183–201.
25. Sumida, S., Ehara, T., Osatune, T., and Hase, E. (1987) *Plant Cell Physiol.* **28,**1587–1592.
26. Barras, D. R., and Stone, B. A. (1968) *in* The Biology of *Euglena,* (Buetow, D. E., Ed.), Vol. II, Chap. 7, pp. 175–183, Academic Press, New York.
27. Smillie, R. M. (1968) *in* The Biology of *Euglena* (Buetow, D. E., Ed.), Vol. II, Chap. 1, pp. 2–54, Academic Press, New York.
28. Armstrong, J. M. (1964) *Biochim. Biophys. Acta* **86,** 194–197.
29. Devars, S., Hernández, R., Covián, R., García-Horsman, A., Barquera, B., and Moreno-Sánchez, R. (1998) *J. Eukaryotic Microbiol.* **45,** 122–130.
30. Wanders, R. J. A., Van Woerkom, G. M., Nooteboom, R. F., Meijer, A. J., and Tager, J. M. (1981) *Eur. J. Biochem.* **113,** 295–302.
31. Laemmli, U. K. (1970) *Nature* **227,** 680–685.
32. Marshall, C. J., and Leevers, S. J. (1995) *Methods Enzymol.* **255,** 273–279.
33. Segel, Y. H. (1975) Enzyme Kinetics, Wiley, New York.
34. Allison, N., O'Donell, M. J., Hoey, M. E., and Fewson, C. A. (1985) *Biochem. J.* **231,** 407–416.
35. Ingledew, W. J., and Poole, R. K. (1989) *Microbiol. Rev.* **48,** 222–271.
36. Gondry, M., and Lederer, F. (1996) *Biochemistry* **35,** 8587–8594.
37. Kohn, L. D., and Kaback, H. R. (1973) *J. Biol. Chem.* **248,** 7012–7017.
38. Leatherbarrow, R. J. (1990) *Trends Biochem. Sci.* **15,** 455–458.
39. Sharp, R. E., Chapman, S. K., and Reid, G. A. (1996) *Biochem. J.* **316,** 507–513.
40. Singer, T. P., Kearney, E. B., and Kenney, W. C. (1973) *Adv. Enzymol.* **37,** 189–272.
41. Tielens, A. G. M., and Van Hellemond, J. J. (1998) *Biochim. Biophys. Acta.* **1365,** 71–78.
42. Garrib, A., and McMurray, W. C. (1986) *J. Biol. Chem.* **261,** 8042–8048.
43. Furuta, S., Miyazawa, S., and Hashimoto, T. (1981) *J. Biochem.* **90,** 1739–1750.
44. Kempner, E. S. (1982) *in* The Biology of *Euglena* (Buetow, D. E., Ed.), Vol. III, pp. 197–252, Academic Press, New York.
45. Reed, D. W., and Hartzell, P. L. (1999) *J. Bacteriol.* **181,** 7580–7587.
46. Pratt, E. A., Fung, L. W-M., Flowers, J. A., and Ho, C. (1979) *Biochemistry* **18,** 312–316.
47. Short, S. A., and Kaback, H. R. (1975) *J. Biol. Chem.* **250,** 4291–4296.
48. Fewson, C. A., Baker, D. P., Chalmers, R. M., Keen, J. N., Hamilton, I. D., Scott, A. J., and Yasin, M. (1993) *J. Gen. Microbiol.* **139,** 1345–1352.
49. Knoll, A. H. (1992) *Science* **256,** 622–627.

PROBLEMA BIOQUÍMICO

TEMA: Cinética enzimática
INACTIVACIÓN TÉRMICA.

Las mitocondrias del protista *Euglena gracilis* oxidan L- y D-lactato por medio de deshidrogenasas membranales que están conectadas a la cadena respiratoria, y son independientes de piridín nucleótidos (iLDH). Con el propósito de distinguir entre (1) la presencia de dos proteínas diferentes que catalizan la misma reacción pero con isómeros diferentes y (2), una sola enzima con afinidad para los dos isómeros, se determinó la termoestabilidad de la deshidrogenación con L- y D-lactato. Las mitocondrias de *E. gracilis* se incubaron a diferentes temperaturas por los tiempos indicados. La actividad de iLDH se determinó espectrofotometricamente, después de la adición de uno de los isómeros del lactato midiendo la reducción del aceptor artificial de electrones diclorofenolindofenol (DCPIP), siguiendo el cambio en la absorbancia a 600 nm. A continuación se presentan las velocidades iniciales a concentraciones saturantes de lactato.

Actividad de L-iLDH 8nmol DCPIP/min/mg prot)											
t (min)	Act 45°C	t (min)	Act 50°C	t (min)	Act 55°C	t (min)	Act 60°C	t (min)	Act 65°C	t (min)	Act 70°C
2	186	1	145	1	193	0.5	175	0.25	177	0.2	232
3	162	2	135	2	61	1	165	0.5	165	0.5	179
4	152	3	84	3	56	1.5	107	0.75	136	0.6	63
5	150	4	99	4	22	2	19	1	78	0.8	15.5
		5	87	5	16	2.5	10	1.25	22		
						3	5				

Actividad de D-iLDH (nmol DCPIP/min/mg prot)													
t	Act	t	Act	Act	Act	t	Act	t	Act	t	Act	t	Act
(min)	55°C	(min)	60°C	65°C	70°C	(min)	75°C	(min)	80°C	(min)	85°C	(min)	90°C
3	390	2	357	401	275	1.5	244	1	141	0.5	287	0.16	353
6	378	4	345	353	188	3	42	2	37	1	12	0.33	367
9	376.9	6	329	319	150	4.5	22	3	35	1.5	8	0.5	349
12	376	8	340	299	149	6	31	4	10	2	6	0.66	190
15	370	10	327	289	126	7.5	20	5	5	2.5	4	0.83	19

Determinar para los dos isómeros: las constantes de velocidad de inactivación térmica para cada temperatura, determinar en cuantos eventos se lleva a cabo el proceso de inactivación térmica y calcular la energía de activación de desnaturalización.

PROBLEMA BIOQUÍMICO

RESPUESTAS:

El logaritmo de las velocidades obtenidas a las diferentes temperaturas se grafican *vs* el tiempo al cual se tomó la muestra como se muestra en la primera gráfica, de acuerdo con la ecuación: $\log v = \log v_0 - (k_{inac}\, t/2.303)$ de esta forma, se obtiene una constante de velocidad de primer orden (k_{inac}) a partir del valor de la pendiente.

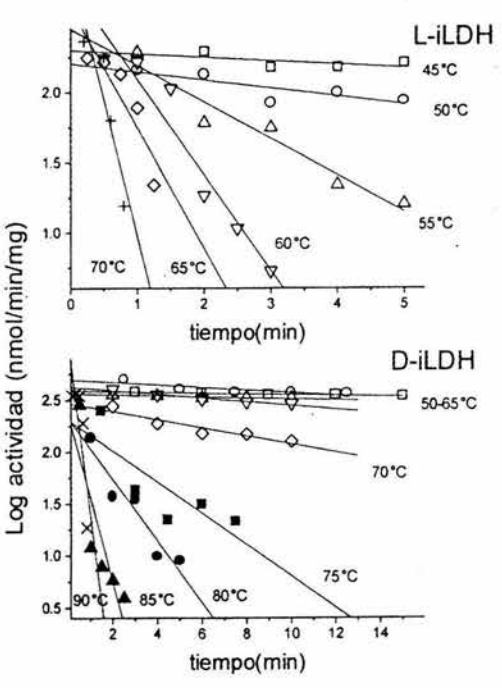

Para determinar el número de eventos en que se lleva a cabo la inactivación térmica de la L- y D-iLDH, se grafican los valores obtenidos de k_{inac} *vs* la temperatura a las que fueron calculadas. En la parte superior de la segunda figura se observa claramente que la inactivación de ambas iLDH es un solo proceso, se dice entonces que es un proceso monotónico. Además con este gráfico se observa que la actividad de D-iLDH es mucho más resistente a la temperatura que la actividad de L-iLDH, lo que indicala presencia de dos enzimas.

Para obtener el valor de la energía de activación (Ea) para la desnaturalización térmica, se grafica el logaritmo de la k_{inac} *vs* el inverso de la temperatura absoluta, de acuerdo con la ecuación de Arrhenius:

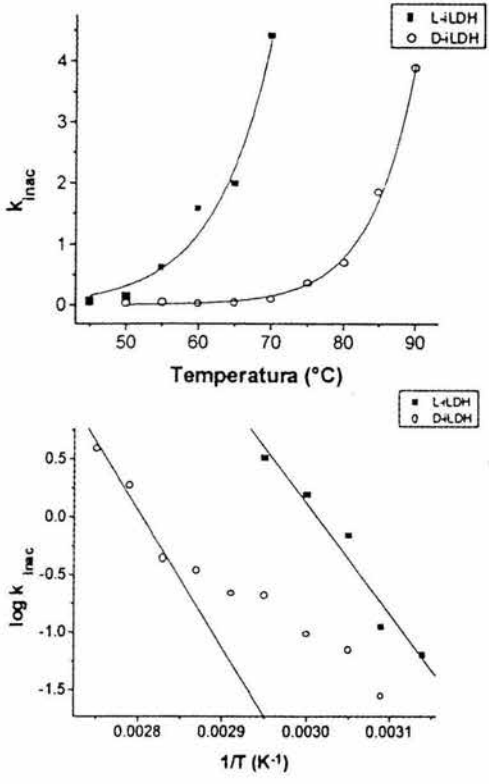

$\log k_{inac} = -(Ea/2.303R)(1/T) + \log k_0$ donde Ea es el valor de la pendiente multiplicado por la constante de los gases R (1.9872 cal/mol K) y por 2.303. Nótese que para la D-iLDH, sólo se consideraron los valores de k_{inac} de las tempe-

raturas mas altas, ya que como se observa en gráfica superior de la segunda figura, la inactivación se observa hasta los 80°C.

Los valores de Ea fueron de 44 y 55 Kcal/mol para la L-iLDH y D-iLDH respectivamente. Estos datos apoyan la presencia de enzimas específicas para cada isómero y descarta la posibilidad de una sola enzima con especificidad para los dos isómeros

Bibliografía

Segel IH (1975). Enzyme Kinetics. John Wiley and Sons, New York. Cap 11B pp 927-935
Dixon MW and Webb EC (1979) Enzymes. Academic Press, New York. Cap 3, pp 164-182

PROBLEMA BIOQUÍMICO

Ricardo Jasso Chávez y Rafael Moreno Sánchez

TEMA: Cinética enzimática
Inhibición de tipo mixto.

La L-lactato deshidrogenasa del protista *Euglena gracilis* es una enzima localizada en la membrana interna mitocondrial, es independiente de piridín nucleótidos (L-iLDH) y está conectada a la cadena respiratoria. En sistemas bacterianos esta enzima se inhibe por oxalato de manera competitiva o no competitiva. Los parámetros cinéticos de la L-iLDH se determinaron en mitocondrias aisladas variando las concentraciones de L-lactato en presencia de concentraciones crecientes del inhibidor. La actividad enzimática de la L-iLDH se midió espectrofotométricamente mediante la reducción a 600 nm del 2,6-Diclorofenolindofenol (DCPIP) como el aceptor artificial de electrones a 30° C y pH de 7.6. A continuación se presentan las velocidades iniciales.

ACTIVIDAD DE L-iLDH (nmol/min/mg prot)						
	[oxalato] mM					
[L-lactato] mM	0	0.1	0.25	0.50	0.75	2.0
0	0	0	0	0	0	0
1	47	41	33	27	23	21
3	79	68	56	49	40	32
5	89	82	68	55	45	42
7.5	93	85	75	56	53	43
10	97	88	77	62	56	48

Determinar los parámetros cinéticos de la L-iLDH, *Ks* y *V*, así como el tipo de inhibición y la *Ki* del oxalato.

PROBLEMA BIOQUÍMICO

RESPUESTAS:

El gráfico Lineweaver-Burk o de dobles recíprocos, es la forma más utilizada para obtener los parámetros cinéticos, así como los diferentes tipos de inhibición. Este gráfico se basa en un re-arreglo de la ecuación de Michaelis-Menten:

$$v/V = [S] / Ks + [S]$$

para formar una ecuación de forma lineal cuando invertimos los componentes de la ecuación y multiplicamos la ecuación por V:

$$1/v = (Ks / V) * (1 / [S]) + (1 / V)$$

donde V es la velocidad máxima, [S] la concentración del sustrato y Ks la constante de disociación del complejo enzima-sustrato.

Así, la gráfica de dobles recíprocos entre el L-lactato y los valores de velocidad inicial a las diversas concentraciones de oxalato (Fig. 1, gráfica superior) muestra que las líneas que unen los puntos para cada concentración de inhibidor se interceptan en el segundo cuadrante, característica de las inhibiciones de tipo mixto, que como su nombre lo indica, afectan tanto a la Ks como a la V.

De este gráfico se puede calcular Ks y V a partir de las ordenadas a las abscisas y al origen respectivamente, en ausencia de oxalato. En este caso la Ks de la L-iLDH por L-lactato es de 1.4 mM y la V = 115 nmol/min/mg prot.

La ecuación que explica una inhibición de tipo mixto es [1]:

$$v = [S] * V' / Ks' + [S]$$

donde

$$Ks' = Ks\,[(1+(I/Ki)) / (1+(I/(\alpha Ki)))] \text{ y}$$

$$V' = V / [1+(I/(\alpha Ki))]$$

I es la concentración del inhibidor y α es el factor que indica el número de veces que se ve afectada la Ks por la unión del inhibidor a la enzima. En este caso $\alpha > 1$.

De la ecuación anterior podemos observar que la Ks y V se encuentran afectadas por la concentración del inhibidor y por el factor α.

Entonces, si regraficamos los valores aparentes de $1/V$ (ordenadas al origen) y de Ks/V (pendientes) contra cada una de las concentraciones de oxalato, podemos obtener los valores de Ki y de α (Fig. 1, gráfica inferior). De esta forma, determinamos que la Ki para el oxalato fue de 0.3 mM y el factor α fue de 3.6.

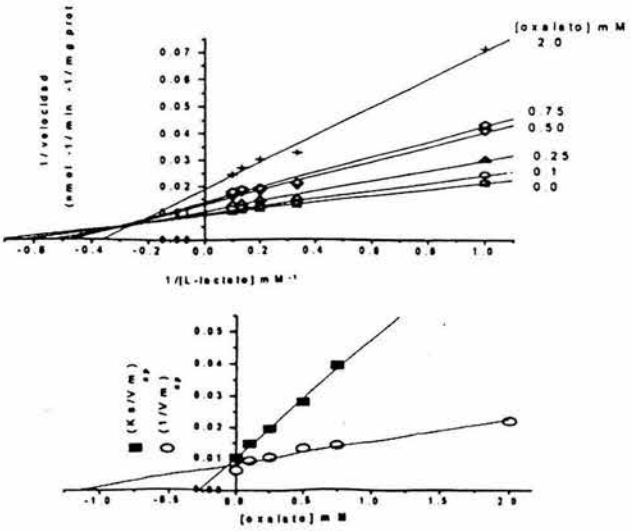

Figura 1.

Aunque el gráfico de dobles recíprocos es el más utilizado no es recomendable, pues conlleva una falsa impresión del error experimental: A valores bajos de velocidad inicial, errores pequeños en velocidad conducen a una gran dispersión de $1/V$; a valores altos de velocidad inicial, errores significativos en v_o se traducen en una baja dispersión de $1/V$ [2].Otra forma de obtener los parámetros cinéticos y el tipo de inhibición de una forma más confiable es editando la ecuación en un programa de cómputo y realizar el ajuste global no-lineal de todos los datos (Fig. 2). De esta manera, cada punto experimental tiene el mismo peso específico en la dispersión del ajuste. Los valores del ajuste no lineal para una inhibición de tipo mixto fueron: $Ks = 1.21$ mM, $Ki = 0.32$ mM, $\alpha = 3.97$ y $V = 108$ nmol/min/mg prot., valores que son muy similares a los encontrados por regresión lineal o de dobles recíprocos.

Estos resultados indican que el oxalato inhibe a la L-iLDH de *E. gracilis* con la misma potencia que a la de bacterias. Esta enzima sólo se ha localizado en mitocondrias de tripanosomátidos y euglenoides, que son dos grupos de eucariontes más primitivos que contiene organelos. Como la enzima de bacteria también es membranal y unida a la cadena respiratoria, estos resultados sugieren un posible origen común.

REFERENCIAS

1. Segel IH. Enzyme Kinetics. John Wiley and Sons, New York, 1975 Cap 11B pp 927-935.
2. Cornish-Bowden A. Fundamentals of Enzyme Kinetics. Portland Press, London. 1995.

Ricardo Jasso Chávez y Rafael Moreno Sánchez

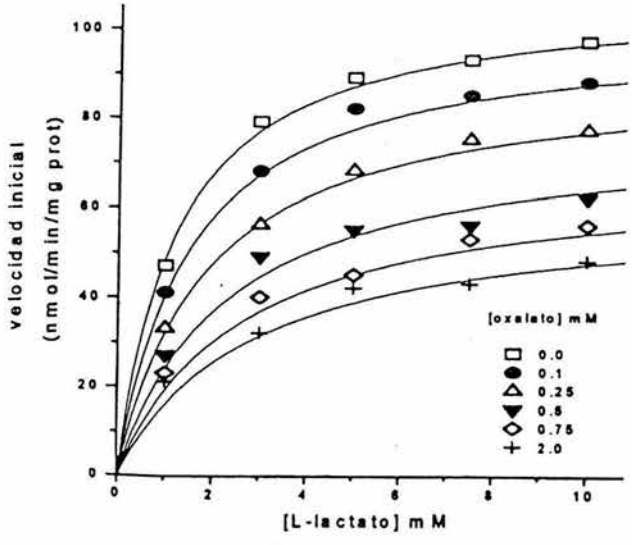

Figura 2.

Otras publicaciones realizadas durante el postgrado

ELSEVIER

Biochimica et Biophysica Acta 1457 (2000) 200–210

BIOCHIMICA ET BIOPHYSICA ACTA
BBA

www.elsevier.com/locate/bba

Oxidative phosphorylation supported by an alternative respiratory pathway in mitochondria from *Euglena*

Rafael Moreno-Sánchez [a,*], Raúl Covián [a], Ricardo Jasso-Chávez [b], Sara Rodríguez-Enríquez [a], Fermín Pacheco-Moisés [a], M. Eugenia Torres-Márquez [b]

[a] *Departamento de Bioquímica, Instituto Nacional de Cardiología, Juan Badiano # 1, Col. Sección XVI, Tlalpan, Mexico D.F. 14080, Mexico*

[b] *Departamento de Bioquímica, Facultad de Medicina, Universidad Nacional Autónoma de México, Mexico D.F., Mexico*

Received 17 November 1999; received in revised form 3 February 2000; accepted 11 February 2000

Abstract

The effect of antimycin, myxothiazol, 2-heptyl-4-hydroxyquinoline-*N*-oxide, stigmatellin and cyanide on respiration, ATP synthesis, cytochrome *c* reductase, and membrane potential in mitochondria isolated from dark-grown *Euglena* cells was determined. With L-lactate as substrate, ATP synthesis was partially inhibited by antimycin, but the other four inhibitors completely abolished the process. Cyanide also inhibited the antimycin-resistant ATP synthesis. Membrane potential was collapsed (<60 mV) by cyanide and stigmatellin. However, in the presence of antimycin, a H^+ gradient (>60 mV) that sufficed to drive ATP synthesis remained. Cytochrome *c* reductase, with L-lactate as donor, was diminished by antimycin and myxothiazol. Cytochrome bc_1 complex activity was fully inhibited by antimycin, but it was resistant to myxothiazol. Stigmatellin inhibited both L-lactate-dependent cytochrome *c* reductase and cytochrome bc_1 complex activities. Respiration was partially inhibited by the five inhibitors. The cyanide-resistant respiration was strongly inhibited by diphenylamine, *n*-propyl-gallate, salicylhydroxamic acid and disulfiram. Based on these results, a model of the respiratory chain of *Euglena* mitochondria is proposed, in which a quinol-cytochrome *c* oxidoreductase resistant to antimycin, and a quinol oxidase resistant to antimycin and cyanide are included.

Keywords: ATP synthesis; Antimycin; Cyanide-resistant respiration; *Euglena*

1. Introduction

Mitochondria isolated from dark-grown *Euglena gracilis* have respiratory components that are resistant to antimycin and cyanide [1–3]. The cyanide-resistant respiratory pathway is inhibited by diphenylamine (DPA) [2,4], preferentially oxidizes L-lactate [4,14], and builds up a small, uncoupler-sensitive membrane potential [4,5], that supports the energy-dependent uptake of Ca^{2+} [6]. This pathway is partially inhibited by salicylhydroxamic acid (SHAM) [4,7], a potent inhibitor of alternative respiratory pathways in plant mitochondria [8]. Cell growth in the presence of antimycin [1,2,9], cyanide [10] or ethanol [10] as carbon source, induces an increase in the content of a *b*-type cytochrome, that reacts with carbon monoxide. This last observation has been interpreted in terms of an adaptable enhancement of an alternative oxidase, which is resistant to the stress conditions of the culture [1,2,10]. However,

* Corresponding author. Fax: +52-5-573-0926; E-mail: morenosanchez@hotmail.com

0005-2728/00/$ – see front matter
PII: S0005-2728(00)00102-X

the semipurified antimycin-sensitive cytochrome *b* also reacts with carbon monoxide [10] and, hence, such an interpretation should be further evaluated.

Based on studies of respiratory inhibition by antimycin and cyanide, and of spectral characteristics of *Euglena* mitochondria, Buetow [3] proposed a respiratory chain in which L-lactate oxidation could occur through both an alternative terminal oxidase and the classical pathway (cytochromes bc_1 and aa_3), by transferring electrons from the dehydrogenase to either the quinone pool or directly to cytochrome *c*. In an effort to elucidate the site of branching for the alternative pathway, the effect of several inhibitors of the mammalian cytochrome bc_1 complex [11] on the rates of respiration, ATP synthesis, cytochrome *c* reductase and quinol oxidase was determined. The effect of SHAM [8], DPA [2,4], *n*-propylgallate [12], and disulfiram [13], inhibitors of alternative respiratory pathways in plant mitochondria, on the cyanide-resistant respiration was also examined.

2. Materials and methods

2.1. Materials

Antimycin, myxothiazol, SHAM, 2-heptyl-4-hydroxyquinoline-*N*-oxide (HQNO), L-lactic acid, D-lactate, duroquinone, decylbenzoquinone (DBQone), *N*,*N*,*N*′,*N*′, tetramethyl-*p*-phenylene diamine (TMPD), disulfiram, fatty acid-free bovine serum albumin, hexokinase, cytochrome *c*, oligomycin, carbonyl cyanide *m*-chlorophenylhydrazone (CCCP), 2,6-dichlorophenol indophenol (DCPIP), and phenazine methosulfate (PMS) were purchased from Sigma. Stigmatellin was from Fluka, *n*-propyl gallate (nPG) from ICN, DPA from Aldrich, and $^{32}P_i$ and ^{3}H-tetraphenylphosphonium (^{3}H–TPP^+) from New England Nuclear.

2.2. Cell culture and preparation of mitochondria

E. gracilis Klebs (a Z-like strain), kept in the dark in liquid medium for several months, was reactivated and axenically grown as described [4,5,14]. The cells were grown in the dark in the Hutner's acidic organotrophic medium with glutamate+malate as carbon source [15,16] at 25 ± 1°C under orbital agitation (125 rpm). Cells were harvested after 82–86 h, in the late exponential phase of growth, by centrifugation at 1000×*g* for 10 min at 4°C and washed once in SHE medium (250 mM sucrose, 10 mM HEPES, 1 mM EGTA, pH 7.3).

The procedure previously described [4,5,10] for isolation of mitochondria by sonication of cells was used with slight modifications. Cells were resuspended at a density of 2×10^9 cells in 25 ml of SHE medium, supplemented with 0.4% (w/v) fatty acid-free bovine serum albumin. The cell suspension was sonicated in ice with a microprobe of 12 mm tip diameter for 10 s three times, with 1 min resting period, at 50–60% of maximal output in a Branson sonifier. The sonicate was diluted with 2–3 volumes of SHE medium and centrifuged at 600×*g* for 10 min at 4°C. The supernatant was centrifuged at 8500×*g* for 10 min at 4°C. The mitochondrial pellet was carefully resuspended in 2–3 ml of SHE medium supplemented with 0.2% fatty acid-free albumin, 1 mM ADP, and incubated for 10 min in ice with occasional agitation. The mitochondrial suspension was diluted with 10–15 volumes of fresh SHE medium and centrifuged at 7800×*g* for 10 min at 4°C. The pellet was resuspended in SHE medium (+0.2% fatty acid-free albumin) to a final concentration of 40–70 mg protein/ml. The usual yield was 45–60 mg protein per l of culture. The respiratory control and ADP/O ratio values, with 10 mM L-lactate as oxidizable substrate, were 2.0 ± 0.1 (14) and 1.1 ± 0.1 (14) (mean ± S.E.M., *n*), respectively. Mitochondrial protein was determined by the biuret method as described previously [4].

2.3. Oxygen uptake and ATP synthesis

The rate of respiration of *Euglena* mitochondria was measured at 30°C, with a Clark-type oxygen electrode, in an air-saturated standard medium that contained 120 mM KCl, 20 mM MOPS, 1 mM EGTA, 5 mM K-phosphate, 1 mM $MgCl_2$, of pH 7.25. For ATP synthesis, mitochondria were incubated at 30°C in 1 ml of standard medium which also contained $^{32}P_i$ (0.3–0.6 μCi/μmol), 10 mM glucose, and five units hexokinase. At predetermined times the reaction was stopped with ice-cold 5% (w/v) trichloroacetic acid. After centrifugation of denatured protein, an aliquot was withdrawn for $^{32}P_i$

extraction from the aqueous phase by reaction with ammonium molybdate/sulfuric acid, and using acetone plus *n*-butyl acetate as organic phase [17]. The $^{32}P_i$-free aqueous phase was used for determination of $^{32}P_i$ incorporated into ATP and glucose-6-phosphate by measuring the Cerenkov radiation in water.

2.4. Quinol and TMPD oxidases

These activities were determined at 30°C by measuring the rate of O_2 uptake stimulated by 0.25 mM duroquinol, and 5 mM ascorbate plus 2.5 mM TMPD, respectively [10]. Irradiation of mitochondria (25–30 mg protein/ml) with ultraviolet light was made in SHE medium supplemented with 1 mM ADP, 2 mM $MgCl_2$ and 0.2–0.5% (w/v) fatty acid-free albumin at 4°C, under occasional stirring. The lamp (Mineralight, UVG-54, 254 nm) was placed at about 1.5–2 cm from the suspension. Extraction of quinones was made according to Ding et al., [18]. Aliquots of 50 mg of mitochondrial protein were freeze-dried, resuspended in 100 ml iso-octane and incubated for 1 h at room temperature under gentle orbital shaking. The supernatant was discarded and the pellet was extracted five more times with iso-octane. The final mitochondrial extract was brought to dryness using a stream of N_2 and resuspended in SHE medium.

2.5. Cytochrome c reductase and NAD-independent L-lactate dehydrogenase (iLDH) activities

Euglena mitochondria (0.08–0.14 mg protein/ml) were incubated at 30°C in SHE medium plus 1 mM ADP, 5 mM K-phosphate, 1 mM $MgCl_2$ and 30 μM oxidized horse heart cytochrome *c*. The reaction was started by addition of either 10 mM L-lactate, 10 mM succinate, or 60 μM decylbenzoquinol (DBQ), which was reduced according to Rieske [19]. The rate of cytochrome *c* reduction was followed by the increase in the absorbance difference at 550 minus 540 nm in a dual wavelength SLM-Aminco DW-2000 spectrophotometer; an extinction coefficient of 21.1 mM^{-1} cm^{-1} was used in the calculations [20]. For iLDH activity determination, mitochondria (0.05–0.1 mg protein) were incubated at 30°C in 1 ml of standard medium, which also contained 0.2 mM DCPIP and 0.25 mM PMS. The rate of variation in the absorbance at 600 nm was measured after addition of 10 mM L-lactate. The extinction coefficient for DCPIP was taken as 21.3 mM^{-1} cm^{-1} at pH 7.5 [21].

2.6. Membrane potential

The distribution of ^3H–TPP^+ (0.06–0.07 μCi/nmol) was used to estimate the difference of electrical potential across the inner mitochondrial membrane, following the formulations proposed by Rottenberg [22], which involve corrections for nonspecific binding to the external and internal faces of the inner mitochondrial membrane.

3. Results

We previously reported that inhibition of respiration by cyanide in *Euglena* mitochondria was lower with L-lactate than with NADH or succinate as substrate [4,10]. This observation suggested that the alternative respiratory pathway preferentially oxidized L-lactate. In an attempt to elucidate the respiratory components involved in L-lactate oxidation, the effect of several inhibitors of the mammalian cytochrome

Table 1
Inhibition of oxidative phosphorylation in *Euglena* mitochondria

Addition	Rate of ATP synthesis (nmol/min/mg protein)	
	L-lactate	Succinate
None	205.5 ± 11 (12)	111 ± 15 (8)
+1 mM NaCN	4.2 ± 1 (8)	6.2 ± 1.4 (3)
+0.5–1 μM Antimycin	91 ± 13 (9)	19 ± 4 (6)
+12.5 μM Oligomycin	2.5 ± 0.1 (5)	1.3
+2.5 μM CCCP	2.1 ± 0.5 (7)	–

Euglena mitochondria (0.35–0.5 mg protein/ml) were incubated as described in Section 2 in the presence of the indicated substrates and inhibitors. After 2 min, 1 mM ADP was added; the reaction was stopped 2 min later and the incorporation of $^{32}P_i$ into ATP was determined. The rates of state 3 respiration for the same mitochondrial preparations were 177 ± 21 (12) and 83 ± 19 (8) ng atoms oxygen/mg protein/min for 10 mM L-lactate and 10 mM succinate, respectively. The data shown are mean ± S.E.M., with the number of preparations assayed between parentheses.

bc_1 complex on respiration and ATP synthesis was assayed.

3.1. ATP synthesis

The rates of ATP synthesis and state 3 (ADP-stimulated) respiration (Table 1) were two-fold higher with L-lactate than with succinate. However, the P/O ratio was identical with the two substrates: 1.25 ± 0.09 (12) for L-lactate and 1.23 ± 0.26 (6) for succinate (mean ± S.E.M.; *n*). With D-lactate, the rates of state 3 respiration reached values of 300–400 ng atoms oxygen/min/mg protein, although the rates of ATP synthesis were similar to those attained with L-lactate (data not shown). Determination of the cell levels of lactate revealed that the L-isomer was at a concentration of 3.8 ± 1.2 mM (7), considering a water intracellular volume of 2.11 μl/10^7 cells, whereas the D-isomer concentration was negligible (< 0.1 mM). Therefore, L-lactate, but not D-lactate, was used throughout the rest of this study.

Oxidative phosphorylation was sensitive to cyanide, oligomycin and the uncoupler CCCP, but partially resistant to a high antimycin concentration, in particular with L-lactate as substrate (Table 1). This observation was made several years ago by our group [10]. The rate of antimycin-resistant ATP synthesis supported by L-lactate oxidation was also fully blocked by 2.5 μM oligomycin, 5 μM CCCP or 1 mM cyanide (data not shown).

3.2. Cytochrome c reductase activities

To explore the existence of a cytochrome bc_1 complex with an unusual low sensitivity to antimycin, as occurs in mitochondria from *Tetrahymena pyriformis* [23] and yeast mutants [24], the activity was directly measured (Table 2). Cytochrome bc_1 complex in *Euglena* mitochondria efficiently reduces added horse heart cytochrome *c*; this is in contrast to *Euglena* cytochrome *c* oxidase, which interacts only with endogenous cytochrome *c* [14]; 30 μM oxidized cytochrome *c* and 60 μM DBQ as substrates sufficed to reach maximal rates of bc_1 complex activity.

Thus, with DBQ as artificial electron donor, the activity of cytochrome bc_1 complex was strongly inhibited by antimycin. With succinate, cytochrome *c* reductase activity was also extensively inhibited by antimycin (Table 2), indicating that electron transfer from succinate flowed preferentially through the cytochrome bc_1 complex. It should be noted that, although the concentrations of antimycin used for inhibition of oxidative phosphorylation and cytochrome *c* reductase were similar, the relation inhibitor/protein was 3–5 times higher for the assays of cytochrome *c* reductase activity. Despite such a high antimycin concentration, cytochrome *c* reductase activity was only partially inhibited when L-lactate was the electron donor. This suggested the presence of an electron flow pathway from quinone to cytochrome *c* that by-passes the cytochrome bc_1 complex.

Myxothiazol, another specific inhibitor of mammalian cytochrome bc_1 complexes [11], exerted a weak effect on *Euglena* cytochrome bc_1 activity using DBQ or succinate as electron donors. Cytochrome bc_1 complexes from closely related trypanosomatids and from *Paramecium* are also resistant to myxothiazol [23]. In contrast, myxothiazol significantly diminished cytochrome *c* reductase activity when L-lactate was the electron donor. This observation indicated the presence of a myxothiazol-sensitive quinol-cytochrome *c* oxidoreductase activity, different to that of the cytochrome bc_1 complex (antimycin-sen-

Table 2
Cytochrome *c* reductase activity

Donor	Activity (nmol cytochrome *c*/mg/min)
60 μM DBQ	96.4 ± 18 (5)
+0.16–0.6 μM Antimycin	0.3 ± 0.2 (5)
+20 μM Myxothiazol	79 ± 24 (3)
10 mM L-Lactate	84.3 ± 8 (6)
+0.16–0.6 μM Antimycin	43 ± 7 (8)
+20 μM Myxothiazol	20.5 ± 5 (3)
+0.16 μM Antimycin+ 20 μM Myxothiazol	6.8 ± 2 (4)
10 mM Succinate	15.6 ± 1.5 (5)
+0.16–0.6 μM Antimycin	2.4 ± 0.4 (5)
+20 μM Myxothiazol	13.4 ± 0.9 (3)

Euglena mitochondria (0.08–0.14 mg protein/ml) were incubated as described in Section 2. After 1–2 min, DBQ, succinate or L-lactate were added. The initial rate of cytochrome *c* reduction was corrected for by the rate of reduction attained in the presence of 1 μM stigmatellin (non-enzymatic reduction) and by the activity due to endogenous substrates, in the same experimental conditions. Mean ± S.D. (*n*).

sitive, myxothiazol-resistant), that is preferentially fed by iLDH, an enzyme that is located in the inner mitochondrial membrane and which does not require pyridine nucleotides ([3]; R. Jasso-Chávez et al., unpublished data). Stigmatellin, a third specific inhibitor of mammalian cytochrome bc_1 complexes [11], fully abolished the activity of cytochrome *c* reductase with the three electron donors (data not shown). This indicated that both quinol-cytochrome *c* oxidoreductases had similar binding sites for this inhibitor.

3.3. Antimycin, HQNO and cyanide

Titration with antimycin of L-lactate-supported state 3 respiration (Fig. 1) and ATP synthesis (Fig. 2A) revealed the presence of an antimycin-resistant respiratory component, which was able to drive oxidative phosphorylation with a lower thermodynamic efficiency; with 500 nM antimycin (1000–1250 pmol antimycin/mg protein), the P/O ratio diminished from 1.25 in control mitochondria to 0.44 (Fig. 2A). Inhibition of succinate oxidation by antimycin (Fig. 1) also exhibited an antimycin-resistant respiratory component. Accordingly, this antimycin-resistant pathway generated a H^+ gradient of a sufficient magnitude (−94 mV; Table 3) able to drive oxidative phosphorylation. It is noted that a H^+ gradient of about 60–80 mV (negative inside) has been determined as threshold value for mitochondrial [25,26] and bacterial [27,28] ATP synthesis.

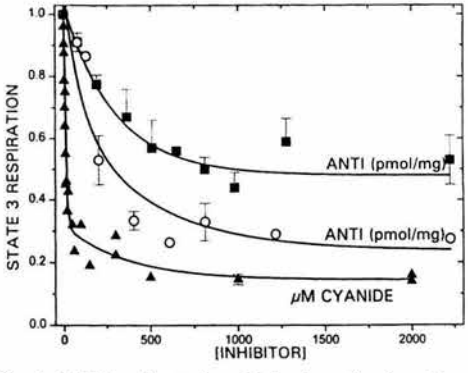

Fig. 1. Inhibition of state 3 respiration by antimycin and cyanide. *Euglena* mitochondria (0.5–1 mg protein/ml) were incubated as described in Section 2 in the presence of 2 mM ADP, 10 mM L-lactate (filled symbols) or 10 mM succinate (empty circles) and the indicated concentrations of antimycin (ANTI) or cyanide. The values shown represent the mean ± S.E.M. of titrations with antimycin of 4–12 different preparations. The experimental values with cyanide are from three different preparations. The rates of state 3 respiration in the absence of inhibitors were 237 ± 17 (33) and 82 ± 12 (14) ng atoms oxygen/mg protein/ min for L-lactate and succinate, respectively. The solid lines represent the best-fit to a second order exponential decay.

The larger inhibition of L-lactate oxidation (Fig. 1), complete suppression of L-lactate dependent oxidative phosphorylation (Fig. 2A), and collapse of the H^+ gradient (Table 3) by cyanide, indicated that a fraction of the electron transfer, resistant to antimycin, required the activity of cyanide-sensitive cytochrome *c* oxidase. This interpretation accounts for the lowering in the P/O ratio in the presence of antimycin, in which only one site of energy conservation participates. In consequence, the respiratory component that by-passes the cytochrome bc_1 complex would not be able to drive ATP synthesis.

The cyanide concentration required to attain half-maximal inhibition (IC_{50}) of ATP synthesis, in the absence (Fig. 2A) or in the presence of 0.5 μM antimycin (IC_{50} = 7.6 μM; data not shown), were similar to K_i values previously reported for inhibition of TMPD oxidase [10,14]. Hence, it appears that cytochrome *c* oxidase is the common terminal oxidase for both, antimycin-sensitive and antimycin-resistant phosphorylating pathways.

HQNO, an inhibitor of alternative quinol oxidases in bacterial respiratory systems [29] and of cytochrome bc_1 complexes [11], was able to abolish oxidative phosphorylation in *Euglena* mitochondria (Fig. 2B) with IC_{50} values in the absence (2.3 μM) and in the presence of 0.5 μM antimycin (14.3 μM) similar to those required for half-maximal inhibition of cytochrome *bo* from *Escherichia coli* [29].

3.4. Myxothiazol and stigmatellin

Myxothiazol completely inhibited L-lactate supported ATP synthesis, but it was partially effective with succinate as substrate (Fig. 3); the respective IC_{50} values were 1.1 and 32.8 μM myxothiazol for L-lactate and succinate, respectively. The respiratory rates with the two substrates were diminished in 85–

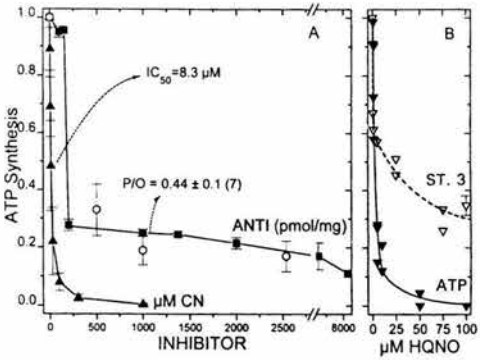

Fig. 2. Inhibition of ATP synthesis by antimycin, cyanide and HQNO. (A) *Euglena* mitochondria (0.35–0.5 mg protein/ml) were incubated with $^{32}P_i$ as described in Section 2 with 10 mM L-lactate (filled symbols) or 10 mM succinate (empty circles) and the indicated concentrations of inhibitors. After 2 min, 1 mM ADP was added and the reaction was stopped 2 min later with trichloroacetic acid. (B) Mitochondria were incubated with L-lactate and the indicated concentrations of HQNO. Respiration and the incorporation of $^{32}P_i$ into ATP were determined as detailed in Section 2. The values shown represent the mean ± S.E.M. of titrations with 3–12 different preparations. The rates of ATP synthesis in the absence of inhibitors were 252.4 ± 27 (14) and 112 ± 24 (5) nmol/mg protein/min for L-lactate and succinate, respectively.

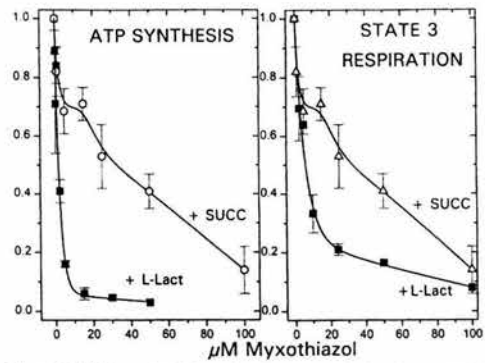

Fig. 3. Inhibition of ATP synthesis and respiration by myxothiazol. See legends to Figs. 1 and 2 for experimental details. The values shown are the mean ± S.E.M. of 3–10 different preparations.

90% by 100 μM myxothiazol; likewise, with both substrates the sensitivity of state 3 respiration to myxothiazol (Fig. 3) was similar (i.e., similar IC_{50} values) to that observed for ATP synthesis, after correction of the non-inhibited fluxes. The biphasic pattern of inhibition by myxothiazol on respiration and ATP synthesis supported by succinate (Fig. 3) was also observed for the L-lactate-cytochrome *c* reductase activity (data not shown). In the latter case, the IC_{50} values for myxothiazol were 0.2 and 24.7 μM ($n = 2$). The low affinity component disappeared when the titration of the reductase activity with myxothiazol was made in the presence of antimycin (not shown). Moreover, in the presence of both antimycin plus myxothiazol, the L-lactate-cytochrome *c* reductase activity was suppressed (Table 2).

With 20 μM myxothiazol, the concentration that inhibited ATP synthesis with L-lactate, but which slightly affected that supported by succinate (Fig. 3), the membrane potential diminished to 105 ± 2 (7) mV with L-lactate (i.e., 12 mV lower H^+ gradient), but it was not affected with succinate.

Stigmatellin, at a concentration of 0.3 nmol/mg protein, suppressed ATP synthesis and state 3 respiration supported by L-lactate or succinate (data not shown); it also collapsed the membrane potential (Table 3). The stigmatellin- and cyanide-resistant respiration was of the same extent; stigmatellin plus

Table 3
Steady-state H^+ gradient in *Euglena* mitochondria

	$\Delta\psi_H$ (mV)	
	L-Lactate	Succinate
State 4	146.4 ± 10 (8)	139.5 ± 6 (8)
State 3	117 ± 7 (16)	104.6 ± 12 (16)
State 3+0.4–1.0 nmol antimycin/mg protein	94 ± 7 (14)	87 ± 7 (7)
State 3+2 mM CN^-	42 ± 3 (6)	
State 3+0.3–0.6 nmol stigmatellin/mg protein	48 ± 8 (6)	

Mitochondria (2.5–3.5 mg protein/ml) were incubated at 30°C in 0.5 ml of standard medium with 0.8 μM [^{3}H]TPP$^+$ and 20 mM L-lactate or 20 mM succinate. After 2 min, 2 mM ADP was added, except for state 4 where no addition was made. The reaction was stopped by rapid centrifugation at 14000 × *g* for 2 min at 4°C in an Eppendorf refrigerated microcentrifuge. Aliquots of the pellet and supernatant were used to calculate the distribution of [^{3}H]TPP$^+$ across the inner membrane following the corrections for unspecific binding to the Nernst equation by Rottenberg [21].

cyanide did not produce further inhibition of the rate of respiration supported by L-lactate. Since iLDH activity was not affected by these inhibitors (data not shown), the site of action of HQNO and stigmatellin on ATP synthesis and respiration supported by L-lactate is very likely located after the reduction of quinones; myxothiazol (50 μM) slightly inhibited (15.5 ± 6%; 5) iLDH activity, but its main site of action may also be after the formation of quinol, because of its more pronounced effect on respiration, cytochrome *c* reductase and ATP synthesis.

3.5. Antimycin-resistant pathway

To determine whether the antimycin-resistant respiratory component oxidizes quinol or receives electrons directly from iLDH, the activity of antimycin-resistant quinol oxidase was determined. Several artificial quinones were assayed, but the two that yielded the higher rates were DBQ and duroquinol (Table 4). For comparison, the activity of antimycin resistant L-lactate oxidase was also measured in the same mitochondrial preparations. The activities were partially inhibited by cyanide, indicating that a fraction of electron flow from the oxidation of quinol reached cytochrome *c* oxidase, notwithstanding the complete blockade of cytochrome bc_1 complex by antimycin. The existence of quinol and L-lactate oxidase activities, in the presence of both antimycin and cyanide, suggests that a second alternative pathway branches from quinone.

Irradiation of mitochondria with ultraviolet light for 100 min, to destroy the quinone pool [30], diminished by 79 and 61% the activities of succinate and L-lactate oxidases, respectively. UV light also affected, but to a lower extent, the activity of quinone independent TMPD oxidase (38% inhibition). The activities of cytochrome *c* reductase, using L-lactate or succinate as electron donors, were also decreased by 20 and 40%, respectively, after UV irradiation; the bc_1 and iLDH activities decreased by 20 and 50%, respectively (data not shown).

Extraction of quinones from mitochondria with iso-octane [18] also decreased the activities of succinate and L-lactate oxidases by 60–90%; these were restored to control values by addition of 0.2 mM DBQone: the L-lactate oxidase activity was enhanced by 4.3 ± 0.5 times (3) and that of succinate oxidase by 2.8 ± 0.3 times (3) by DBQone. The value of stimulation of L-lactate oxidase by DBQone, when corrected for respiration due to endogenous substrates, was 8.4–10.5 times higher for iso-octane extracted mitochondria, and 1.18–1.53 times for control, lyophilized mitochondria. These data indicated an extensive, although incomplete, extraction of quinones. Antimycin (2 μM) strongly inhibited (81 ± 7%; 3) the stimulation of L-lactate oxidase by DBQone, while 20 μM myxothiazol only diminished the activity by 43% (2). The cytochrome *c* reductase activity, with L-lactate or succinate as electron donor, was also restored by added DBQone; these activities were 76 and 50% inhibited by 0.4 μM antimycin, respectively. The activities of succinate and L-lactate oxidases, cytochrome *c* reductase, and cytochrome bc_1 complex were higher in iso-octane treated than in control mitochondria, probably due to a limitation of natural quinones in the latter and saturation by artificial quinones in the former conditions.

Table 4
Antimycin-resistant quinol oxidases

Substrate	Activity (ng atoms oxygen/mg/min)	
		+ Cyanide
DBQ	13.7 ± 1.3 (8)	6.7 ± 1.7 (7)
Duroquinol	23.7 ± 2.8 (8)	15.8 ± 1.7 (7)
L-lactate	109 ± 13 (8)	33 ± 3.9 (8)

Mitochondria (1–1.5 mg protein/ml) were incubated at 30°C in 2 ml of standard medium, which also contained 0.8 μM antimycin (540–810 pmol/mg protein) and 1.25–2.5 mM dithiothreitol. After approximately 5–7 min (to exhaustion of endogenous substrates), 0.22 mM DBQone, 0.25 mM duroquinone or 10 mM L-lactate were added. Where indicated, 1 mM NaCN was present from the beginning of the incubation. The data shown are mean ± S.E.M. (*n*).

3.6. Cyanide-resistant pathway

In all our preparations the rate of respiration with L-lactate as substrate was always partially inhibited (85.4 ± 1.7%; 18) by 1 mM cyanide (or 10 mM azide). One micromolar antimycin, 0.1 mM HQNO or 0.5 μM stigmatellin did not further decrease the rate of cyanide-resistant respiration with 10 mM L-lactate as substrate. On the other hand, inhibitors of plant alternative respiratory pathway strongly inhibited the cyanide-resistant pathway, whereas myxothi-

Table 5
Cyanide-resistant pathway

Inhibitor	0.5 mM DPA	12.5 mM nPG	5 mM SHAM	0.05 mM disulfiram	10 mM azide	50 μM myxothiazol
Activity (% of control)	20 ± 3 (5)	17 ± 4 (4)	37 ± 4 (3)	21 (2)	59 (2)	56.5 (2)

Three milligram protein of mitochondria were incubated at 30°C in 2 ml of standard medium with 1 mM sodium cyanide and the indicated concentrations of the inhibitors. After 5–7 min, 10 mM L-lactate was added and the steady-state rate of 0_2 uptake was measured. The cyanide-resistant respiration in the absence of other inhibitors was 51 ± 8 (9) ng atoms oxygen/mg protein/min, which in turn was 17 ± 2 (9)% of the rate reached in the absence of cyanide. The data shown are mean ± S.E.M. (*n*).

azol and azide inhibited, but to a lower extent (Table 5). Catalase exerted a very small inhibitory effect of the cyanide-resistant respiration, with or without DPA or nPG (data not shown), indicating that this activity was not associated to the production of H_2O_2. Cyanide-resistant respiration was stimulated by 34 ± 5% (7) by 5 mM AMP; oligomycin (2.5 μM) and oleic acid (15–20 nmol/mg protein) partially suppressed AMP stimulation, whereas pyruvate (5 mM) or DTT (1.25 mM) did not induce any effect [31].

4. Discussion

The values of the P/O ratio with L-lactate or succinate indicated the involvement of two energy conservation respiratory sites, i.e., the cytochrome bc_1 complex and the cytochrome *c* oxidase. This is in agreement with the early proposal of Sharpless and Butow [1]. Thus, similarly to succinate oxidation, dehydrogenation of L-lactate produces reduction of the quinone pool. This is further supported by the drastic diminution of L-lactate oxidation and L-lactate dependent cytochrome *c* reduction in iso-octane treated mitochondria, and their restoration by addition of artificial oxidized quinone. In addition, the direct reduction of added Q_1 by iLDH through a reaction inhibited by oxalate, oxamate or sulfite (R. Jasso-Chávez et al., unpublished data), also illustrated their connection to the quinone pool.

The partial inhibition of oxidative phosphorylation by antimycin indicated a branching for the oxidation of quinol, in which electrons flow through the cytochrome bc_1 complex, the reaction completely sensitive to antimycin, or through an alternative route, resistant to antimycin but still able to generate a H^+ gradient. The existence of an alternative respiratory component that catalyzes the same reaction like cytochrome bc_1 complex, by an antimycin-resistant process without the coupled pumping of H^+, was suggested by the following observations. (a) The diminished P/O ratio of 0.44 induced by the presence of antimycin (see also [1]); (b) the reduction of cytochrome *c* by dehydrogenation of L-lactate (or succinate) in the presence of antimycin; and (c) the total suppression of ATP synthesis by cyanide with similar IC_{50} values either in the presence or in the absence of antimycin. In consequence, L-lactate-dependent oxidative phosphorylation, in the presence of antimycin, would be supported by cytochrome *c* oxidase H^+ pumping activity. Cytochrome *c* reductase activity resistant to antimycin has also been reported in *Candida parapsilosis* mitochondria [32]. Antimycin-resistant electron transfer between NADH and cytochrome *c* was described for trypanosomatids [33,34] and *Euglena* mitochondria [1], although quinone involvement was not explored.

Myxothiazol was a weak inhibitor of the activity of cytochrome bc_1 complex as well as of the succinate-dependent activities of respiration, cytochrome *c* reductase and ATP synthesis. This pattern of inhibition by myxothiazol, together with the strong inhibition of the same activities by antimycin, further supported the notion that succinate was preferentially oxidized through the cytochrome bc_1 complex [4,10]. In contrast, the high sensitivity of L-lactate dependent activities to myxothiazol, and the lower inhibition by antimycin, indicated a preferential electron flow through the phosphorylating alternative branch, sensitive to myxothiazol. Stigmatellin was equally effective on both branches. The biphasic pattern of inhibition by myxothiazol (cf. Fig. 3; two slopes in a Dixon plot of [I] versus 1/L-lactate-cytochrome *c* oxidoreductase activity, not shown) suggested the presence of two components; one with high affinity, presumably the alternative quinol:cytochrome c oxidoreductase, and another with low af-

finity, identified as the cytochrome bc_1 complex, in which myxothiazol exerted a partial, mixed-type inhibition (R. Covián et al., unpublished data).

Likewise, the inhibition of the antimycin-resistant pathway from L-lactate to cytochrome *c*, by submicromolar concentrations of myxothiazol or stigmatellin, also indicated that there was a non-bc_1 quinol: cytochrome *c* oxidoreductase, since these two highly hydrophobic molecules interact with membrane-bound enzymes that use quinol or quinone as substrates, such as NADH dehydrogenase [35], bacterial quinol oxidases [36,37] and quinone reductases [38], in addition to cytochrome bc_1 complex [11].

On the basis of the results of the present study a model of the respiratory chain of *Euglena* mitochondria is proposed (Scheme 1). iLDH and succinate dehydrogenase catalyze the transfer of electrons from L-lactate or succinate to quinone; the cytochrome bc_1 complex transfers electrons from quinone to cytochrome *c* in an antimycin-sensitive reaction, which is coupled to H^+ pumping (and ATP synthesis). Cytochrome *c* oxidase (*cyt. c Ox.*) catalyzes the reduction of oxygen in a cyanide-sensitive reaction also coupled to H^+ pumping. There is also a cyanide-resistant quinol oxidase (*Q. Ox.*) that reduces oxygen in a reaction partially blocked by DPA, nPG, SHAM and disulfiram, and an alternative component with an antimycin resistant activity of quinol:cytochrome *c* oxidoreductase (*Q. cyt. c red.*), but sensitive to myxothiazol, stigmatellin and HQNO.

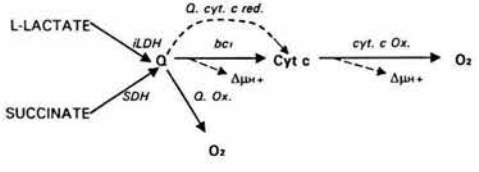

Scheme 1.

iLDHs from yeast mitochondria are soluble enzymes located in the intermembrane space that catalyze the electron transfer from lactate to cytochrome *c* [39], while bacterial iLDHs are membrane-bound enzymes of the respiratory chain that catalyze the electron transfer from lactate to the quinone pool [40,41]. Moreover, the respiratory chain of *Paracoccus denitrificans* has a D-lactate oxidase activity that is also resistant to antimycin [42], and is coupled to the generation of a H^+ gradient, apparently by the activity of a H^+ pumping terminal oxidase [43]. Hence, the involvement of quinones in the oxidation of L-lactate suggests that the *Euglena* iLDH is similar to that present in bacteria.

It is pointed out that some experimental results are not fully explained by the above described model. For instance, inhibition of TMPD oxidase by cyanide exhibits a biphasic pattern which has been interpreted as the presence of two oxidases with different sensitivity to cyanide. The component of high affinity (K_i for cyanide ranging from 1 to 10 μM) has been identified as cytochrome *c* oxidase, while the low affinity component (K_i of 40–100 μM) has been associated to an alternative oxidase [10,41]. However, a biphasic pattern of inhibition may also result from two states of the enzyme with different affinity for the inhibitor [44,45], as consequence of negative cooperativity in inhibitor binding, or from a partial or mixed-type inhibition [46]. Since the TMPD oxidase activity follows a Michaelis–Menten kinetics with respect to the TMPD concentration (i.e., only one component), with a K_m of 0.65 ± 0.06 (3) mM and V_{max} of 604 ± 20 (3) ng atoms oxygen/mg protein/min (data not shown), it is suggested that the biphasic kinetics of cyanide inhibition is the result of the presence of oxidized and reduced enzymes which have different cyanide affinities.

There was a low lactate-dependent ATP synthesis in the presence of high concentrations of myxothiazol (> 10 μM), although a H^+ gradient of a sufficient magnitude to support the process was available. However, at these concentrations, myxothiazol exerted inhibitory effects on other enzymes of the pathway like iLDH (15% inhibition) and ATP synthase ($14 \pm 2\%$; $n = 3$; activity measured as ATP hydrolysis in the presence of 1 μM CCCP).

We previously reported the ability of *Euglena* mitochondria to generate a H^+ gradient supported by L-lactate oxidation in the presence of 0.1 mM cyanide [4,5]. This observation is apparently at variance with the proposed model of the respiratory chain, in which there is only one cyanide-sensitive component (cytochrome *c* oxidase) and, hence, no H^+ gradient should be built up in the presence of cyanide. A low cyanide concentration was previously used, because

it was thought that such concentration could totally inhibit cytochrome *c* oxidase, while still allowing the observation of the low affinity component. However, 0.1 mM cyanide does not completely abolish TMPD oxidase and, therefore, nor respiration or ATP synthesis (see Figs. 1 and 2).

The lower activity of antimycin-resistant quinol oxidase, in comparison to that of antimycin-resistant L-lactate oxidase, could be due to a lower affinity for the artificial quinones used. The natural quinones found in the membranes of *Euglena* mitochondria are ubiquinone-9, traces of ubiquinone-8 and rhodoquinone-9 [47], a quinone with an amine group instead of methoxy in the position 2 of the aromatic ring [48]. This last quinone is abundant in organisms subjected to anoxic environments in which a fumarate reductase activity is increased [49]. Although its function in the respiratory chain of *Euglena* mitochondria is yet unknown, rhodoquinone might be a more specific substrate for the putative antimycin-resistant quinol/cytochrome *c* oxidoreductase, since DBQ and other artificial quinones prompted high rates of the cytochrome bc_1 complex, but they were unable to reconstitute fully the antimycin-resistant activity.

Acknowledgements

This work was partially supported by Grants 25274-M and 25465-M from CONACYT-México. The authors thank Dr. A. Gómez-Puyou for his suggestions and critical reading of the manuscript.

References

[1] T.K. Sharpless, R.A. Butow, J. Biol. Chem. 245 (1970) 50–57.
[2] T.K. Sharpless, R.A. Butow, J. Biol. Chem. 245 (1970) 58–70.
[3] D.E. Buetow, in: D.E. Buetow (Ed.), The Biology of *Euglena*, Vol. IV, Academic Press, New York, 1989, pp. 247–314.
[4] A. Uribe, R. Moreno-Sánchez, Plant Sci. 86 (1992) 21–32.
[5] R. Moreno-Sánchez, J.C. Raya, Plant Sci. 48 (1987) 151–157.
[6] A. Uribe, E. Chávez, M. Jiménez, C. Zazueta, R. Moreno-Sánchez, Biochim. Biophys. Acta 1186 (1994) 107–116.
[7] W.U. Kümmel, K. Brinkmann, Planta 176 (1988) 261–268.
[8] G.R. Schonbaum, W.D. Bonner, B.T. Storey, J.T. Bahr, Plant Physiol. 47 (1971) 124–128.
[9] P. Benichou, R. Calvayrac, M. Claisse, Planta 175 (1988) 23–32.
[10] S. Devars, R. Hernández, R. Covián, A. García-Horsman, B. Barquera, R. Moreno-Sánchez, J. Eukaryot. Microbiol. 45 (1998) 122–130.
[11] G. Von Jagow, T.A. Link, Methods Enzymol. 126 (1986) 253–271.
[12] J. Siedow, M. Grivin, Plant Physiol. 65 (1980) 669–674.
[13] D.S. Grover, G.G. Laties, Plant Physiol. 68 (1981) 393–400.
[14] S. Devars, M.E. Torres-Márquez, D. González-Halphen, A. Uribe, R. Moreno-Sánchez, Plant Sci. 82 (1992) 37–46.
[15] S.H. Hutner, M.K. Bach, G.I.M. Ross, J. Protozool. 3 (1958) 101–105.
[16] J.A. Schiff, H. Lyman, G.K. Russell, Methods Enzymol. 23 (1971) 143–162.
[17] L. De Meis, M.G.C. Carvalho, Biochemistry 13 (1974) 5032–5038.
[18] H. Ding, D.R. Robertson, F. Daldal, P.L. Dutton, Biochemistry 31 (1992) 3144–3158.
[19] J.S. Rieske, Methods Enzymol. 10 (1967) 239–245.
[20] K. Mukai, M. Yoshida, H. Toyosaki, Y. Yao, S. Wakabayashi, H. Matsubara, Eur. J. Biochem. 178 (1989) 649–656.
[21] J.M. Armstrong, Biochim. Biophys. Acta 86 (1964) 194–197.
[22] H. Rottenberg, J. Membr. Biol. 81 (1984) 127–138.
[23] A. Ghelli, M. Crimi, S. Orsini, N. Gradoni, M. Zannotti, G. Lenaz, M. Degli-Esposti, Comp. Biochem. Physiol. 103B (1992) 329–338.
[24] M. Degli-Esposti, S. De Vries, M. Crimi, A. Ghelli, T. Patarnello, A. Meyer, Biochim. Biophys. Acta 1143 (1993) 243–271.
[25] G.F. Azzone, T. Pozzan, S. Massari, M. Bragadin, Biochim. Biophys. Acta 501 (1978) 296–306.
[26] H. Woelders, T. Van der Velden, K. Van Dam, Biochim. Biophys. Acta 934 (1988) 123–134.
[27] A. Guffanti, H. Blumenfeld, T. Krulwich, J. Biol. Chem. 256 (1981) 8416–8421.
[28] J.E. MacCarthy, S.J. Ferguson, Eur. J. Biochem. 132 (1983) 425–431.
[29] K. Kita, K. Konishi, Y. Anraku, Methods Enzymol. 126 (1986) 94–113.
[30] J.E. Escamilla, M.C. Benito, J. Bacteriol. 160 (1984) 473–477.
[31] A.M. Almeida, W. Jarmuszkiewicz, H. Khomsi, P. Arruda, A.E. Vercesi, F.E. Sluse, Plant Physiol. 119 (1999) 1323–1329.
[32] N.M. Camougrand, S. Zniber, M.G. Guerin, Biochim. Biophys. Acta 1057 (1991) 124–130.
[33] K.R. Santhamma, A. Bhaduri, Mol. Biochem. Parasitol. 75 (1995) 43–53.
[34] J.F. Turrens, Biochem. J. 259 (1989) 363–365.
[35] M. Degli-Esposti, A. Ghelli, M. Crimi, E. Estornell, R. Fato, G. Lenaz, Biochem. Biophys. Res. Commun. 190 (1993) 1090–1096.

[36] B. Meunier, S.A. Madgwick, E. Reil, W. Oettmeier, P.R. Rich, Biochemistry 34 (1995) 1076–1083.
[37] A. Magalon, R.A. Rothery, D. Lemesle-Meunier, C. Frixon, J.H. Weiner, F. Blasco, J. Biol. Chem. 273 (1998) 10851–10856.
[38] Y. Shahak, B. Arieli, E. Padan, G. Hauska, FEBS Lett. 299 (1992) 127–130.
[39] G. Daum, P.C. Bohni, G. Sehatz, J. Biol. Chem. 257 (1982) 13028–13033.
[40] H.A. Dailey, J. Bacteriol. 127 (1976) 1286–1291.
[41] W.J. Ingledew, R.K. Poole, Microbiol. Rev. 48 (1984) 222–271.
[42] P. Zboril, V. Wernerová, Biochem. Mol. Biol. Int. 39 (1996) 595–605.
[43] M. Raitio, M. Wikström, Biochim. Biophys. Acta 1186 (1994) 100–106.
[44] K.J.H. Van Buuren, P.F. Zuurendonk, B.F. Van Gelder, A.O. Muijsers, Biochim. Biophys. Acta 256 (1972) 243–257.
[45] M.G. Jones, D. Bickar, M.T. Wilson, M. Brunori, A. Colosimo, P. Sarti, Biochem. J. 220 (1984) 57–66.
[46] I.H. Segel, Enzyme Kinetics, Chapter 4, John Wiley and Sons, New York, 1975.
[47] G.K. Hutson, D.R. Threlfall, in: M. Levandowsky, S.H. Hutner, (Eds.), Biochemistry and Physiology of Protozoa, Vol. 3, Academic Press, New York, 1980, pp. 255–286.
[48] A.G.M. Tielens, J.J. Van Hellemond, Biochim. Biophys. Acta 1365 (1998) 71–78.
[49] J.J. Van Hellemond, M. Klockiewicz, C.P.H. Gaasenbeek, M.H. Roos, A.G.M. Tielens, J. Biol. Chem. 270 (1995) 31065–31070.

REB 21(3): 214, 2002

Problema Bioquímico

Ricardo Jasso Chávez
Instituto Nacional de Cardiología
"Ignacio Chávez"
e-mail: rjasso@hotmail.com

TEMA: Cinética enzimática.
Efecto de la temperatura

El aumento en la temperatura incrementa la actividad de las enzimas hasta un valor en donde empieza a prevalecer la desnaturalización. Mientras que la variación en la velocidad (*Vm* o *kcat*) debida a la temperatura se analiza frecuentemente en las enzimas, la variación de la afinidad por el substrato ha sido menos estudiada (*Km*).

La temperatura es una de las variables ambientales más importantes que establece los límites de viabilidad en los organismos. Para comparar la estabilidad enzimática en organismos expuestos a diferentes temperaturas, se determinó el efecto de la temperatura sobre los parámetros cinéticos de la 3-fosfoglicerato cinasa presente en una bacateria mesofílica (*Zymomonas mobilis*) y en una termofílica (*Thermoanaerobacter sp*). La reacción se ensayó en la dirección de la formación de 1,3-bisfosfoglicerato, acoplando la gliceraldehído3-fosfato deshidrogenasa. Por lo tanto, la actividad enzimática se monitoreó midiendo la desaparición de NADH. La mezcla de reacción se incubó durante 10-15 s y la reacción se midió en los primeros 5 s [1].

Los resultados fueron los siguientes:

Zymomonas mobilis			*Thermoanaerobacter sp*		
Temperatura (°C)	*Vm* (nmol NADH/min/mg)	*Km* (mM) (3PG)	Temperatura (°C)	*Vm* (nmol NADH/min/mg)	*Km* (mM) (3PG)
20	280	1.0625	40	700	0.75
25	340	0.9375	45	800	0.875
30	400	1.0	50	925	0.9375
35	480	1.0625	55	1100	1.00
40	550	—	60	1250	1.0625
45	625	1.125	65	1500	1.125
50	700	1.1875	70	1650	1.25
55	800	1.3125	75	1650	
60	850	1.625	80	1600	
65	1000				
70	950				
75	875				

Determinar la energía de activación y los parámetros termodinámico $\Delta G°$ a 30°C, $\Delta H°$ y $\Delta S°$ para la disociación del complejo Enzima-3PG (suponiendo que la enzima presenta una cinética en equilibrio rápido) a partir de los valores de *Km*. Discutir las diferencias observadas en la 3-fosfoglicerato cinasa entre los dos organismos.

Respuestas al Problema Bioquímico

RESULTADOS:

La velocidad de una reacción enzimática depende de la frecuencia de colisiones entre las moléculas reactantes (enzima + substrato). La energía mínima para que una colisión genere una reacción es la *energía de activación* (Ea).

La cual puede determinarse mediante la ecuación de Arrhenius:

$v = v_0 e^{-Ea/RT}$ o en su forma lineal:

$\log v = \log v_0 - Ea / 2.3\ RT$,

donde v es la velocidad obtenida a cada temperatura de ensayo, v_0 es la velocidad máxima teórica si el número total de colisiones entre los reactantes fueran productivas a una temperatura infinita, T es la temperatura absoluta y R es la constante de los gases.

De esta forma, si relacionamos el logaritmo de las velocidades contra el inverso de la temperatura absoluta a la cual fueron obtenidas obtenemos una gráfica como la siguiente:

Así, el valor de la pendiente es igual $-Ea/ R* 2.3$, por lo que la *Ea* es de 5414 y 6301 cal/mol para las 3-fosfoglicerato cinasas de *Zymomonas mobilis* y de *Thermoanaerobacter sp*, respectivamente. Es importante puntualizar en la figura, que el cambio en la pendiente es indicativo de la inactivación térmica, por lo que estos puntos ya no se toman en cuenta para el cálculo de la Ea.

Suponiendo que la reacción catalizada por la 3-fosfoglicerato cinasa establece un equilibrio rápido para la asociación del substrato ($Km = Ks$), entonces las *Kms* obtenidas a diferentes temperaturas se puede utilizar para calcular los parámetros termodinámicos de acuerdo a la siguiente ecuación [2]

$\log Km = - \Delta H° / 2.3\ RT + \Delta S° / 2.3\ R$,

donde $\Delta H°$ es el cambio en la entalpía estándar, $\Delta S°$ es el cambio en la entropía estándar de la disociación del complejo enzima-substrato y R es la constante de los gases. Entonces, con la linea recta obtenida del gráfico del log *Km* contra el inverso de la temperatura absoluta,

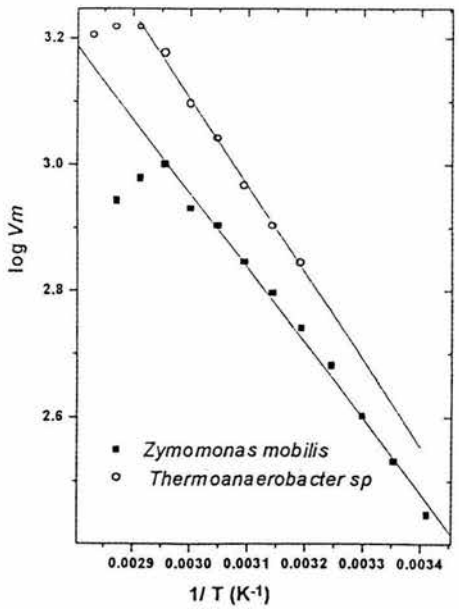

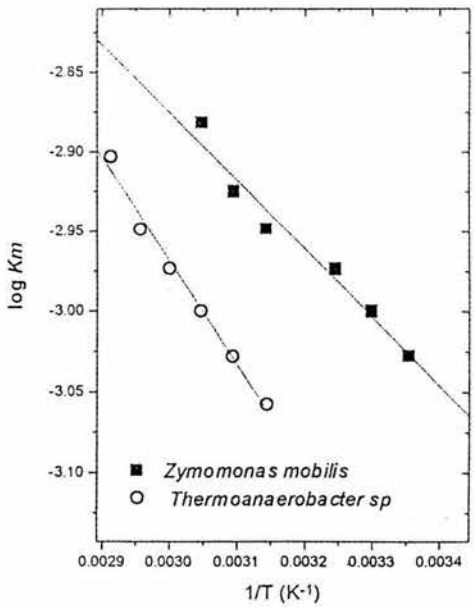

podemos calcular ΔH° a partir del valor de la pendiente y ΔS° de la ordenada al origen. El ajuste de los datos experimentales a una línea recta indica que la suposición de equilibrio rápido es razonable para esta enzima.

De esta forma, los valores de ΔH° fueron +1956 y +2960 cal /mol; y los de ΔS° de -7.29 y -4.7 cal/mol K, para *Zymomonas mobilis* y *Thermoanaerobacter sp*, respectivamente. Estos valores de cambio de entalpía y entropía indican que la disociación del complejo cinasa-3PG es un proceso endergónico con una disminución en la entropía.

Finalmente con la ecuación del cambio de la energía libre:

$$\Delta G° = \Delta H° - T\Delta S°,$$

podemos calcular el cambio en la energía libre de la reacción (ΔG°). En este caso el ΔG° a 30 °C es de +4.17 y +4.4 Kcal/mol para las enzimas de *Zymomonas mobilis* y *Thermoanaerobacter sp*, respectivamente.

El valor positivo en la energía libre de Gibbs para la disociación a 30°C indica que la asociación entre la enzima y el substrato está termodinamicamente favorecida independientemente del organismo del cual provenga.

El aumento en la actividad de la 3-fosfoglicerato cinasa de *Thermobacter* con respecto a la contraparte mesofílica, es un caso contrario a la observación normal que las enzimas termofílicas son menos activas que las mesófilas a una temperatura dada [1]. Sin embargo, las *Ea* para cada una de las enzimas fue muy similar, lo que indica que la termodinámica de una reacción enzimática no se modifica a pesar de la temperatura del ambiente en el cual se desarrolle un organismo sino a la naturaleza conservada de esta enzima.

BIBLIOGRAFÍA

1. Thomas, T., M., and Scopes, R. K.(1998). Biochem. J. 330,1087-10
2. Segel, I., H. (1975) Enzyme kinetics. Cap. 11, pp 926-935. John Wiley & Sons.

ACADEMIC PRESS

Archives of Biochemistry and Biophysics 404 (2002) 48–54

ABB

www.academicpress.com

Kinetic and thermodynamic characterization of adenylyl cyclase from *Euglena gracilis*

Ricardo Jasso-Chávez,[a,b] Alicia Vega-Segura,[a] Mohammed El-Hafidi,[b] Rafael Moreno-Sánchez,[b] and M. Eugenia Torres-Márquez[a,*]

[a] *Departamento de Bioquímica, Facultad de Medicina, UNAM, Apdo. Postal 70-159, Mexico 04510, DF, Mexico*
[b] *Departamento de Bioquímica, Instituto Nacional de Cardiología, Mexico 14080, DF, Mexico*

Received 11 February 2002, and in revised form 15 May 2002

Abstract

Some kinetic and thermodynamic properties of the plasma membrane adenylyl cyclase (AC) from the protist *Euglena gracilis* were examined. The AC kinetics for Mg-ATP was hyperbolic with a K_m value of 0.33–0.43 mM, whereas the inhibition exerted by 2′,5′-dideoxyadenosine was of the mixed type with a K_i of 80–147 μM. The V_m value (0.9 or 1.8 nmol (mg protein)$^{-1}$ min^{-1}) changed, depending upon the carbon source in the growth medium (lactic acid or glutamate plus malate). Lactic acid membrane AC was slightly more thermolabile (from 28 to 40 °C) and showed higher activation energy (range 15–25 °C). With lactate, the total and saturated fatty acid percentage content in the plasma membrane was significantly greater than with glutamate plus malate, whereas the percentage content of polyunsaturated ($n - 3$) fatty acids was lower. The data suggest that the fatty acid composition, as changed by the carbon source in the growth medium, may modulate the AC activity in *Euglena*.

Keywords: Adenylyl cyclase; cAMP; Enzyme kinetics; *Euglena gracilis*; Fatty acids; Protist; Signal transduction

Adenylyl cyclase (AC)[1] is an essential enzyme within the signal transduction pathway that operates downstream of the activation of G-protein-coupled receptors (GPCR), particularly those associated with G_s or G_i. Mammalian ACs are the best known enzymes of their class, and so far nine membrane-bound isoforms have been described [1]. The characteristics of each isoform, including their regulation by $G_s\alpha$ or $G_i\alpha$ subunits and the $G\beta\gamma$ complex, Ca^{2+}-calmodulin-dependent kinase and protein kinase C, have been reviewed by Tang and Hurley [2]. Except for isoform IX and the soluble mammalian AC [3], all particulate mammalian ACs are activated by forskolin. Another very different group of ACs includes soluble enzymes found in bacteria [4,5]. There are also some other ACs which, although located in the plasma membrane, are forskolin insensitive. These last ACs have been identified in many insect tissues [6], leech [7], *Paramecium* [8], octopus [9], and sea urchin sperm [10].

We [11] and Keirns et al. [12] have previously reported forskolin-insensitive AC activity in plasma membranes from the free-living flagellate protist *Euglena gracilis*. Apparently, the activity of this enzyme is regulated by G proteins and GPCR, as suggested by its stimulation by GTPγS and cholera toxin [11] and the activation by some GPCR agonists [12], respectively. The potency of GTPγS or GPCR agonists to activate *Euglena* AC was very low, which implies that the proper, physiological agonist is yet to be found or that this activation mechanism is not operating as the upstream pathway for the enzyme in this microorganism. Changes in AC activation and isoenzyme expression with the progress of the life cycle have been reported in flagellates [13]. It is not known whether *Euglena* faces such changes, but it might become challenged by nutrient availability. Indeed, different growth rates and cellular densities are achieved in *Euglena*, depending on the carbon source in the culture medium [14–16]. Change of metabolic patterns and of signal transduction

* Corresponding author. Fax: +525-616-2419.
E-mail address: metorres@servidor.unam.mx (M. Eugenia Torres-Márquez).

[1] *Abbreviations used:* AC, adenylyl cyclase; GPCR, G-protein-coupled receptor; Mops, 4-morpholinepropanesulfonic acid; BHT, butylhydroxytoluene; ddAdo, 2′,5′-dideoxyadenosine.

0003-9861/02/$ - see front matter
PII: S0003-9861(02)00235-7

pathways may be involved in this process. Therefore, we performed a kinetic and thermodynamic characterization of the *E. gracilis* AC activity in plasma membranes isolated from cells grown with different carbon sources, in a continuing effort to determine the signal transduction pathways involved in the physiological regulation of this microorganism.

Materials and methods

Plasma membrane preparation

Plasma membranes were obtained as described by Nakano et al. [17] with some modifications. *E. gracilis* Klebs, a Z-like strain, was grown axenically in the dark in Hutner's acidic organotrophic medium with either 35 mM glutamate plus 15 mM malate (glu plus mal) or 36 mM lactate as carbon source, as described previously [18]. After 4 days (in the early stationary phase of growth), cells were harvested by centrifugation at 1000*g* for 10 min at 4 °C and washed with 10 mM KH_2PO_4, pH 7. Cells were resuspended in a buffer containing 250 mM sucrose, 5 mM Mops, 2 mM EGTA, and 0.1% bovine serum albumin (SMEA buffer) and then sonicated four times for 30 s at 20–25 μm potency (80% maximal output) in a Branson sonifier. The suspension of broken cells was centrifuged at 1000*g* to eliminate debris and paramylon. The supernatant was centrifuged at 7000*g* for 10 min; the pellet was discarded to eliminate the mitochondrial fraction [19]. Centrifugation of the second supernatant at 33,000*g* for 1 h was used to sediment plasma membranes, which were washed once and resuspended in 50 mM Tris, pH 7.4, and 10 mM $MgCl_2$. The plasma membrane fraction was stored at −70 °C until use. Following this procedure, the discontinuous sucrose gradient centrifugation step described by Nakano et al. [17], and previously used by our group [11], was replaced by simple differential centrifugation steps, which resulted in a 10- to 20-times enriched AC activity. When membranes were used to determine their lipid composition 0.001% butylhydroxytoluene (BHT) was added. Protein concentration was determined by the method of Lowry et al. [20] with bovine serum albumin as standard.

Adenylyl cyclase determination

AC activity was measured as described by Salomon et al. [21], using 30–50 μg membrane protein per assay, with a reaction time of 20 min at 25 °C; under these conditions the activity was linear with time and protein concentration.

Determination of total fatty acids

This was achieved using the procedure described by Folch et al. [22], as follows. Aliquots of 10 mg plasma membrane protein were thawed and 1 ml BHT in 0.02% (v/v) methanol, 60 μg margaric acid (as standard), 1 ml 0.9% NaCl, and 2 ml chloroform were added and mixed for 1 min. The suspension was centrifuged at 1600*g* for 10 min at 4 °C. The organic phase was then recovered and the aqueous phase extracted two or three times more with chloroform. The organic phase was dehydrated by addition of 1.5 g Na_2SO_4 anhydrous. The solvent was evaporated under a stream of N_2. For *trans*-esterification of phospholipids, and derivatization of free fatty acids to methyl esters [23], dried samples were mixed with 0.1 ml toluene, 2 ml methanol anhydrous, and 0.04 ml sulfuric acid. This mixture was heated at 65 °C for 2 h. Then, the samples were mixed with 1 ml 5% NaCl and 2 ml hexane, stirred vigorously, evaporated under a N_2 stream, and stored at −72 °C until gas chromatography (GC) analysis was carried out. The conditions for GC were 198 °C, with H_2 as carrier at a pressure of 0.5 kg cm^{-2}. The column used was CP SIL 8CB in a Carlo Erba (Chromopack) instrument.

Results

Kinetics of adenylyl cyclase

The effect of different ATP concentrations on the rate of cAMP production by AC followed a Michaelis–Menten kinetics pattern, regardless of the carbon source under which *Euglena* cells were grown (Fig. 1). The affinity for Mg-ATP was similar for both types of membranes; however, the maximal rate (V_m) was 1.9-fold

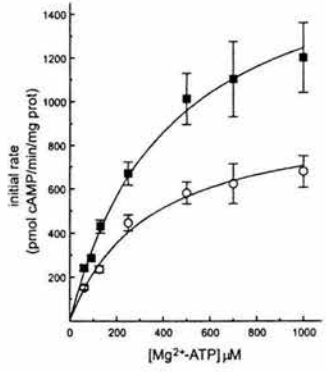

Fig. 1. Kinetics of adenylyl cyclase basal activity from *E. gracilis*. Plasma membranes (30–50 μg protein) were incubated at 25 °C with the indicated concentrations of Mg-ATP, and the rate of cAMP production was measured as described under Materials and methods. Membranes were isolated from cells grown with glu plus mal (○) or lactic acid (■) as carbon source. The experimental points were fitted to the Michaelis–Menten equation, using the commercial computer program Microcal Origin version 5. Values are the mean ± SE of the mean of five independent experiments made in duplicate.

higher in lactic acid membrane preparations (Table 1). In consequence, the catalytic efficiency (V_m/K_m) for lactic acid membrane AC was larger than that for glu plus mal membrane AC: 0.0041 versus 0.0028 ml (mg protein)$^{-1}$ min^{-1}. Stimulation of AC activity by GTPγS, a nonhydrolyzable GTP analogue that activates $G_s\alpha$ [25], was similar in both membrane preparations (22% for glu plus mal and 36% for lactic acid at 1 μM). The P-site inhibitor 2′,5′-dideoxyadenosine (ddAdo) [26] was able to inhibit *Euglena* AC activity. Double reciprocal plots (Figs. 2A and B) showed that ddAdo exerted a mixed-type inhibition, regardless of the membrane preparation. Nonlinear regression analysis of the ddAdo effect in lactic acid membranes showed a fitting of a quality similar to both simple noncompetitive and mixed-type inhibition (not shown). Since the former is a partic-

Table 1
Kinetic parameters for basal adenylyl cyclase in two membrane preparations from *E. gracilis*

	Lactic membranes	Glu plus mal membranes
$K_{s\ (25\,°C)}$ (μM)	427 ± 74 (5)	327 ± 48 (5)
$V_{m\ (25\,°C)}$ (pmol/min/mg)	1777 ± 235 (5)[a]	933 ± 88 (5)
	Linear regression	Linear regression
$K_{i\ 2',5'\text{-ddAdo}}$ (μM) mixed-type inhibition	80	147
	$\alpha = 0.63$	$\alpha = 0.5$
	Nonlinear regression	Nonlinear regression
	51 ± 14	121 ± 16
	$\alpha = 1.94 \pm 1.17$ (8)	$\alpha = 0.43(8) \pm 0.23$

Values are means ± SE with the number of different preparations assayed between parentheses. The equation used for mixed-type inhibition was [24] $v = (V_{m_{app}}[S])/(K_{s_{app}} + [S])$, where $V_{m_{app}}$ is $V_m/(1 + I/\alpha K_i)$ and $K_{s_{app}}$ is $K_s(1 + I/K_i)/(1 + I/\alpha K_i)$ and α is the factor by which the inhibitor affects the substrate binding.

[a] $P < 0.05$ vs glu plus mal membranes.

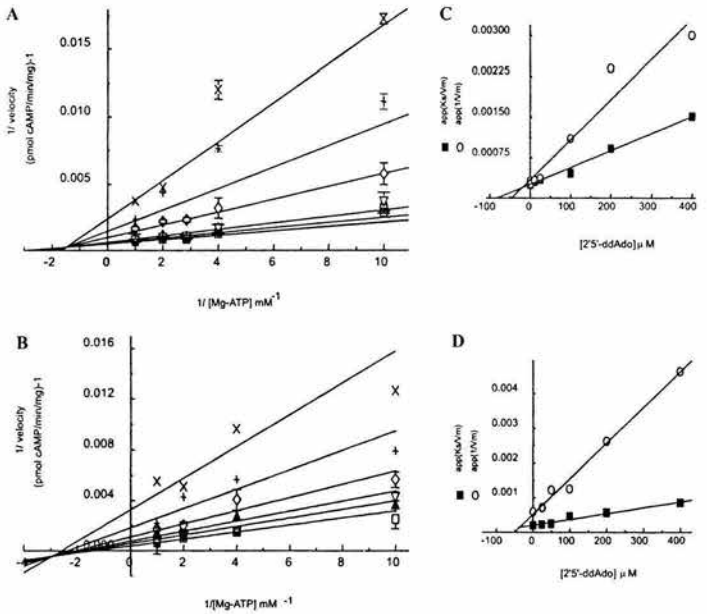

Fig. 2. Inhibition of basal adenylyl cyclase activity by ddAdo. Assays with 30–50 μg of membrane protein were made in the presence of 0.1–1 mM Mg-ATP and with no inhibitor added (□) or 1 (○), 10 (△), 25 (▲), 50 (▽), 100 (◇), 200 (+), or 400 μM (×) ddAdo. (A) Lactic acid membranes. (B) Glu plus mal membranes. Replots (C and D) of slopes (■) and intercepts (○) were used to estimate the inhibition constant (K_i) value. Solid lines in A and B are the result of a nonlinear regression analysis. Values are the means ± SE of six or seven experiments in duplicate for 0–100 μM ddAdo or two or three experiments in duplicate for 200–400 μM ddAdo.

ular case of the latter pattern ($\alpha = 1$), a mixed-type inhibition was assigned to ddAdo in lactic acid membranes, as well as in glu plus mal membranes (Table 1).

Thermostability of AC activity

Preincubation of plasma membranes with increasing temperature from 28 to 40 °C induced a diminution of AC activity. The thermal inactivation followed first-order exponential decay kinetics. Inactivation rate constants (k_{inac}) for each temperature were obtained from the slope derived by plotting log activity versus time (Figs. 3A and B). The k_{inac} vs temperature plot (Fig. 3C) indicated that AC from lactic acid-grown cells was slightly more thermolabile than AC from glu plus mal cells.

To determine the changes in enthalpy ($\Delta H°$) and entropy ($\Delta S°$) for the binding of Mg-ATP to the enzyme, the dissociation constants obtained at different temperatures (Fig. 4) were obtained applying the following equation [24]:

$$\log K_s = -\frac{\Delta H^0}{2.303RT} + \frac{\Delta S^0}{2.303R}. \quad (1)$$

Similar to the mammalian isoforms [2], it was assumed that the binding reaction established a rapid equilibrium, i.e., $K_m = K_s$. The straight lines in the $\log K_s$ versus $1/T$ plot for both types of membrane preparations (Figs. 4A and B) indicated that the dissociation of ATP was an endothermic process with an increase in entropy (Table 2). The resulting positive change in Gibbs free energy for the dissociation at 25 °C indicated that the association was thermodynamically favored. Arrhenius plots in the temperature range from 15 to 25 °C showed that the activation energies for both membrane preparations were slightly different (Table 2). These activation energies were substantially lower than those reported for canine heart AC of 23–32 kcal mol^{-1} [27], but similar to that obtained for the mussel [28] and rat heart enzymes [29].

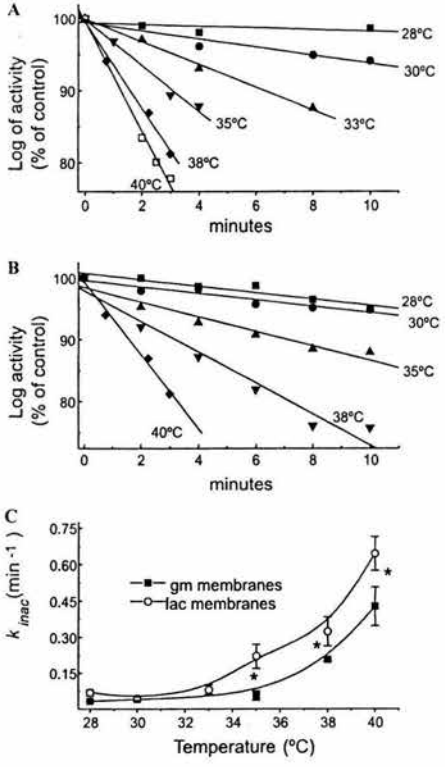

Fig. 3. Temperature inactivation of adenylyl cyclase. Membranes (30–50 μg protein) were preincubated at the indicated temperatures. Aliquots were withdrawn at the indicated times to assay the AC activity at 25 °C as described under Materials and methods. Values are the means ± SD of five experiments in duplicate. *$P < 0.05$.

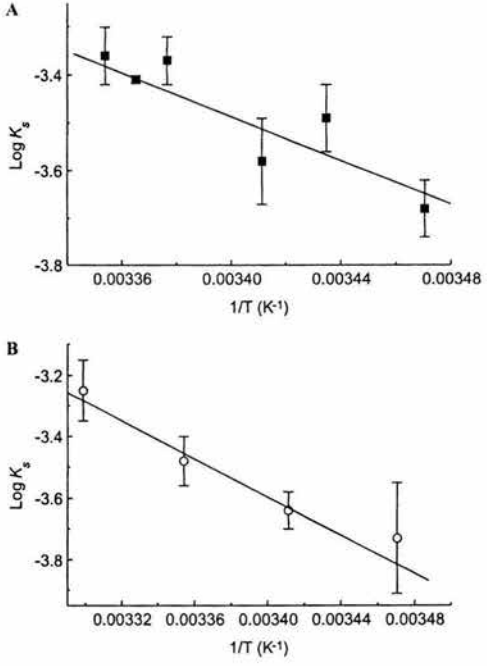

Fig. 4. Thermodynamic parameters. AC activity was measured at 15, 18, 20, 23, 24, and 25 °C in lactic acid membranes (A) or 15, 20, 25, and 30 °C in glu plus mal membranes (B) The values of the dissociation constants (K_s) were derived from fitting the experimental points to the Michaelis–Menten equation at each temperature. Values are the means ± SE of five experiments in duplicate.

Table 2
Estimated thermodynamic parameters of the adenylyl cyclase–Mg-ATP interaction

	Activation energy (kcal/mol) (15–25°C)	Enthalpy of dissociation (kcal/mol)	Entropy of dissociation (cal/mol × K)	Dissociation free energy at 25°C (kcal/mol)
Lactic acid membranes	18 ± 1.4	+10.5 ± 2	+19.6 ± 7	+4.6
Glu plus mal membranes	12 ± 2	+14 ± 2	+32 ± 6	+4.6

The values shown are the means ± SE of at least four different preparations made in duplicate.

Fatty acid composition of plasma membranes

The differences in AC activity between the two membrane preparations could be related to different amounts of AC, expression of different isoenzymes, or different lipid environments. To assess the third possibility, the fatty acid composition of both cell membrane preparations was determined (Table 3). The glu plus mal membranes showed smaller contents of *total* and several individual fatty acids than those of lactic acid membranes. However, the polyunsaturated fatty acids araquidonic (C20:4$n-6$) and eicosapentaenoic (C20:5$n-3$) acids represented a two times higher percentage content in glu plus mal membranes than in lactic acid membranes (Table 3). The unsaturated/saturated fatty acids ratio was also greater in glu plus mal membranes (2.48) than in lactic acid membranes (2.14). The cholesterol content in both membrane preparations was negligible (not shown). A significant content of the $\Delta^{7,10}$ hexadecenoic acid (C16:2$n-6$), a fatty acid not commonly found in mammalian plasma membranes [30], was detected in both *Euglena* membrane preparations.

Discussion

The K_m value for Mg-ATP found in this work for the AC from *E. gracilis* is within the range reported for other mammalian ACs [2]. This conserved characteristic is in accordance with the high homology of the catalytic site in mammalian AC [2] and AC from the flagellate protist *Leishmania donovani* [31], the phylogenetically closest organism to Euglena with a cloned AC. The V_m values showed that AC activities from *E. gracilis* were strikingly larger than those found in mammalian plasma membranes [32–36] and in other eukaryotic systems, including some invertebrates [6–8,37,38]. Nevertheless, *Euglena* AC rates were still remarkably smaller than those from bacterial AC [4,39], although the latter are soluble, while the protist enzyme was located in the

Table 3
Fatty acid composition of plasma membranes from *Euglena*

Content (μg/mg protein)				Percentage		
Fatty acids	Glu + mal	Lactic acid	*P*	Glu + mal	Lactic acid	*P*
C16:0	230 ± 29	662 ± 56	0.0002	14.8 ± 0.9	20 ± 2.7	0.002
C16:1$n-7$	55 ± 16	130 ± 13	0.003	3.5 ± 0.5	4 ± 0.5	ns
C16:2$n-6$	46 ± 26	335 ± 263	ns	3 ± 2	10 ± 6.7	ns
C18:0	39 ± 11	122 ± 28	0.008	2.5 ± 0.9	3.8 ± 0.4	ns
C18:1$n-9$	77 ± 14	292 ± 124	0.04	5 ± 1.3	9 ± 2.7	ns
C18:2$n-6$	47 ± 14	167 ± 17	0.0006	3 ± 0.9	5.1 ± 0.1	0.01
C18:3$n-3$	15 ± 3	44 ± 24	ns	0.9 ± 0.04	1.3 ± 0.6	ns
C20:3$n-6$	22 ± 17	18 ± 5	ns	1.4 ± 1.1	0.5 ± 0.09	ns
C20:2$n-6$	46 ± 7	199 ± 11	0.00003	2.9 ± 0.1	6.2 ± 0.6	0.0007
C20:3$n-6$	17 ± 3	53 ± 1	0.000005	1.07 ± 0.09	1.6 ± 0.2	0.008
C20:4$n-6$	262 ± 69	285 ± 25	ns	16.8 ± 1.6	8.8 ± 1.5	0.004
C20:5$n-3$	298 ± 81	286 ± 20	ns	19 ± 1.8	8.8 ± 1.2	0.001
C22:4$n-6$	107 ± 27	203 ± 7	0.003	6.9 ± 0.6	6.3 ± 1	ns
C22:5$n-3$	8 ± 0.3	16 ± 5	0.05	0.5 ± 0.06	0.5 ± 0.1	ns
C22:6$n-3$	288 ± 76	414 ± 35	0.001	18.5 ± 1.7	13 ± 2	0.02
TFA	1553 ± 267	3228 ± 425	0.004			
SFA				17.3 ± 1.5	24.5 ± 2	0.01
MUFA				8.6 ± 1.4	13 ± 2	0.04
PUFA($n-6$)				34.4 ± 1.4	39.6 ± 3	0.06
PUFA($n-3$)				39 ± 2.7	23 ± 3	0.002

Data represent the means ± SD; $N = 3$ different preparations, ns, not significant; TFA, total fatty acids; SFA, MUFA, and PUFA, saturated, monounsaturated, and polyunsaturated fatty acids.

particulate fraction. A particulate bacterial AC was recently found in *Mycobacterium tuberculosis* [40], but with a V_m approximately 12–20 times higher than that of *Euglena* AC.

The relatively high V_m values of the *Euglena* AC bring about high levels of basal cAMP in both cultures (15 ± 2, $N = 6$, and 32 ± 2.5, $N = 6$ pmol cAMP/10^7 cells for lactic acid and glu plus mal cells, respectively). Similar values of cAMP have also been described for leech [7], *Paramecium* [8], sea urchin sperm [10], and rat C6 glioma cells [41]. However, a tight correlation between V_m and basal cAMP in *Euglena* was not attained (cells from lactic acid medium exhibited a higher AC V_m, but a lower cAMP level, than cells from glu plus mal medium). This suggests that other factors are also involved in the establishment of the steady-state levels of intracellular cAMP, such as the activities of cAMP phosphodiesterases and pyrophosphatases.

Except for type IX, all particulate mammalian types of AC are potently activated by forskolin. However, Yang et al. [42] reported that the exchange of Tyr1082 for Leu in the murine type IX AC isoform transforms a forskolin-insensitive enzyme into a sensitive one. Similar to mammalian AC isoforms, *E. gracilis* AC was associated with the particulate fraction, although it was forskolin-insensitive and showed a 30- to 60-fold lower sensitivity to ddAdo [43]. These differences between the *Euglena* and the mammalian ACs suggest that either a different isoform is expressed in the protist or the change in the enzyme lipid microenvironment modulates the kinetics of the AC. The difference in V_m between lactic acid and glu plus mal membranes may reflect different amounts of active AC. However, a different content of AC does not explain the difference in (1) ddAdo sensitivity, (2) thermal activation, or (3) thermostability found between both membrane preparations.

P-site inhibition of mammalian AC with respect to ATP may be noncompetitive, uncompetitive, or mixed type in the presence of Mn^{2+} [26,44] and noncompetitive or uncompetitive in the presence of Mg^{2+} [35,44]. In contrast, in the present work a mixed-type inhibition exerted by ddAdo versus Mg-ATP on the *Euglena* AC was found, which suggests that the inhibitor may bind to both the PP_i–enzyme complex [43] and the free enzyme. The Mn^{2+} effect on P-site inhibition has been related to an effect on the enzyme conformation when studied in membranes [35]. Hence, it is possible that the different sensitivity of the *Euglena* AC toward ddAdo, depending on the carbon source in the growth medium, may also reflect different AC conformations, as a consequence of different lipid environments.

In this regard, the AC from lactic acid membranes showed a larger activation energy in the temperature range of 15–25 °C and a lower thermostability in the temperature range of 28–40 °C; the former may be related to the lower unsaturated/saturated fatty acid ratio, which induces a decrease in the membrane fluidity. Free PUFA such as araquidonic and eicosapentaenoic acids, but not phospholipids with esterified PUFA, are potent inhibitors of the AC activity [45]. Although a higher percentage content of these two PUFA correlated with a lower AC activity in glu plus mal membranes, *free* PUFA, in addition to *total* PUFA (free + esterified), remains to be determined in *Euglena* membranes. Modifications in membrane lipid composition and fluidity, together with a higher expression of β-adrenergic receptors, contribute to thermal compensation of the β-adrenergic response in trout liver [46]. Thus, *Euglena* may also change its plasma membrane lipid composition as part of compensatory mechanisms to temperature fluctuations.

The physiological relevance of the relatively high AC activity from *Euglena* is unknown. However, it implies that the signal transduction cAMP pathway is important in this free-living protist for the regulation of cellular processes and metabolic networks.

Acknowledgment

This paper was partially supported by Grant 25465N from CONACYT.

References

[1] T.B. Patel, Z.S. Du Pierre, L. Cartin, K. Scholich, Gene 269 (2001) 13–25.
[2] W.-J. Tang, J.H. Hurley, Mol. Pharmacol. 54 (1998) 231–240.
[3] J. Buck, M.L. Sinclair, L. Schapal, M.J. Cann, L.R. Levin, Proc. Natl. Acad. Sci. USA 96 (1999) 79–84.
[4] S.-Z. Yang, Z.-M. Huang, R.K. Andrews, W.-J. Tang, Mol. Pharmacol. 53 (1998) 182–187.
[5] C.L. Drum, S.-Z. Yang, R. Sarac, Y. Mabuchi, K. Beckingham, A. Bohm, Z. Grabarek, W.-J. Tang, J. Biol. Chem. 275 (2000) 36334–36340.
[6] D.B. Morton, Comp. Biochem. Physiol. 78C (1984) 153–158.
[7] M.E. Ferretti, M.C. Portolan, M.C. Pareschi, A.L. Campi, C. Biondi, Comp. Biochem. Physiol. 94C (1989) 635–640.
[8] J.E. Schultz, S. Klumpp, R. Benz, W.J.C.H. Schürhoff-Goeters, A. Schmid, Science 255 (1992) 600–603.
[9] A. Capasso, V. Carginale, L. Borrelli, E. Parisi, Comp. Biochem. Physiol. 106C (1993) 555–559.
[10] C. Beltran, O. Zapata, A. Darszon, Biochemistry 35 (1996) 7591–7598.
[11] M.E. Torres-Márquez, M. Macias-Silva, A. Vega-Segura, Comp. Biochem. Physiol. 115C (1996) 233–237.
[12] J.J. Keirns, B. Carritt, J. Freeman, J.M. Eisenstadt, M.W. Bitensky, Life Sci. 13 (1973) 287–302.
[13] S. Alexandre, P. Paindavoine, P. Tebabi, A. Pays, S. Halleux, M. Steinert, E. Pays, Mol. Biochem. Parasitol. 43 (1990) 279–288.
[14] J. Briand, R. Calvayrac, D. Laval-Martin, S. Falineau, Planta 151 (1981) 168–175.
[15] S. Sumida, T. Ehara, T. Osafune, E. Hase, Plant Cell Physiol. 28 (1987) 1587–1592.
[16] L. Navarro, M.E. Torres-Márquez, S. González-Moreno, S. Devars, R. Hernández, R. Moreno-Sánchez, Comp. Biochem. Physiol. 116C (1997) 265–272.

[17] Y. Nakano, Y. Urade, R. Urade, S. Kitaoka, J. Biochem. (Tokyo) 102 (1987) 1053–1063.
[18] R. Moreno-Sánchez, R. Covián, R. Jasso-Chávez, S. Rodríguez-Enríquez, F. Pacheco-Moisés, M.E. Torres-Márquez, Biochim. Biophys. Acta 1457 (2000) 200–210.
[19] R. Moreno-Sanchez, J.C. Raya, Plant Sci. 48 (1987) 151–157.
[20] O.H. Lowry, N.J. Rosebrough, A.L. Farr, R.J. Randall, J. Biol. Chem. 193 (1951) 265–275.
[21] Y. Salomon, C. Londos, M. Rodbell, Anal. Biochem. 58 (1974) 541–548.
[22] J. Folch, M. Lees, G.M. Sloane-Stanley, J. Biol. Chem. 226 (1957) 497–509.
[23] W.W. Christie, J. Lipid Res. 23 (1982) 1072–1075.
[24] I.H. Segel, Enzyme Kinetics, Wiley, New York, 1975.
[25] J.K. Northup, M.D. Smigel, A.G. Gilman, J. Biol. Chem. 257 (1982) 11416.
[26] R.A. Johnson, I. Shoshani, J. Biol. Chem. 265 (1990) 11595–11600.
[27] R.A. Colvin, R.A. Allen, Arch. Biochem. Biophys. 289 (1991) 337–342.
[28] M.J. Mancebo, M. Trevino, J. Espinosa, Comp. Biochem. Physiol. 99B (1991) 355–357.
[29] P. Chatelain, P. Robberecht, M. Waelbroeck, P. De Neef, J. Camus, J. Christophe, Mol. Pharmacol. 22 (1982) 342–348.
[30] F. Destaillats, R.L. Wolff, D. Precht, J. Molkentin, Lipids 35 (2000) 1027–1032.
[31] M.A. Sanchez, D. Zeoli, E.M. Klamo, M.P. Kavanaugh, S.M. Landfear, J. Biol. Chem. 270 (1995) 17551–17558.
[32] J.F. Krall, S.C. Leshon, S.G. Korenman, Biochem. J. 205 (1982) 249–255.
[33] H.A. Bakalyar, R.R. Reed, Science 250 (1990) 1403–1406.
[34] J.J. Cali, J.C. Zwaagstra, N. Mons, D.M. Cooper, J. Krupinski, J. Biol. Chem. 269 (1994) 12190–12195.
[35] C.W. Dessauer, A.G. Gilman, J. Biol. Chem. 272 (1997) 27787–27795.
[36] G. Zimmermann, R. Taussig, J. Biol. Chem. 271 (1996) 27161–27166.
[37] G. Venturini, O. Silei, G. Palladini, A. Carolei, V. Margotta, Comp. Biochem. Physiol. 78C (1984) 345–348.
[38] T. Kataoka, D. Broek, M. Wigler, Cell 43 (1985) 493–505.
[39] D.C. Ladant, Brezin, J.-M. Alonso, I. Crenon, N. Guiso, J. Biol. Chem. 261 (1986) 16264–16269.
[40] Y.L. Guo, T. Seebacher, U. Kurz, J.U. Linder, J. Schultz, EMBO J. 20 (2001) 3667–3675.
[41] L. Roef, E. Witters, J. Gadeyne, J. Mercussen, Anal. Biochem. 233 (1996) 188–196.
[42] J. Yang, W. Epstein, J. Biol. Chem. 258 (1983) 3750–3758.
[43] R.A. Johnson, L. Desaubry, G. Bianchi, I. Shoshani, E. Lyons, R. Taussig, P.A. Watson, J.J. Cali, J. Krupinski, J.P. Pieroni, R.J. Iyengar, Biol. Chem. 272 (1997) 8962–8966.
[44] J.J. Tesmer, C.W. Dessauer, R.K. Sunahara, L.D. Murray, R.A. Johnson, A.G. Gilman, S.R. Sprang, Biochemistry 39 (2000) 14464–14471.
[45] J. Nakamura, N. Okamura, S. Usuki, S. Bannai, Arch. Biochem. Biophys. 389 (2001) 68–76.
[46] S.J. McKinley, J.R. Hazel, J. Exp. Biol. 203 (2000) 631–640.